

Research outputs 2022 to 2026

---

2-1-2022

## Recent advances in carbon dioxide geological storage, experimental procedures, influencing parameters, and future outlook

Muhammad Ali

Nilesh Kumar Jha

Nilanjan Pal

Alireza Keshavarz

*Edith Cowan University*, [a.keshavarz@ecu.edu.au](mailto:a.keshavarz@ecu.edu.au)

Hussein Hoteit

*See next page for additional authors*

Follow this and additional works at: <https://ro.ecu.edu.au/ecuworks2022-2026>

 Part of the Civil and Environmental Engineering Commons

---

[10.1016/j.earscirev.2021.103895](https://doi.org/10.1016/j.earscirev.2021.103895)

Ali, M., Jha, N. K., Pal, N., Keshavarz, A., Hoteit, H., & Sarmadivaleh, M. (2022). Recent advances in carbon dioxide geological storage, experimental procedures, influencing parameters, and future outlook. *Earth-Science Reviews*, 225, article 103895.

<https://doi.org/10.1016/j.earscirev.2021.103895>

This Journal Article is posted at Research Online.

<https://ro.ecu.edu.au/ecuworks2022-2026/50>

---

## Authors

Muhammad Ali, Nilesh Kumar Jha, Nilanjan Pal, Alireza Keshavarz, Hussein Hoteit, and Mohammad Sarmadivaleh



## Recent advances in carbon dioxide geological storage, experimental procedures, influencing parameters, and future outlook



Muhammad Ali <sup>a,b,\*</sup>, Nilesh Kumar Jha <sup>c</sup>, Nilanjan Pal <sup>a</sup>, Alireza Keshavarz <sup>d</sup>, Hussein Hoteit <sup>a, \*\*</sup>, Mohammad Sarmadivaleh <sup>b</sup>

<sup>a</sup> Physical Science and Engineering Division, King Abdullah University of Science and Technology (KAUST), Thuwal 23955, Saudi Arabia

<sup>b</sup> Western Australia School of Mines, Minerals, Energy and Chemical Engineering, Curtin University, 26 Dick Perry Avenue, Kensington 6151, WA, Australia

<sup>c</sup> School of Petroleum Technology, Pandit Deendayal Petroleum University, Knowledge Corridor, Raisan, Gandhinagar 382007, Gujarat, India

<sup>d</sup> School of Engineering, Edith Cowan University, Joondalup 6027, WA, Australia

### ARTICLE INFO

#### Keywords:

CO<sub>2</sub> geo-storage  
Deep saline aquifers  
Wettability  
Organic acids  
Nanoparticles

### ABSTRACT

The oxidation of fossil fuels produces billions of tons of anthropogenic carbon dioxide (CO<sub>2</sub>) emissions from stationary and nonstationary sources per annum, contributing to global warming. The natural carbon cycle consumes a portion of CO<sub>2</sub> emissions from the atmosphere. In contrast, substantial CO<sub>2</sub> emissions accumulate, making it the largest contributor to greenhouse gas emissions and causing a rise in the planet's temperature. The Earth's temperature was estimated to be 1 °C higher in 2017 compared to the mid-twentieth century. A solution to this problem is CO<sub>2</sub> storage in underground formations, abundant throughout the world. Millions of tons of CO<sub>2</sub> are stored underground into geological formations annually, including deep saline aquifers. However, these geological formations have minute concentrations of organic material, significantly influencing the CO<sub>2</sub> containment security, fluid dynamics, and storage potential. Examining the wetting characteristics and influencing parameters of geological formations is pertinent to understanding the supercritical CO<sub>2</sub> behavior in rock/brine systems. Wettability is an important parameter governing the ability of injected CO<sub>2</sub> to displace formation water and determine the containment security and storage capacity. Previously, many studies have provided comprehensive overviews of CO<sub>2</sub>-wettability depending on various factors, such as pressure, temperature, salinity, formation type, surfactants, and chemicals. However, mineral surfaces in these wettability studies are chemically cleaned, and natural geological storage conditions are anoxic (containing organic molecules) where reductive conditions ensue. A severe gap exists in the literature to comprehend the effects of organic material for determining the CO<sub>2</sub> storage capacities and how this effect can be reversed using nanomaterial for increased CO<sub>2</sub> storage potential. Therefore, we conducted a thorough literature review to comprehend the recent advances in rock/CO<sub>2</sub>/brine and rock/oil/brine systems containing organic material in different geo-storage formations. We also present recent advances in anoxic rock/CO<sub>2</sub>/brine and rock/oil/brine systems that have employed nanomaterial for wettability reversal to be more water-wet. This comprehensive review is divided into four parts: 1) reviewing CO<sub>2</sub> emissions and geological systems, 2) recent advances in direct quantitative experimental procedures in anoxic rock/CO<sub>2</sub>/brine systems and effects of organic contaminations on experimental methodology and their controls, 3) effects of organics and nanomaterial in rock/CO<sub>2</sub>/brine and rock/oil/brine systems, and 4) the future outlook of this study.

### 1. Introduction

Carbon dioxide (CO<sub>2</sub>) storage in porous geological media is a

promising technique to mitigate anthropogenic CO<sub>2</sub> greenhouse gas emissions, which are proven contributors to global warming (Blunt et al., 1993; Bui et al., 2018; III, 2013), resulting in a considerable

\* Corresponding author at: Physical Science and Engineering Division, King Abdullah University of Science and Technology (KAUST), Thuwal 23955, Saudi Arabia (M. Ali).

\*\* Corresponding author at: Physical Science and Engineering Division, King Abdullah University of Science and Technology (KAUST), Thuwal 23955, Saudi Arabia (H. Hoteit).

E-mail addresses: [Muhammad.ali.2@kaust.edu.sa](mailto:Muhammad.ali.2@kaust.edu.sa), [Muhammad.ali7@postgrad.curtin.edu.au](mailto:Muhammad.ali7@postgrad.curtin.edu.au) (M. Ali), [Hussein.hoteit@kaust.edu.sa](mailto:Hussein.hoteit@kaust.edu.sa) (H. Hoteit).

increase in the temperature of the Earth (Davis et al., 2010; Karl et al., 2009; Solomon et al., 2009). Based on a combined report from the National Oceanic and Atmospheric Administration (NOAA) and National Aeronautics and Space Administration (NASA), the Earth's average temperature in the middle of the twentieth century rose by 0.99 °C (1.78 °F) in 2016 (NASA and NOAA, 2016). The rise in temperature at these elevated levels holds a direct risk to the planet's species, including humans. The CO<sub>2</sub> emissions around the globe have risen dramatically from 280 ppm in 1750 to 410 ppm in 2020 over the timescale of two centuries (Davis et al., 2016; Grim, 2017; Nordhaus, 2014). Many alternative approaches have been applied to diminish CO<sub>2</sub> emissions, including carbon-free solar panels, carbon-free wind power, geothermal energy, hydrogen production, and CO<sub>2</sub> geological storage (Chu and Majumdar, 2012; Gerber et al., 2013; Herrero et al., 2016; Lackner, 2003; Mohanty et al., 2021a; Schiermeier et al., 2008).

Moreover, CO<sub>2</sub> geological storage has proven to be an efficient method for reducing anthropogenic greenhouse gas emissions (Lackner, 2003; Matter and Kelemen, 2009; Matter et al., 2016). Through this method, million tons of CO<sub>2</sub> emissions are stored globally in geological storage formations (i.e., deep saline aquifers, basaltic rocks, coal bed methane formations, tight shale formations, and depleted hydrocarbon reservoirs; (Al-Rubaye et al., 2021; Ali et al., 2020a; Dahraj et al., 2016; Memon et al., 2021b; Page et al., 2020). The estimated worldwide CO<sub>2</sub> emissions in 2020 were 36.8 billion tons, which was reduced by 2.94 billion tons (8% reduction) compared to 2019. This reduction resulted from the slowdown of global industry caused by the 2019 coronavirus disease (COVID-19) pandemic, representing the sharpest reduction of CO<sub>2</sub> emissions since World War II (IEA, 2020). However, with business proceeding as usual, CO<sub>2</sub> emissions are expected to exceed 40 billion tons by 2030 (Newell et al., 2019), which is an alarming condition. Therefore, it is pertinent to capture and store a significant amount of CO<sub>2</sub> emissions in geological formations to mitigate the damage to the climate (Metz et al., 2005; Orr, 2009).

Carbon capture and storage (CCS) is primarily based on capturing CO<sub>2</sub> from anthropogenic sources (e.g., coal-based thermal power plants) and further transporting it to a location where it can be injected into the geological storage media (destined sinks, such as deep saline aquifers and depleted hydrocarbon reservoirs; (Ali, 2018; Holloway, 2007; Rackley, 2017). Globally, these formations are abundant, providing long-term safe storage for permanent CO<sub>2</sub> immobilization (Ali et al., 2020a; Ali et al., 2019a; Ali et al., 2019b; Ali et al., 2020c; Metz et al., 2005). Once CO<sub>2</sub> is injected into geological storage formations, it is rendered into a porous medium following various trapping mechanisms. These trapping mechanisms include structural or hydrodynamic trapping, which is a dominant trapping mechanism in caprocks and sedimentary formations (Al-Khdheeawi et al., 2020; Ali et al., 2020a; Arif et al., 2016a; Arif et al., 2016c; Iglauer et al., 2015a; Iglauer et al., 2015b). Residual or capillary trapping, which is a dominant trapping mechanism in sedimentary formations (Iglauer et al., 2011; Pentland et al., 2011a). Adsorption trapping, which is a dominant trapping mechanism in organic-rich shale and coal seams (Akhondzadeh et al., 2021; Arif et al., 2017c; Busch et al., 2008; Golding et al., 2011; Kaveh et al., 2012; Keshavarz et al., 2022). Dissolution in brine and mineral trapping, which are dominant trapping mechanisms in basaltic and sedimentary formations (Agartan et al., 2015; Al-Khdheeawi et al., 2017b; Golding et al., 2011; Iglauer, 2011; Matter et al., 2016).

In this context, the geo-storage rock property, which measures its adhering behavior in the surroundings of CO<sub>2</sub> with other aqueous fluids (e.g., brine in porous media), is widely known as wettability (Arif et al., 2020; Fauziah et al., 2019; Iglauer, 2017; Iglauer et al., 2015a; Iglauer et al., 2015b). It is a critical parameter directly or indirectly related to determining the structural and residual trapping potential. Previous studies have found that geo-storage formations that are less water-wet are prone to reduced CO<sub>2</sub> storage capacities (Al-Khdheeawi et al., 2017a; Arif et al., 2017b; Chaudhary et al., 2013; Iglauer et al., 2015a; Rahman et al., 2016). Moreover, CO<sub>2</sub> geo-storage formations (i.e., deep

saline aquifers and depleted hydrocarbon reservoirs) are typically weakly water-wet in the presence of CO<sub>2</sub>; hence, the porous media is filled with formation water (Al-Yaseri et al., 2016a, 2016b; Arif et al., 2016a; Sarmadivaleh et al., 2015). Wettability governs the ability of the injected CO<sub>2</sub> to displace the formation water and accumulate below the seal (caprock) due to the buoyancy factor, causing structural trapping (Iglauer, 2017; Iglauer et al., 2015a; Iglauer et al., 2015b). Once CO<sub>2</sub> injection is stopped, the previously displaced column of formation water exerts pressure back on the CO<sub>2</sub> flooded zone, resulting in CO<sub>2</sub> capillary trapping (Al-Menhal and Krevor, 2016; Iglauer et al., 2011; Krevor et al., 2015; Tokunaga and Wan, 2013). This phenomenon may take decades to occur (Iglauer et al., 2015b). However, a thorough review of the CO<sub>2</sub> wettability of geological storage media unveils various complexities of wettability mechanisms affecting CO<sub>2</sub> trapping in rock/brine systems (Arif et al., 2019a; Arif et al., 2020; Iglauer, 2017; Iglauer et al., 2015a; Iglauer et al., 2015b; Pentland et al., 2011a; Rahman et al., 2016).

Many approaches have been considered (e.g., capillary pressure curve, Amott–Harvey Index, US Bureau of Mines (USBM), core flood method, molecular dynamic simulation, micromodel experiments, x-ray microcomputed tomography, and nuclear magnetic resonance) to examine the behavior of wettability in supercritical rock/CO<sub>2</sub>/brine systems. However, all these approaches provide indirect wettability assessments. In contrast, a practical way to characterize the wettability of mineral/CO<sub>2</sub>/brine systems is to conduct contact angle (advancing and receding contact angles on a tilted plate) experiments that provide direct quantitative wettability assessment (Al-Anssari et al., 2016; Ali et al., 2020c; Arif et al., 2016c; Iglauer et al., 2015a; Iglauer et al., 2015b). Previously, many studies have presented comprehensive reviews of CO<sub>2</sub>-wettability depending on various factors, such as pressure, temperature, salinity, formation type, surfactants, and chemicals (Abbaszadeh et al., 2020; Abramov et al., 2019; Al-Yaseri et al., 2016a, 2016b; Arif et al., 2019a; Chiquet et al., 2007; Fauziah et al., 2019; Haghghi et al., 2020; Hansen et al., 2000; Iglauer et al., 2015a; Jha et al., 2019b).

However, mineral surfaces used in these wettability studies are chemically cleaned, which can only be obtained in strongly oxidizing conditions, such as an ultraviolet-ozone or oxygen plasma atmosphere (Iglauer et al., 2014; Love et al., 2005). Such an overview of the wettability information facilitates the quantitative analysis of the residual and structural trapping capacities in ideal geo-storage situations. In comparison, natural geological storage conditions are anoxic where reductive conditions ensue (Froelich et al., 1979; Townsend et al., 2003). These geo-storage formations contain dissolved organic material (Akob et al., 2015; Louk et al., 2017; Lundegard and Kharaka, 1994; Stalker et al., 2013), which is enough to significantly alter the wettability of the rock/CO<sub>2</sub>/brine system (Ali, 2018; Ali et al., 2021b; Gomari and Hamouda, 2006; Iglauer et al., 2020). Indeed, the adsorption of an organic (partial mono molecular) layer on the mineral surface is competent enough to influence the wettability of the reservoir rocks (sandstone, carbonate, and caprock; (Adamson and Gast, 1967; Gaines, 1966; Kuhn and Möbius, 1971; Kumar et al., 2020; Maboudian and Howe, 1997; Shafirin and Zisman, 1962; Zasadzinski et al., 1994)). Nevertheless, organic-acid contamination can diminish CO<sub>2</sub> containment security and geo-storage capacity. Thus, it is pertinent to augment threshold concentrations of organic acids and their influence on CO<sub>2</sub>-wettability of reservoir rock to ensure optimized conditions for CO<sub>2</sub> geo-storage (Al-Anssari et al., 2018b; Tosun, 2020).

Moreover, many approaches have been adopted to improve the wetting characteristics of oil-wet (due to organic acids) geo-storage formations, including nanoparticles (NPs) and surfactants (Al-Anssari et al., 2017b; Al-Anssari et al., 2017c; Al-Anssari et al., 2018b; Al-Anssari et al., 2016; Jha et al., 2018; Jha et al., 2019a; Jha et al., 2019b; Jha et al., 2017; Jha et al., 2020a; Nwiedee et al., 2016). However, nanoformulations have shown great potential for reversing the wettability to more water-wet conditions resulting in positive progress toward CO<sub>2</sub>

geo-storage trapping potential (various NPs are used depending on the formation type; [Ali et al., 2021a](#); [Ali et al., 2020c](#)). The viability of the CO<sub>2</sub> underground storage process can be improved with both concerns, such as optimization of wettability of reservoir rock through nanofluid interaction and augmenting the effects of organic acids on the geological storage potential. Thus, in the present work, the influence of various organic acids and their threshold concentrations (commonly dissolved in hydrocarbon traces) and NPs on various types of geo-storage formations (e.g., sandstone, carbonate, and caprock) are discussed to determine the CO<sub>2</sub> geo-storage potential. This information is valuable for reservoir modeling and assessing the feasibility of CO<sub>2</sub> geo-storage, including the thresholds of organic acids and nanofluids (NFs), so that better decisions can be made with lower uncertainty.

## 2. Background

This section reviews the importance of CO<sub>2</sub> storage and environmental problems caused by CO<sub>2</sub> emissions into the atmosphere. The possible options for underground CO<sub>2</sub> storage are discussed using CCS in geological storage formations. This section initially focuses on supercritical CO<sub>2</sub> behavior and its operational principles and storage options. Afterward, trapping mechanisms responsible for the long-term immobilization of CO<sub>2</sub> in underground formations are evaluated.

### 2.1. Climate protection and CO<sub>2</sub> storage

The oxidation of fossil fuels (i.e., crude oil, natural gas, and coal) is the main cause of anthropogenic CO<sub>2</sub> emissions, with an estimated 30 billion tons per year ([Administration, 2011](#)). The change in climate temperature to CO<sub>2</sub> emissions is defined by the term *carbon-climate response*, the ratio of cumulative CO<sub>2</sub> emissions to the increase in temperature. It is estimated that climate temperature rises by 1.0 °C to 2.1 °C per 3600 billion tons of CO<sub>2</sub> emissions ([Matthews et al., 2009](#)). However, the natural carbon cycle consumes a portion of CO<sub>2</sub> emissions from the atmosphere, including terrestrial vegetation and ocean beds. In comparison, substantial CO<sub>2</sub> emissions remain untouched.

In addition, CO<sub>2</sub> is recognized as the most significant contributor to greenhouse gas emissions ([Hussain et al., 2019](#)). The CO<sub>2</sub> storage is considered an environmentally friendly and operationally feasible practice to create a high-cost pathway for protecting the environment by controlling global warming to be below 2 °C by the end of the twenty-first century ([Huang et al., 2017](#); [Klutse et al., 2018](#); [Meinshausen et al., 2009](#)). Scholars believe that deforestation and the release of toxic chemicals in flora and fauna ended 2020 with unprecedented challenges (medical, economic, social, and environmental) that have caused global warming ([Chahal, 2020](#); [Toquero, 2020](#)).

However, it was found that critical factors, such as an increase in temperature due to CO<sub>2</sub> emissions, may have promoted viral problems ([Aguilar et al., 2015](#)). Additionally, researchers found that this climate issue has caused infection in living organisms, resulting in pathogen growth. Thus, investigators are working together to minimize the effect of CO<sub>2</sub> by storing it in underground formations to mitigate climate change via CCS ([Kalam et al., 2020](#)). Nevertheless, this technique is not implemented at an adequate scale owing to its commercial, economic, and technical challenges. Efforts are currently focused on balancing commercial, policy, environmental, and scientific priorities via CO<sub>2</sub> sequestration in underground reservoirs, including utilization for enhanced oil recovery (EOR; [Pal et al., 2022](#); [Ali et al., 2017](#); [Ali et al., 2015](#); [Ampomah et al., 2016](#)).

### 2.2. Underground CO<sub>2</sub> behavior

As an essential component of the atmosphere, the environmental concentration of CO<sub>2</sub> usually ranges up to 350 ppm ([Rosenberg, 1981](#)). Moreover, CO<sub>2</sub> is a nontoxic, colorless, odorless, and nonflammable gas ([Zhang et al., 2014](#)). [Fig. 1](#) illustrates the thermodynamic phase

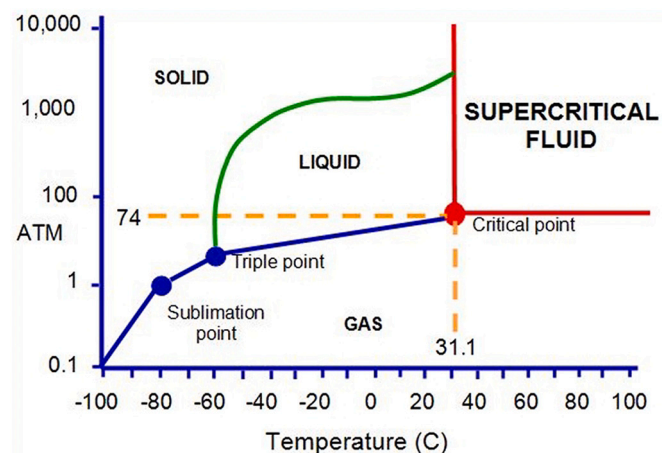


**Fig. 1.** Phase diagram of carbon dioxide (CO<sub>2</sub>); ATM: atmospheric pressure. Adapted from [King and Bott \(2012\)](#).

behavior of CO<sub>2</sub> as a function of temperature and pressure. In addition, CO<sub>2</sub> changes its state into a solid, liquid, gas, or supercritical state at specific temperatures and pressures. Typically, CO<sub>2</sub> maintains a gaseous state below 0.5 MPa and changes into a liquid state above this pressure. Further, CO<sub>2</sub> can coexist in three different states at 56.56 °C and 0.5 MPa ([Ali, 2018](#)), called the triple point. However, at 31.10 °C and 7.38 MPa, a critical point occurs in the CO<sub>2</sub> phase behavior ([Zheng et al., 2018](#)). Above these pressure and temperature conditions, CO<sub>2</sub> changes into a dense liquid state, commonly called the supercritical fluid state ([Ingrosso and Ruiz-López, 2017](#); [Rao et al., 2020](#)). Thus, supercritical CO<sub>2</sub> establishes the behavior of both gas and liquid phases ([Budisa and Schulze-Makuch, 2014](#)). Therefore, it is used in supercritical form for oil and gas industry applications (i.e., CO<sub>2</sub> geo-storage and EOR; [Al-Bayati et al., 2019](#); [Blunt et al., 1993](#); [Godec et al., 2013](#); [Qin et al., 2020a](#)).

### 2.3. Carbon capture and geo-storage

The CCS technique is considered the most attractive to capture CO<sub>2</sub> emissions (greenhouse gas) from stationary (power plants) and nonstationary (automobiles) sources and introduce emissions into geological rock for sustainable environmental growth and CO<sub>2</sub> storage durability ([Nunes et al., 2020](#); [Reddy et al., 2019](#); [Tang et al., 2020](#)). The CO<sub>2</sub> emissions from stationary sources are estimated at approximately 13 billion tons per year, and nonstationary sources are estimated at around 2.5 billion tons per year ([Administration, 2011](#)). The other CO<sub>2</sub> emissions are sourced from chemical processes to form cement and steel, but their portion of cumulative values is minor ([Boden et al., 1995](#)).

This process aims to protect the environment from anthropogenic CO<sub>2</sub> release, which is responsible for climate change ([Hinkle et al., 2017](#); [Nunes et al., 2020](#)), and global warming ([Hinkle et al., 2017](#); [Hussain et al., 2019](#)). [Fig. 2](#) presents a forecast by IEA to mitigate the CO<sub>2</sub> emissions into the environment ([dell'energia, 2010](#)).

#### 2.3.1. CCS operational principle

The CO<sub>2</sub> capture and storage process consists of four components: i) capturing, ii) compressing, iii) transporting, and iv) injecting CO<sub>2</sub> ([Porrostami et al., 2020](#); [Sahle et al., 2018](#)). Initially, CO<sub>2</sub> is captured from stationary CO<sub>2</sub> sources (e.g., power generation plants, chemical processing plants, coal-fired based plants, and several other nonstationary carbon emitters, such as automobiles). These sources are responsible for emitting billions of tons of CO<sub>2</sub> into the environment, half of which is used in natural carbon cycles and other mechanisms. About half of the remaining amount accumulates in the atmosphere, resulting in an annual growth of 2 ppm of CO<sub>2</sub> ([Lemonnier and Ainsworth, 2018](#)). The CO<sub>2</sub> capturing technique is typically based on

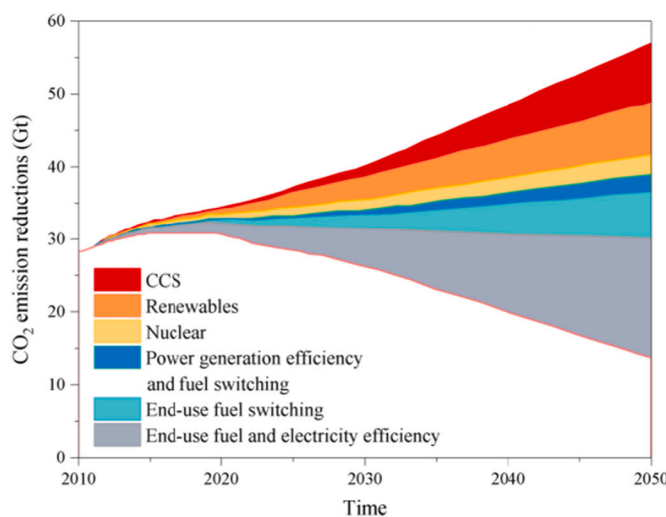


**Fig. 2.** IEA unveils technologies expected to be used to mitigate carbon dioxide ( $\text{CO}_2$ ) emissions.

Adapted from dell'energia (2010).

precombustion, oxyfuel combustion, and postcombustion capture (Porrostami et al., 2020; Sahle et al., 2018). Then,  $\text{CO}_2$  (captured) is compressed using high-pressure compressors (with an operational capacity of more than 10 MPa). They are transported to storage locations via pipelines and cargo ships. The transportation of  $\text{CO}_2$  is considered safe due to its nonflammable nature compared to natural gas (Xu et al., 2018). Finally, compressed  $\text{CO}_2$  is injected into underground formations at adequate injection parameters (e.g., rate of injection and injection pressure) for permanent immobilization. The overall flow process of CCS is illustrated in Fig. 3. These parameters depend on the petro-physical and physiochemical properties of the geological rock, which are determined through careful screening via pilot and simulated experimental trials ((Berger et al., 2019; Plaisant et al., 2017)).

### 2.3.2. Geological $\text{CO}_2$ storage media

Carbon capture and storage provide an appropriate option for removing  $\text{CO}_2$  from the atmosphere via permanent immobilization in underground geological storage formations (Ajayi et al., 2019). The primary  $\text{CO}_2$  sinks are categorized into various types of geological formations, such as depleted and existing hydrocarbon reservoirs for the EOR process (Blunt et al., 1993; Metz et al., 2005), deep saline aquifers (Ali et al., 2020a; Ali et al., 2019a; Ali et al., 2019b; Ji and Zhu, 2015), basaltic rocks (Al-Yaseri and Jha, 2021; Matter et al., 2007), coal seams (Awan et al., 2020; Su et al., 2019; Viete and Ranjith, 2006), and organic-rich shales (Arif et al., 2017c; Kang et al., 2011).

Deep saline aquifers and depleted and existing hydrocarbon reservoir rocks are considered major potential  $\text{CO}_2$  storage media. Both storage media have a vast capacity for storing  $\text{CO}_2$  and are abundantly present worldwide (Ali et al., 2020a; Blunt et al., 1993). The amount of  $\text{CO}_2$  that can be stored in both formations may comprise the majority of the total accumulated underground  $\text{CO}_2$  storage capacity.

These geological formations are typically sandstone or carbonate rocks (Al-Khdheeawi et al., 2021; Arif et al., 2019b). Carbonate rocks are considered highly permeable and provide ease for a large amount of  $\text{CO}_2$  injection compared to sandstone rocks with low permeability (Durand, 2005). The caprock, which provides a seal to trap buoyant  $\text{CO}_2$  to prevent capillary leakage, is typically shale (Ali et al., 2021d; Ali et al., 2022b; Arif et al., 2016a; Arif et al., 2016c).

Globally, the Intergovernmental Panel on Climate Change (IPCC) information reveals that hydrocarbon reservoirs can store between 675 and 900 billion tons of  $\text{CO}_2$ . In contrast, saline aquifers have between 1000 and 100,000 billion tons of estimated  $\text{CO}_2$  storage capacity

(Durand, 2005; Metz et al., 2005). In addition to these, basaltic rocks have recently displayed great potential for storing  $\text{CO}_2$  in mineralized form through a process developed by CarbFix (Abdullah et al., 2021; Gislason et al., 2018; Gislason et al., 2010). In this process,  $\text{CO}_2$  and water are injected together in basalt formations, inducing a rapid chemical reaction for storing  $\text{CO}_2$  in carbonized form (Gislason and Oelkers, 2014). An advantage of this process is that it does not require concentrated  $\text{CO}_2$  during injection, which can store up to 100 kg of  $\text{CO}_2$  in a cubic meter area of basalt (Gislason et al., 2018).

Further, organic-rich shales are another adequate candidate for permanent immobilization of  $\text{CO}_2$ . These geological formations are widely known as low porous, impermeable sedimentary rocks that can store a substantial amount of  $\text{CO}_2$  (Kang et al., 2011). In these formations,  $\text{CO}_2$  is permanently trapped in an adsorbed state within exceptionally distributed organic matter, such as kerogen. Finally, coal seam reservoirs have also been depicted as promising candidates for storing  $\text{CO}_2$  in deep and unminable coal seams for the application of enhanced coal bed methane recovery (Su et al., 2019; Viete and Ranjith, 2006). In coal seam reservoirs,  $\text{CO}_2$  can exist in three different scenarios: 1) a pore matrix filled with free  $\text{CO}_2$ , 2)  $\text{CO}_2$  dissolution in pore matrix liquid, and 3) gas trapped as adsorbate on a coal surface. However, not all porous media can be suited for permanent storage of  $\text{CO}_2$ , and some may lack the proper storage environment, caprock seal, or trapping mechanism. In that context, physical trapping of gas may prevail or create a free gas cap that may not provide long-term storage potential.

### 2.4. $\text{CO}_2$ trapping mechanisms in geological storage media

In carbon geo-storage locations, the pertinent hazard is the leakage of  $\text{CO}_2$  into the environment through artificial (e.g., wells) or natural (e.g., fractures and faults) methods. This outcome is due to the buoyant nature of  $\text{CO}_2$ , which flows in an upward direction in any given storage conditions (Iglauer et al., 2015b). However, keeping the nano- to micropore size specifications in the geological formations,  $\text{CO}_2$  is preferred to be injected in the supercritical phase. The supercritical state of  $\text{CO}_2$  may have the ability to vary its phase relative to the physicochemical conditions.

Various trapping mechanisms have been investigated to restrict the upward migration and leakage of  $\text{CO}_2$ . These trapping mechanisms include structural or hydrodynamic trapping in sandstone, carbonate, and caprock formations; (Ali et al., 2020a; Arif et al., 2016a; Arif et al., 2016c; Iglauer et al., 2015a; Iglauer et al., 2015b). Capillary or residual trapping in carbonate and sandstone formations (Ali et al., 2021b; Iglauer et al., 2011; Pentland et al., 2011a). Mineral and dissolution trapping in carbonate, sandstone, and basaltic formations (Agartan et al., 2015; Al-Khdheeawi et al., 2020; Al-Khdheeawi et al., 2017b; Gislason and Oelkers, 2014; Iglauer, 2011). Adsorption and diffusion trapping in organic-rich shales, clay interlayers, and coal seams (Busch et al., 2008; Golding et al., 2011; Kang et al., 2011; Kaveh et al., 2012; Su et al., 2019). It requires a thorough investigation of different physicochemical interactions and complexities to select feasible storage formation to ensure the containment security of the above trapping mechanisms to mitigate upward  $\text{CO}_2$  movement.

#### 2.4.1. Structural (hydrodynamic) trapping of $\text{CO}_2$

Structural (hydrodynamic) trapping can be referred to as the trapping of  $\text{CO}_2$  in the supercritical or liquid phase beneath the caprock (impermeable rock), which has greater capillary entry pressure than the buoyancy force of  $\text{CO}_2$  (Iglauer et al., 2015b). When  $\text{CO}_2$  gas is injected into the geological storage formation, it exerts pressure on the aqueous phase (brine), and free  $\text{CO}_2$  moves upward due to the density differences between the formation fluids in the reservoir. This upward movement of  $\text{CO}_2$  is credited to the balance between capillary forces (the force retaining  $\text{CO}_2$  in the pore matrix) and buoyancy forces (the force supporting upward movement; (Zhang and Song, 2014)). This upward movement of  $\text{CO}_2$  is not paralleled with gravity forces and displaces

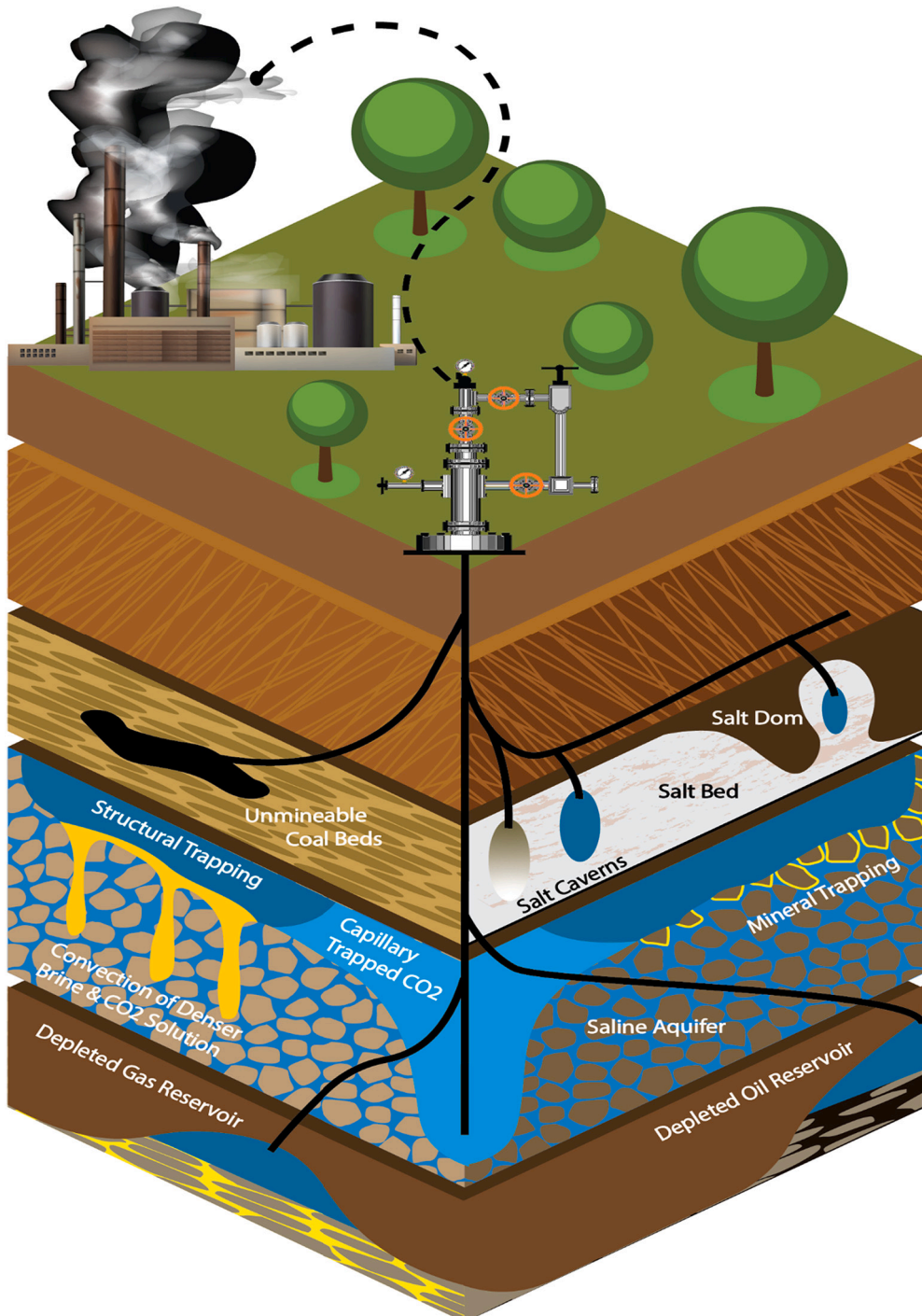


**Fig. 3.** Carbon capture and storage mechanisms.

density fluids lower than the formation fluid below the caprock (Mackay, 2013), trapping itself structurally. This physical trapping should have lateral and vertical seals (Iglauer et al., 2015a) and is also known as structural/stratigraphic or hydrodynamic trapping. This process is pivotal for any storage location to mitigate CO<sub>2</sub> leakage via caprock during the first decade while other trapping mechanisms come into effect (Bachu et al., 1994).

There are several types of stratigraphic and structural traps or a combination of these, which are used for physically trapping CO<sub>2</sub>. Traditional structural traps have anticline folds or sealed fault blocks, as illustrated in Fig. 4.

Stratigraphic or structural traps are commonly found in geological

formations containing oil and gas for millions of years. In such geological formations, the storage capacity is based on the pore-space volume. Hydrodynamic trapping systems are primarily found in sedimentary basins (saline aquifers) with significantly poor flow rates. The CO<sub>2</sub> injected into these deep structural traps can take millions of years to flow back to the surface (due to buoyancy forces) and discharge back into the atmosphere. For this trapping mechanism, the storage capacity of the rock is affected by the formation permeability and absolute porosity (Gunter et al., 2004). Nevertheless, the CO<sub>2</sub> storage by structural mechanism is primarily based on the sealing potential of the caprock, posing a significant challenge to select the appropriate location (Song and Zhang, 2013).

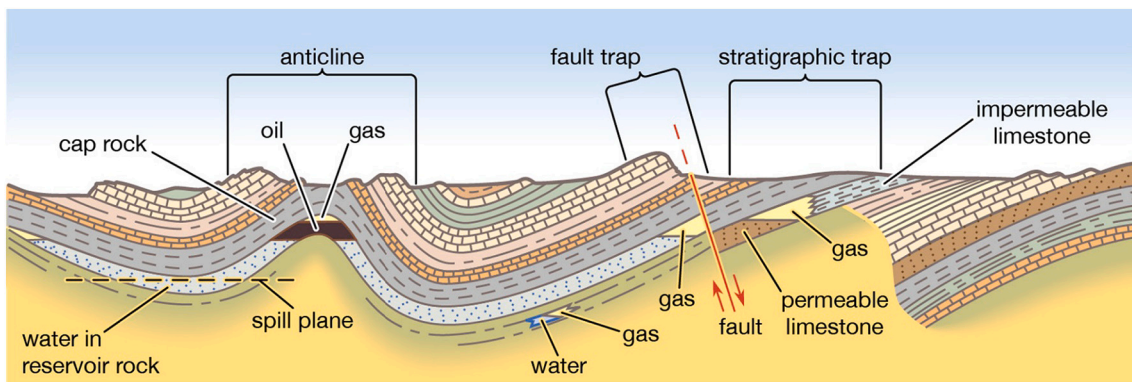


**Fig. 4.** Structural or stratigraphic trapping for storing CO<sub>2</sub>. Adapted from Britannica (2017).

#### 2.4.2. Residual trapping of CO<sub>2</sub>

During CO<sub>2</sub> injection in the geological formation, it exerts pressure and relocates the formation water (brine) in a cocurrent way. Once the injection of CO<sub>2</sub> is paused, the brine column exerts backpressure due to differences in the density of brine and CO<sub>2</sub>, and fluids start to flow in a counter-current way, resulting in the upward flow of CO<sub>2</sub> and downward flow of brine (Zhang et al., 2017). Consequently, the wetting fluid (brine) reinvades the pore matrix formerly occupied by CO<sub>2</sub> (Garcia et al., 2010). In such a mechanism, the brine pushes the CO<sub>2</sub>; thus, a considerable volume of CO<sub>2</sub> becomes trapped in small clusters of porous media, as depicted in Fig. 5. Hence, the separated CO<sub>2</sub> becomes trapped for permanent immobilization, known as residual trapping (Iglauer et al., 2019). Fundamentally, once the nonwetting phase is isolated in the narrow and small pore spaces, it remains captured by capillarity for permanent immobilization. The residual trapping mechanism thwarts a considerable journey of the CO<sub>2</sub> to the subsurface, diminishing the chance for upward CO<sub>2</sub> movement and coincidental delivery to the groundwater or atmosphere. This mechanism separates the moderately enormous continuous CO<sub>2</sub> (subcritical) plume into numerous little ganglia with bigger surface-region-to-volume proportions, encouraging long-term disintegration and precipitation response, which further improves the trapping security (Sun et al., 2020).

Various trials have contemplated exploring immiscible CO<sub>2</sub> (near critical) flow and residual catching conduct at the pore-to-core scale (e.g., μm to cm) inside porous geological storage media, such as 2D

micromodels (Gunning et al., 2020; Kazemifar et al., 2016), sandstones (Ali et al., 2020c; Rushton et al., 2020), sand packs (Chaturvedi and Sharma, 2020; Gauteplass et al., 2020), shales (Goodman et al., 2020; Li et al., 2020b), and carbonates (Snippe et al., 2020; Walpurguer et al., 2010). In addition, the simulations were conducted to determine the capillary trapping capacities in geological storage formations (Al-Khdheeawi et al., 2017a; Al-Khdheeawi et al., 2017). For this, two major approaches were used to investigate the residual trapping capacities (Krevor et al., 2012):

1. Measurement of the relative permeability data and
2. Measurement of the capillary pressure curves and gas saturation profile.

Through these measurements, residual trapping could significantly prevent the movement of CO<sub>2</sub>, resulting in a high volume of CO<sub>2</sub> being trapped in geological formations (Iglauer et al., 2015b; Ruprecht et al., 2014). Moreover, the heterogeneity, injection rate, and ratio of viscous forces to gravity forces significantly affect the immobilized fraction of CO<sub>2</sub>. Thus, increasing the ratio of viscous to gravity forces and the injection rate improves sweeping behavior, consequently providing a significant enhancement in CO<sub>2</sub> residual trapping capacities (Rezk et al., 2019).

#### 2.4.3. Solubility (dissolution) trapping of CO<sub>2</sub>

The dissolution of CO<sub>2</sub> in formation fluid is commonly referred to as solubility trapping (Li et al., 2020a). Importantly, after CO<sub>2</sub> injection, it travels upward to the interface between the caprock and reservoir and

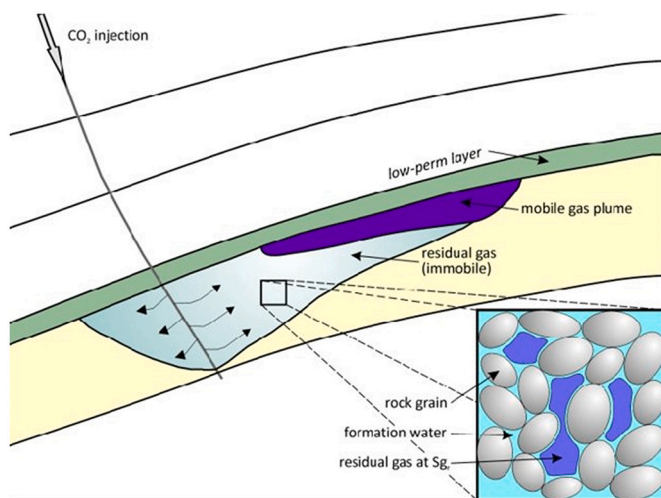


**Fig. 5.** Schematic of the entrapped carbon dioxide (CO<sub>2</sub>) in small clusters of porous media.

Adapted from Juanes et al. (2006).

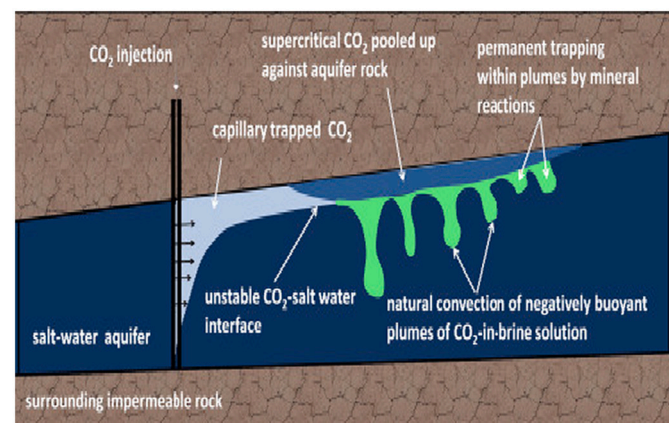


**Fig. 6.** Injected carbon dioxide (CO<sub>2</sub>) moves up to develop an interface and is laterally distributed under the cap rock (e.g., shale) as a distinct phase. Adapted from Riaz and Cinar (2014).

laterally distributes under the caprock as a distinct phase (Fig. 6). Afterward, the CO<sub>2</sub> contacts hydrocarbons (in depleted oil reservoirs) and the formation brine (in deep saline aquifers), resulting in mass transfer due to the CO<sub>2</sub> dissolution in the formation fluids. This process continues until the equilibrium state is achieved, improving the residual and structural trapping capacities (Ali, 2018; Gutiérrez and Lizaga, 2016). The CO<sub>2</sub> solubility in the formation fluid is based on the temperature, pressure, and salinity of the formation brine (Chang et al., 1996). The dissolution of CO<sub>2</sub> in formation water is driven by the molecular diffusion at the interface of the formation water and free gas phase. However, the CO<sub>2</sub> dissolution process is very lengthy due to the small molecular diffusion coefficient. It is believed that it may take thousands of years for CO<sub>2</sub> to dissolve in the formation water completely (Lindeberg and Wessel-Berg, 1997).

When CO<sub>2</sub> dissolves in formation brine, it slightly increases the density of the formation water. Previous studies have demonstrated that the CO<sub>2</sub> dissolution increases the density of the formation brine by 1% compared to normal formation water (Bachu and Adams, 2003; Kumar et al., 2004), making it heavier and triggering a downward flow of formation brine due to gravity forces. Such a process further improves the mixing of the formation brine and CO<sub>2</sub>, causing a diffusion mechanism at a rapid scale, resulting in the high dissolution of CO<sub>2</sub>. This process provides two main benefits: minimizing the upward movement of CO<sub>2</sub> and improving the storage capacity of the geological formation (Ajayi et al., 2019; Zhang et al., 2009; Zheng et al., 2020).

#### 2.4.4. Mineral trapping of CO<sub>2</sub>

When CO<sub>2</sub> is incorporated in a stable mineral phase via various reactions with different organic matters and minerals in geological storage formation, it is known as mineral trapping (Zhang and Song, 2014). On a geological time scale: the dissolution of CO<sub>2</sub> occurs in formation water, initiating different geochemical reactions and forming a weak carbonic acid (Eqs. (1) to (2)):



Afterward, an increase in acidity dissolves the primary host rock minerals, forming dissolved cations with bicarbonate ions (Eq. (3)):



Thereafter, dissolved bicarbonate ions react with divalent cations (primarily Ca<sup>2+</sup>, Fe<sup>2+</sup>, and Mg<sup>2+</sup>), forming precipitation of carbonaceous minerals (Ding et al., 2018); Eqs. (4) to (6)):



The reaction sequence (from Eqs. (1) to (6)) is dependent on pH, hydrogeology, mineralogy, and the formation structure (Liu and Maroto-Valer, 2011; Rochelle et al., 2004). For instance, the production of H<sub>2</sub>CO<sub>3</sub> controls at a lower pH (~4 pKA), the production of HCO<sub>3</sub><sup>-</sup> controls at a mid pH (~6 pKA), and the production of CO<sub>3</sub><sup>2-</sup> controls at a higher pH (~9 pKA) (Druckenmiller et al., 2006; Stumm and Morgan, 1996). The CO<sub>2</sub> geological formations, such as deep saline aquifers or depleted hydrocarbon reservoirs, are generally acidic, with pH values ranging from 2 to 6 (Soong et al., 2006). The formation of mineral carbonates cannot occur in an acidic environment, and it requires a higher pH range (e.g., ~9 pKA; (Soong et al., 2004)). This process contains CO<sub>2</sub> in the form of carbonate minerals and aids other trapping mechanisms for the permanent immobilization of CO<sub>2</sub>. Therefore, it is better suited for CO<sub>2</sub> storage to select geological formations that contain divalent cations (Ca<sup>2+</sup>, Fe<sup>2+</sup>, and Mg<sup>2+</sup>) for mineral trapping purposes.

Pearce et al. (2019) examined drilled core samples and found variations in the mineralogy of the rock samples exposed to CO<sub>2</sub> (Pearce et al., 2019). Natural chlorite and plagioclase formed ankerite and siderite after interacting with CO<sub>2</sub> (Fig. 7a and b). This process is well-matched with the natural system, which is highly saturated with CO<sub>2</sub>. The mineral trapping and alteration in the porous media may provide an adequate environment for CO<sub>2</sub> storage (Fig. 7b, c, and d).

Table 1 provides minerals usually engaged in mineral trapping responses and includes the subatomic weight, specific gravity limit, and possible load of CO<sub>2</sub> fixed by a response with 1 m<sup>3</sup> to 1 kg of mineral. The second section of the table records the related response items.

Whether these particles stay in the solution for a more extended term or add to mineral trapping responses, they highly rely on the brine water pH and ionic loading, as demonstrated schematically in Fig. 8.

### 3. Experimental procedures

Underground CO<sub>2</sub> storage has been highly influenced by the wetting characteristics of rock-forming minerals, which govern the capability of CO<sub>2</sub> to dispense through the geo-storage formation. It also governs CO<sub>2</sub> injection flow rates, fluid flow dynamics across the formation, containment security, and the project certainty of the underground CO<sub>2</sub> (Akhondzadeh et al., 2020; Iglauer, 2017; Iglauer et al., 2015a; Iglauer et al., 2015b). The wetting characteristics of the geo-storage formations are directly responsible for determining the structural and residual trapping capacities of CO<sub>2</sub> (Al-Khdheeawi et al., 2017a; Al-Menhal and Krevor, 2016; Iglauer et al., 2015a; Iglauer et al., 2015b; Rahman et al., 2016), and wettability has an indirect effect on dissolution and mineral trapping capacities (Agartan et al., 2015; Al-Khdheeawi et al., 2017a; Al-Khdheeawi et al., 2017b; Al-Khdheeawi et al., 2017; Iglauer, 2011). Wettability is a pertinent parameter that is very intricate, and all characteristics should be contemplated at realistic underground conditions to augment this influence. Therefore, the application of wettability in the rock/fluid system and its experimental techniques are discussed to emphasize the importance of advancing and receding contact angles and their relationship with structural and residual trapping capacities.

#### 3.1. Application of rock wettability for CO<sub>2</sub> geo-storage formation

The CO<sub>2</sub> geological storage formations comprise a three-phase system containing nonaqueous and aqueous-phase liquid denoted by hydrophobic and hydrophilic terminology, respectively. This terminology is used for the aqueous phase to cover the deep pore matrix (hydrophilic) and for the nonaqueous phase that does not cover it (hydrophobic; (Ali et al., 2020a; Ali et al., 2021a; Ali et al., 2020c)). Wettability has a direct and substantial influence on key parameters, such as interfacial areas of fluids and morphology (Al-Yaseri et al., 2021a; Iglauer et al., 2012a; Pentland et al., 2012), relative permeability (McCaffery and Bennion, 1974; Morrow, 1990), residual nonaqueous phase saturation (Chaudhary et al., 2013; Jadhunandan and Morrow, 1995; Morrow, 1990; Pentland et al., 2011b), and the aqueous phase saturation ( $S_w$ ) and capillary pressure ( $P_c$ ) relationship ( $S_w[P_c]$ ). This relationship controls the ability of the reservoir fluids to distribute with the buoyancy-capillary equilibrium force statically (Donaldson and Alam, 2013; Jackson et al., 2005). Therefore, the wettability must be investigated in detail despite the greater physiochemical complications. In CCS applications, wettability is directly responsible for the CO<sub>2</sub> distribution across the geo-storage formation and governs the containment security, residual and structural trapping potential, fluid dynamics, and injection rates. It is also indirectly responsible for the mineral and dissolution trapping potential (via liquid-mineral and liquid-liquid interfaces). Thus, wettability should be investigated sufficiently for accurate storage potential estimations and risk assessment.

Wettability can be defined as a fundamental surface property affected by dynamic intermolecular interactions and controls the capability and relative attraction of one fluid on the solid surface in the

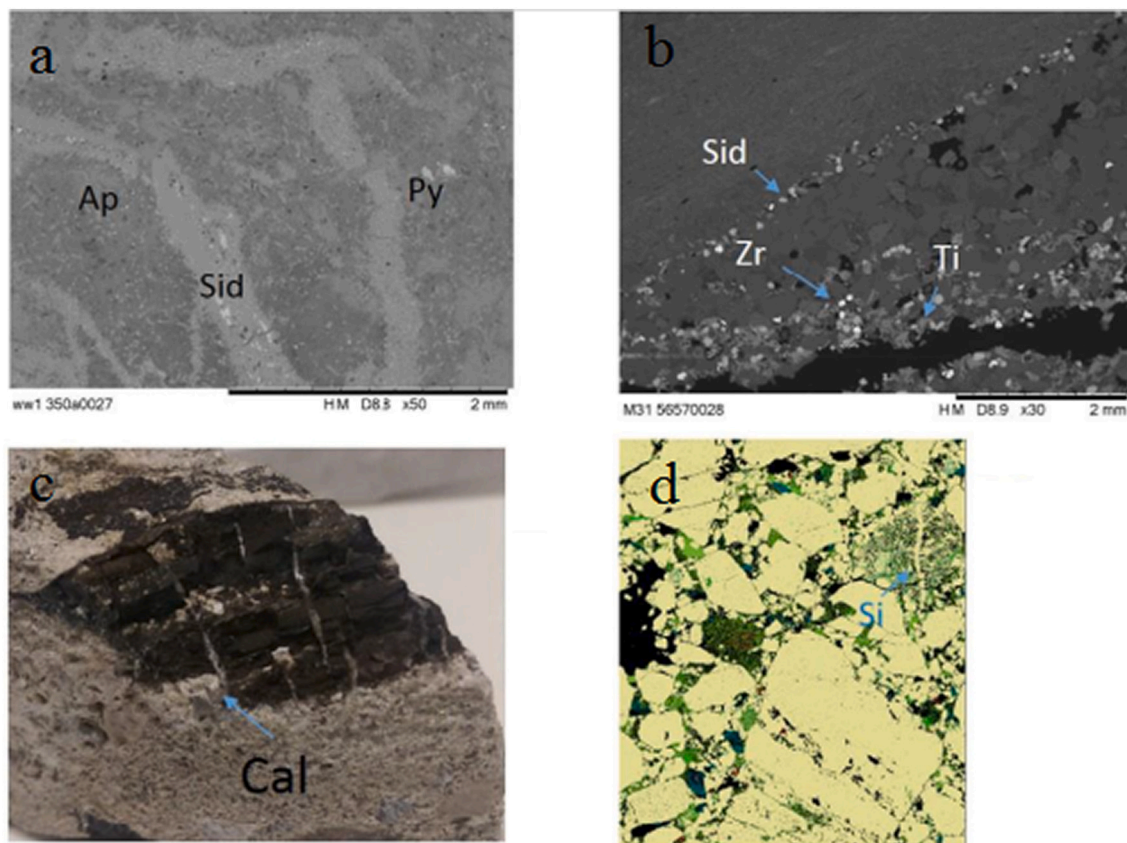


**Fig. 7.** Natural fractures and mineral trapping in core well samples (Wandon), (a) seal rock and (b, c, and d) transition zone; Abbreviations: Apatite: Ap, Cement Titanium oxide: Ti, Calcite: Cal, Silica cement: Si, and Siderite: Sid.

Adapted from Pearce et al. (2019).

**Table 1**  
Mineral trapping and its reaction products.

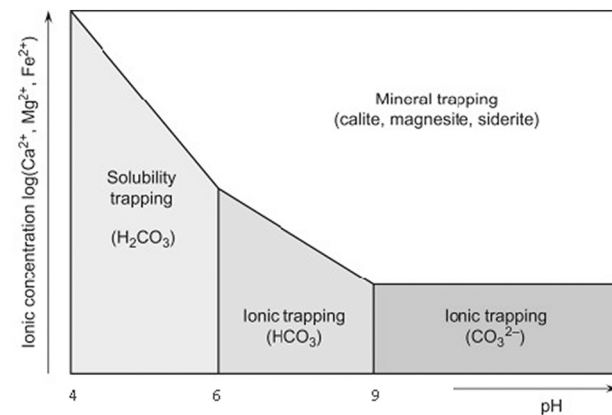
Fixed CO <sub>2</sub> potential					
Reactants minerals	Formula	Sp. gravity	Mol. weight	Kg/m <sup>3</sup> mineral	Kg/Kg mineral
Wollastonite	CaSiO <sub>3</sub>	2.9–3.1	116.2	1140	0.38
Diopside	MgCaSi <sub>2</sub> O <sub>6</sub>	3.3–3.6	216.6	1400	0.41
Fayalite	Fe <sub>2</sub> SiO <sub>4</sub>	4.39	203.8	1890	0.43
Forsterite	Mg <sub>2</sub> SiO <sub>4</sub>	3.2–3.3	140.7	2020	0.62

Products of reaction					
Anhydrite	CaSO <sub>4</sub>	Chalcedony	SiO <sub>2</sub>		
Siderite	FeCO <sub>3</sub>	Alunite	KAl <sub>3</sub> (OH) <sub>6</sub> (SO <sub>4</sub> ) <sub>2</sub>		
Magnesite	MgCO <sub>3</sub>	Ankerite	CaMg <sub>0.3</sub> Fe <sub>0.7</sub> (CO <sub>3</sub> ) <sub>2</sub>		
Calcite	CaCO <sub>3</sub>	Dawsonite	NaAlCO <sub>3</sub> (OH) <sub>2</sub>		

Adapted from Rackley (2017).

presence of another fluid (De, 1985). When CO<sub>2</sub> is injected in geological storage formations, three immiscible phases, the aqueous phase (brine), nonaqueous phase (supercritical CO<sub>2</sub> – ScCO<sub>2</sub>), and rock formation, intermingle. In this scenario, the influence of three interfacial force tensions ( $\gamma$ ) is considered: the interfacial force field between liquid and fluid (in this case, brine and ScCO<sub>2</sub>) and the tension of each liquid or fluid and the rock surface (e.g., calcite represents a clean carbonate geological formation). In this example, three different forces are induced by three interfacial tensions (IFTs) acting in separate directions (Fig. 9). These interfacial forces are acting at the same time (assuming the absence of all other external forces, such as buoyancy and viscous forces), resulting from the final force that governs the precise fluid



**Fig. 8.** Dependencies of geochemical trapping on pH.  
Adapted from Rackley (2017).

formation on the rock surface, calculated by the contact angle ( $\theta$ ), as depicted in Fig. 9. The value of the contact angle ( $\theta$ ) can be determined between 0° and 180° and is wholly derived due to the intermolecular force balance, as expressed by Young's equation (7):

$$\cos\theta = \gamma_{SL} - \gamma_{SF}/\gamma_{LF}, \quad (7)$$

where  $\theta$  is the contact angle derived due to the intermolecular force balance,  $\gamma$  is the IFT force for the solid-liquid (SL; mineral-brine), solid-fluid (SF; mineral-ScCO<sub>2</sub>), and liquid-fluid (LF; brine-ScCO<sub>2</sub>) interfaces, respectively. Previous studies have found that  $\gamma_{LF}$  is experimentally derived, which is the function of the liquid-fluid intermolecular

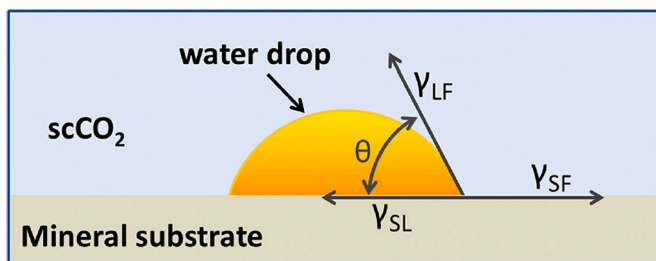


**Fig. 9.** Three interfacial force tensions acting on a water drop on a rock surface in the presence of supercritical CO<sub>2</sub>.  
Adapted from Iglauer et al. (2015b).

interactions influenced by geo-storage thermo-physical conditions (e.g., temperature and pressure; (Al-Anssari et al., 2018a; Arif et al., 2016a; Iglauer et al., 2012b; Sarmadivaleh et al., 2015). However, the other two IFTs ( $\gamma_{SL}$  and  $\gamma_{SF}$ ) cannot be measured (Butt et al., 2006). They can only be estimated via theoretical and indirect calculations, such as semi-empirical equations and molecular dynamic simulation (Good and Girifalco, 1960). Therefore, the contact angle ( $\theta$ ) from Eq. (7) cannot be calculated but requires experimental investigation.

Furthermore, this section also discusses wettability (contact angle,  $\theta$ ) in detail and how it behaves in various thermo-physical conditions, liquid-fluid systems, and geo-storage formations. In the CCS context, wettability is directly related to structural and residual trapping capacities of geo-storage formation, which depends on the idea that the upward movement of CO<sub>2</sub> can be retained via the sufficient strength of capillary forces in a subsurface formation (Arif et al., 2019b). These capillary forces are dependent on the contact angle ( $\theta$ ) between the rock-brine CO<sub>2</sub> and the nonwetting (CO<sub>2</sub>) and wetting (formation brine) phase IFT ( $\gamma$ ), as presented in the equations below:

$$P_c = P_{CO_2} - P_{water}, \quad (8)$$

$$P_c = \frac{2\gamma \cos(\theta)}{R}, \quad (9)$$

where  $P_c$  denotes the capillary pressure,  $P_{CO_2}$  is the rock nonwetting phase pressure,  $P_{water}$  represents the rock wetting phase pressure,  $\gamma$  indicates the interfacial forces between water and CO<sub>2</sub>,  $R$  denotes the radius of the largest pore throat, and  $\theta$  represents the contact angle.

Once CO<sub>2</sub> is injected into the geo-storage formation, it displaces the wetting phase (formation water), which is related to the receding contact angle (this assumption is based on the ideal pore matrix for determining the first approximation, however, in real situations, pore matrix also plays a crucial role; (Broseta et al., 2012; Iglauer, 2018; Iglauer et al., 2015a)). In CO<sub>2</sub>-wet systems, when the receding contact angle ( $\theta_r$ ) is more than 90° (e.g., in Eq. (9), where  $\cos(\theta_r) = 0$ ), capillary leakage can occur due to the upward suction force in the caprock, causing a significant decrease in structural trapping. Afterward, once CO<sub>2</sub> injection is stopped, the wetting phase (formation brine) reinvades the pore matrix, which was previously occupied by clusters of CO<sub>2</sub>. This phenomenon is related to the advancing contact angle ( $\theta_a$ ), where primary drainage is not affected by wettability if ( $\theta_a$ ) is less than 50° (Chiquet et al., 2007; Rahman et al., 2016). This process is crucial for providing containment security via additional trapping support called residual trapping.

Iglauer et al. (2015b) defined the classification of wettability in geo-storage formations, where the rock is highly water-wet when the contact angle is smaller than 50°, poorly water-wet from 50° to 70°, and intermediate water-wet from 70° to 110° (Iglauer et al., 2015b). The wettability system transforms into poorly CO<sub>2</sub>-wet when the contact angle is from 110° to 130°, highly CO<sub>2</sub>-wet when the contact angle ranges from 130° to 180°, and completely nonwetting when the contact angle is 180°. These classifications are physically proven on rock-brine-

mineral surfaces (Iglauer, 2017; Sarmadivaleh et al., 2015).

### 3.2. Wettability determination using various approaches

Wettability is a pertinent factor in CO<sub>2</sub> geo-storage calculations. Various direct (quantitative) and indirect (qualitative) methods have evolved to classify wettability in a given rock-fluid system at various physio-thermal geo-storage conditions. For instance, relative permeability and capillary pressure curve determination by typical core flooding via material balance method (Haghghi et al., 2020), nuclear magnetic resonance imaging via wettability shift method (Looyestijn, 2008), X-ray computed tomography (MacAllister et al., 1993), and micro-computed tomography (μCT) imaging via dynamic saturation profile method; (Idowu et al., 2015), and USBM (Donaldson et al., 1969) and Amott-Harvey index (Anderson, 1986) via primary imbibition method can provide wettability assessment at the macroscopic and microscopic level.

In addition, 2D micromodels represent geo-storage formations to determine the wetting characteristics at the pore scale in brine-CO<sub>2</sub> systems at high-pressure and high-temperature conditions (Chalbaud et al., 2009). Molecular dynamic simulations are also used for CO<sub>2</sub>-water interfaces at various thermo-physical geo-storage conditions (Iglauer et al., 2012b). However, all of the above methods only provide an indirect qualitative assessment of wettability, and the contact angle method is the only method used to determine direct quantitative wettability assessment (Ali, 2018; Lander et al., 1993).

However, the efficiency of this method depends on proper cleaning procedures for rock minerals and experimental apparatus. Therefore, in the sections below, we systematically review recent advances in methods for contact angle systems and explain the effect of organic contamination on the experimental apparatus and rock surfaces. The proper cleaning methodology is also suggested for quantifying wettability studies.

#### 3.2.1. Wettability determination using direct quantitative approaches

Direct quantitative assessment of wettability (via the contact angle) in a given rock-fluid system is widely accepted (Al-Anssari et al., 2016; Ali et al., 2020c; Arif et al., 2016c; Iglauer et al., 2015a; Iglauer et al., 2015b). This method involves several configurations for measuring the contact angle; however, the gas bubble (captive bubble), pendant drop (sessile drop), and tilted-plate (advancing and receding contact angles) methods are primarily used in the oil and gas industry (Sarmadivaleh et al., 2015). An IFT cell (goniometric cell) is used in these methods, comprising stainless steel or Hastelloy material (for CO<sub>2</sub>).

This IFT cell can sustain a high temperature (up to 433 K) and high pressure (up to 70 MPa) and contains a sample holder. The IFT cell is connected with two high-precision syringe pumps supplying gas and fluid, the heating mechanism (for providing high temperature), and a mixing reactor (providing equilibrium between gas and liquid). This mechanism offers a direct quantitative measurement of the wettability on a rock substrate (Al-Anssari et al., 2016; Ali et al., 2019b; Ali et al., 2021b). However, these methods are only used for rock-mineral substrates and pure fluids (Al-Yaseri et al., 2015; Arif et al., 2016a). Furthermore, this mechanism can conduct the contact angle measurement at a wide variety of geo-storage conditions that provide a wettability investigation as a function of salinity, surface roughness, aging, temperature, and pressure.

In the pendant drop (sessile drop) method for a typical CO<sub>2</sub>-brine-mineral system, the high-precision syringe pumps are initially filled with CO<sub>2</sub> and brine (salinity can differ based on reservoir condition) at geo-storage conditions (syringe pumps in this system control the flow rate and pressure; Teledyne ISCO, Model D-500, pressure accuracy = 0.1%). The temperature of high-precision syringe pumps is controlled by a heating bath (model 900F, from Julabo). High-precision syringe pumps inject CO<sub>2</sub> and brine at high pressure and high temperature (HPHT) conditions in a mixing reactor (Parr mixing reactor, volume 500 mL),

which already contains mineral substrates. These fluids are mixed at 1200 rpm for 1 h with mineral substrates at HPHT until a live brine is formed and equilibrium is achieved. This equilibrium is essential for avoiding the mass transfer of brine and CO<sub>2</sub> during contact angle measurements on mineral substrates (El-Maghraby et al., 2012). Afterward, live brine is transferred to a high-precision syringe pump, and a clean mineral or polished rock surface is placed on the sample holder, followed by tightly closing the IFT cell. Then, CO<sub>2</sub> is gradually introduced via a high-precision syringe pump in an IFT cell until HPHT reservoir conditions are met. The temperature of the IFT cell is controlled via a different mechanism, such as heating tape and a controller (Model No. HTC101-002 from Omega Company). Once the IFT cell is full of CO<sub>2</sub>, a droplet (mean droplet size:  $4.5 \pm 0.6 \mu\text{L}$ ) of live brine is introduced from another high-precision syringe pump on the mineral substrate surrounded by CO<sub>2</sub> at HPHT conditions. Newly developed contact angle systems were equipped with a high-performance video camera (Fujinon CCTV lens: HF35HA-1B; 1:1.6/35 mm, frame rate = 71 fps; pixel size = 7.4  $\mu\text{m}$ ; Basler scA 640–70 fm) and contact angle interpreting software (e.g., ImageJ) to video-record the complete procedure and interpret the images for measuring the contact angle, respectively. A schematic of the HPHT contact angle system is depicted in Fig. 10.

However, other contact angle measurement configurations are almost the same, with slight variations in the method. For example, in the gas bubble (captive bubble) method, a CO<sub>2</sub> bubble is dispensed from below the mineral substrate instead of a liquid drop, whereas the IFT cell is filled with live brine in geo-storage conditions (HPHT). Similarly, in the tilted-plate contact angle method, the IFT cell contains a sample holder in a tilted position. A droplet of live brine forms two angles (advancing and receding) at the leading and trailing corners of the droplet (Lander et al., 1993). Typically, receding contact angles are less than advancing contact angles, and the difference between these angles is due to wettability hysteresis, which ranges from 5° to 20°. Wettability hysteresis is a function of variables, such as adsorption/absorption of

molecules on reactive surfaces, structural or chemical heterogeneity, and surface roughness (Carré et al., 1996; Eral and Oh, 2013; Neumann and Good, 1972), and is depicted in Fig. 11.

### 3.3. Effect of organic contamination on experimental methodology

Concerns regarding the cleaning procedure of rock representative substrates for wettability measurements have historically been raised (Bikkina, 2011; Bikkina, 2012; Iglauer et al., 2014; Mahadevan, 2012; Saraji et al., 2014). These debates are of high interest in experimental results and surface chemistry in general. Contamination significantly affects the wettability measurement results regardless of the applied method. Fig. 12 exhibits significant variation and uncertainties in the water contact angle ( $\theta = \sim 7^\circ$  to  $92^\circ$ ) in the experimental CO<sub>2</sub>–water–silica contact angle (Iglauer et al., 2014). These were tested for various temperatures ( $\sim 296$  K to  $396$  K), pressures ( $\sim 0$  to  $40$  MPa), and salinities ( $\sim 0$  to  $7$  M of NaCl), which do not reveal any specific trend lines or obvious explanation for the variation (Iglauer et al., 2014). The reason for this large variation and high uncertainty was apparatus and surface contamination due to discrepancies in the cleaning procedures

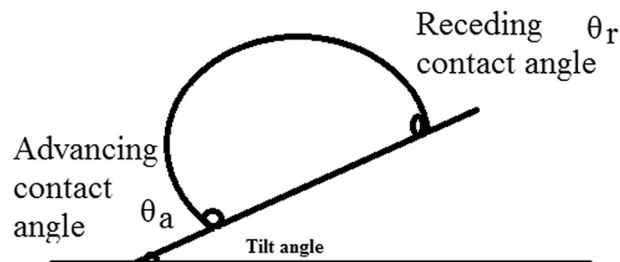


Fig. 11. Wettability hysteresis.

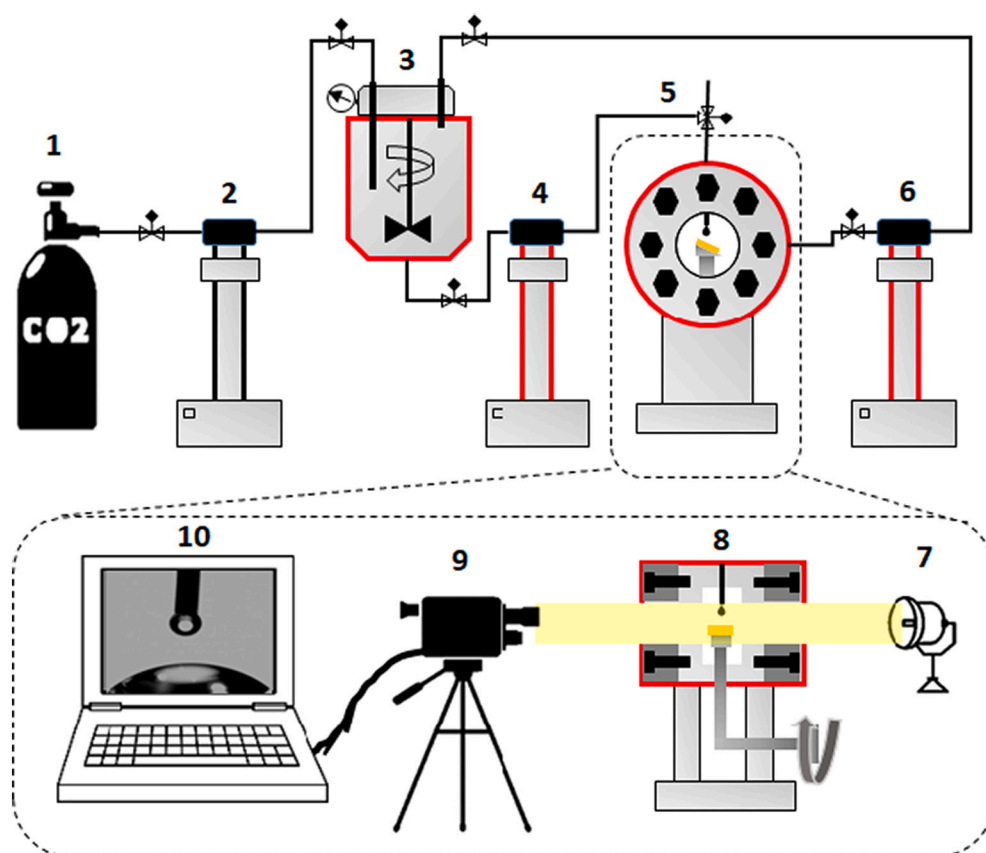
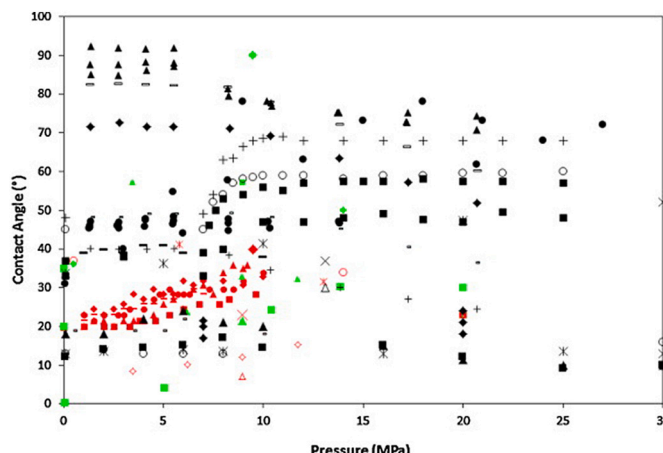


Fig. 10. Schematic of the high-pressure, high-temperature contact angle system: (1) carbon dioxide (CO<sub>2</sub>) supply, (2) high-precision syringe pump for CO<sub>2</sub>, (3) mixing reactor, (4) high-precision syringe pump for brine, (5) interfacial tension (IFT) cell with sample holder, front view, (6) high-precision syringe pump for back pressure, (7) brightness from light, (8) IFT cell with sample holder, side view, (9) video camera for recording the procedure, and (10) contact angle interpretation software.  
Adapted from Ali et al. (2021a).



**Fig. 12.** Reported experimental carbon dioxide ( $\text{CO}_2$ ) aqueous-phase sandstone representative contact angles. Sessile  $\theta$ : open or closed black; advancing  $\theta$ : green; receding  $\theta$ : red. (For interpretation of the references to colour in this figure legend, the reader is referred to the web version of this article.) Adapted from Iglauer et al. (2014).

(Iglauer et al., 2014). For instance, some of the main causes of organic contamination are using a paper towel for water adsorption from the surface of the substrate/glassware and the metallic and nonmetallic parts of the inner chamber of the IFT cell and the subsequent adsorption of organic molecules from the air or fingers of the researchers (Iglauer et al., 2014). Equipment and apparatus reuse for different experiments with residual organic contaminants from inconsistent prior cleaning can also significantly contribute to such contamination (Iglauer et al., 2014).

Some natural rock substrates from the subsurface can leave residual organic contaminants due to the dissolution of associated organic matter during interaction with other fluids during measurements. The potential sources of post-depositional organic matter contamination (also called modern organic contaminants) are attributed to subsurface biological activity, groundwater penetration, sampling, and storage (Brocks, 2011; Brocks et al., 2003a; Brocks et al., 2003b; Gerard et al., 2009). These contamination issues have also been reported in biomarker studies (i.e., bitumen) of Precambrian rocks (Brocks, 2011; Brocks et al., 2008; Illing et al., 2014). In contrast, the insoluble macromolecular organic matter (i.e., kerogen) is considered unaffected by modern organic contamination (Brocks et al., 2003b; Marshall et al., 2007). Different solvents (e.g., dichloromethane-ethanol mixtures, acetone, and toluene) are frequently used to remove modern organic contaminants from experimental apparatus and rock samples, assuming that the modern organic contaminants did not percolate into the porous space of the sample (Beaumont and Robert, 1999; Derenne et al., 2008; Wright et al., 1997). Moreover, organic solvents, along with trace impurities, can contaminate samples, contributing to errors in the total organic carbon (TOC) values (Arif et al., 2017c; Pan et al., 2020; Wright et al., 1997). The TOC values affect the wettability data so that an increase in TOC indicates an increase in  $\text{CO}_2$  wetting (Arif et al., 2017c; Pan et al., 2020). This error in wetting values can provide a misleading evaluation of the containment security and  $\text{CO}_2$  storage feasibility. Therefore, various cleaning procedures were evaluated and proposed to obtain accurate measurements (Al-Anssari et al., 2018b; Al-Yaseri et al., 2021b; Ali, 2021; Ali et al., 2020a; Ali et al., 2021c; Arif et al., 2016c; Arif et al., 2021; Sarmadivaleh et al., 2015). The following section discusses the prevalent cleaning procedures in the literature and their implications in wettability evaluation.

### 3.3.1. Controls of organic contamination on substrates and experimental apparatus

Various cleaning methods were applied (Table 2); however, they were inconsistent, which affects the measured data, as discussed in the

**Table 2**

Cleaning procedures for sandstone samples for contact angle measurements.

Reported cleaning process for sandstone representative substrates	References
First clean substrates with DI water to remove surface organic contamination, blow with ultra-pure nitrogen to clear the water film using air plasma to clean adsorbed organic contamination, ionize substrates in pH 4 calibrated 2 wt% NaCl brine, clean substrates again with ultra-pure nitrogen to remove excessive brine film, age the sample with wettability modifiers (e.g., organic acids), and dry the substrates at 343 K for 1 h	(Ali et al., 2019b)
Soak in acetone for 3 h, heat to 393 K for 2 h, sonicate in DI water, and blow-dry with nitrogen	(Wang et al., 2013a)
Rinse with 2-propanol; 30 min of sonication in sulfuric acid containing 10 wt% Nochromix, soak in the same solution overnight, wash with water and boil in DI water for 2 h, store in DI water after rinsing with it, dry the substrate by adsorption of bulk water with a filter paper, and blow-dry with ultra-pure nitrogen before the test	(Wang et al., 2013b)
Wash with Deconex cleaning detergent solution, 20 min of sonication in the same solution, DI water wash, rinse with 6 wt% nitric acid solution of the heated sample (303 K), DI water wash	(Farokhpoor et al., 2013)
Ethanol	(Jung and Wan, 2012)
Substrate cleaning using the standard silica wafer cleaning technique: submersion in a solution (five parts DI water, one part 27 wt% ammonium hydroxide, and one part hydrogen peroxide) for 10 mins at 343 K; DI water, chloroform, 2-propanol, and ethanol rinse; ultraviolet-ozone treatment for 30 mins	(Grate et al., 2012)
30 min of sonication in acetone and 30 min sonication in ultra-pure water	(Bikkina, 2011)
For first use: clean in toluene, methanol, acetone, 2-propanol; for subsequent use: rinse in methanol, DI water, and ultrasonication (in a beaker)	(Mills et al., 2011)
30 mins of ultra-sonic agitation in tension-active solution, rinse with a 10 wt% nitric acid solution, and DI water wash	(Chiquet et al., 2007)
Wash with acetone and dry in an oven	(Wesch et al., 1997)

previous section. Iglauer et al. (2014) conducted several contact angle measurements to measure the effect of the pressure at isothermal conditions (323 K) by dispensing the aqueous phase with (i) deionized (DI) water, (ii) 0.342 M of NaCl brine, and (iii) 1 M of  $\text{NaHCO}_3$  brine on  $\alpha$ -quartz surfaces in separate runs (Iglauer et al., 2014). The substrates were initially cleaned with acetone and DI water. The measured aqueous-phase contact angle was mostly relatively high (sometimes  $\theta > 90^\circ$ ) with some exceptions (e.g., data for 1 M of  $\text{NaHCO}_3$ ).

In theory, the aqueous-phase contact angle at 0.1 MPa (ambient pressure) should be  $\sim 0^\circ$  (Grate et al., 2012). Following this discrepancy in measurements, (Iglauer et al., 2014) cleaned an  $\alpha$ -quartz single crystal with piranha solution (5:1 vol,  $\text{H}_2\text{SO}_4:\text{H}_2\text{O}_2$ ), resulting in a contact angle of approximately  $0^\circ$  at ambient conditions in the presence of  $\text{CO}_2$ . Wiping the same substrate with a clean paper towel and repeating the measurements at the same conditions resulted in a contact angle of  $\sim 25^\circ$ . Initially, a cleaned sample exposed to laboratory air for several weeks resulted in a contact angle of  $\sim 70^\circ$ . They prescribed cleaning wetted parts of the contact angle measurement apparatus three times, flushing with toluene, acetone, and DI water. Furthermore, cleaning the substrate with air plasma for 15 mins instead of piranha solution (due to the serious health and safety hazards) helped produce highly reproducible results.

This cleaning recommendation by Iglauer et al. (2014) was followed in almost all contact angle measurements by their group to date (Al-Anssari et al., 2018b; Al-Yaseri et al., 2021b; Ali, 2021; Ali et al., 2020a; Ali et al., 2021c; Arif et al., 2016c; Arif et al., 2021; Sarmadivaleh et al., 2015). Previously, the pumps used to inject the aqueous phase (e.g., brine) and gaseous phase (e.g.,  $\text{CO}_2$ ) were kept in communication with the inside of the IFT cell to dispense the aqueous phase on the substrate at the desired flow rate and maintain the pressure of the gaseous phase.

This is the span of the experiment when the cylinder of the pumps can become contaminated, and the suggested cleaning steps are often ignored (this is due to operational limitations and is subject to the service warranty provided by the manufacturers) during repeated or new measurements. Cleaning the inner portions (cylinder) of pumps with organic solvents is not recommended. However, recently, Jha et al. (2019a, 2021) modified the contact angle apparatus to better control the contamination by improvising this process using a floating piston accumulator between the pump and IFT cell (Jha et al., 2019a; Jha et al., 2021).

The natural rock samples from the formation are reported to be contaminated by the solvent during the contaminant removal process that causes an error in the measurements of organic carbon content (TOC), especially for low TOC samples. Independent investigations in three different laboratories to quantify the effect of this contamination exhibited similar results (Muller et al., 2018). The results suggest that ethanol cleaning after dichloromethane treatment on rock samples can potentially solve contamination issues. An important observation is that ethanol does not introduce contamination. Ethanol alone cannot remove the preexisting nonpolar contaminants (e.g., hydrocarbon, bitumen, oil, or drilling fluid) by extraction.

Therefore, despite the reported observation of dichloromethane being the most contaminating solvent, it is still used for nonpolar contaminant removal from real rock samples (Muller et al., 2018). Fauziah et al. (2020) reported carbon dioxide wettability of natural rock samples from Southwest Hub sandstone, Western Australia, before and after dichloromethane treatment and found some influence on the wetting characteristics and organic content removal due to dichloromethane treatment (Fauziah et al., 2020); however, the effect of dichloromethane as a contaminant could not be quantified. Muller et al. (2018) also suggested conducting extra experiments on various minerals (with some peculiar properties, e.g., chlorite), natural samples (with variation in TOC content, kerogen types, and thermal maturities) to correlate the contamination rate with the mineralogy in the natural samples (Muller et al., 2018). It is advised to improve the experimental procedures by reducing the contact of organic contamination in the apparatus to avoid errors in the experimental results. Similarly, substrate cleaning methods are still evolving, and devising a proper cleaning method requires extensive insight from researchers.

#### 4. Influencing parameters

This section discusses the effects of realistic geo-storage conditions, such as temperature, pressure, variable salinity, and formation type, on the wettability alteration of the reservoir rock, forming a basis for technical evaluation. Next, the focus shifts to examining the effects of organic acids, which are generally found in depleted hydrocarbon reservoirs or deep saline aquifers and significantly influence the wettability shift. Finally, the effect of nanomaterial on the optimization and alteration of wettability for the mineral/CO<sub>2</sub>/brine system are discussed in the presence of organic acids. In this context, we critically analyze the most fundamental factors and gaps in the current knowledge in the context of underground CO<sub>2</sub> storage.

##### 4.1. Influencing parameters on CO<sub>2</sub> wettability in ideal geo-storage conditions

The parameters influencing CO<sub>2</sub> wettability in a given rock-fluid system for clean minerals or polished rock surfaces include geo-storage thermo-physical conditions, such as temperature (Abbaszadeh et al., 2020; Hamouda and Rezaei Gomari, 2006; Jing et al., 2021) and pressure (Al-Yaseri et al., 2016a, 2016b; Fauziah et al., 2019; Hansen et al., 2000). The parameters also include the composition of brine in geo-storage formation (Al-Yaseri et al., 2016a, 2016b; Arif et al., 2016b; Arif et al., 2016c; Saraji et al., 2014), surface roughness (Al-Yaseri et al., 2016a, 2016b; Marmur, 2006), and formation heterogeneity (Arif et al.,

2016b).

Previous studies have demonstrated that pressure has a substantial effect on CO<sub>2</sub>-wettability by shifting it toward more CO<sub>2</sub>-wet conditions irrespective of the formation type or wetting characteristics (Al-Yaseri et al., 2016a, 2016b; Arif et al., 2016a; Arif et al., 2017b; Fauziah et al., 2019; Hansen et al., 2000; Sarmadivaleh et al., 2015). However, some studies have found little or no effect on the contact angle due to increased pressure (Espinoza and Santamarina, 2010; Farokhpoor et al., 2013; Mills et al., 2011). In contrast, temperature behaves differently in various formations. For instance, the contact angle increases with an increase in temperature in sandstone formations (quartz mineral substrates; (Sarmadivaleh et al., 2015) and decreases with an increase in temperature in carbonate (calcite mineral substrate; (Arif et al., 2017b) or caprock (mica substrate) formations (Arif et al., 2016a).

Wetting characteristics have also exhibited different behaviors for temperature. For example, the contact angle decreases in hydrophobic dolomite with an increase in temperature, and the contact angle increases in hydrophilic dolomite with an increase in temperature (Al-Yaseri et al., 2017). In contrast, several other studies have also shown contradictions from this perspective (Al-Anssari et al., 2018a; Fauziah et al., 2019; Lu et al., 2017; Yang et al., 2008). The composition of formation brine differs substantially in different geo-storage formations. However, the influence of salinity on the contact angle demonstrates mixed behavior. Some studies have found that with an increase in salinity, the contact angle also increases (Al-Yaseri et al., 2016a, 2016b; Iglauder et al., 2015b), whereas some studies have discovered little or no effect on the contact angle due to the change in salinity (Ali et al., 2021b).

In addition, geo-storage formation contains a mixture of monovalent ions (i.e., NaCl and KCl) and divalent cations (i.e., CaCl<sub>2</sub> and MgCl<sub>2</sub>), and previous studies have reported that both salinities negatively affect hydrophilic surfaces. In contrast, compared to the monovalent ions, divalent cations have more effect on the contact angle, owing to the cation screening effect (Al-Yaseri et al., 2016a, 2016b; Iglauder, 2017).

Another crucial parameter that influences the contact angle is the surface roughness of the rock mineral; therefore, mineral surfaces are polished before conducting contact angle measurements. This parameter can be represented in various forms, such as the roughness ratio *rs* (Tudek et al., 2017) or the route mean square (Ali et al., 2022a; Mahesar et al., 2020a; Mahesar et al., 2020b; Memon et al., 2021a; Memon et al., 2020) and can be measured via atomic force microscopy. The effect of surface roughness on the contact angle differs based on the wetting characteristics. For instance, the contact angle decreases in hydrophilic surfaces (calcite or quartz) with an increase in surface roughness, whereas it increases in hydrophobic surfaces with an increase in surface roughness (Al-Yaseri et al., 2016a, 2016b; Arif et al., 2017b).

Moreover, contact angle studies comprise various experimental techniques that can substantially influence wettability studies, such as surface contamination (i.e., organic acids), equilibrium fluid procedures, and substrate cleaning procedures (Ali et al., 2020a; Ali et al., 2019a; Ali et al., 2019b). In addition, the use of different chemicals and surfactants may also substantially change the surface coverage of substrates, significantly affecting the wetting behavior of various minerals (Iglauder, 2017).

Arif et al. (2017a) examined the CO<sub>2</sub>/brine/rock system by measuring the contact angles (advancing and receding contact angles) relative to influencing factors, such as variable values of temperature (298 K to 343 K), pressure (0.1 MPa to 20 MPa), surface roughness (containing minerals, shale, and coal seams), and salinity (0 to 20 wt% of NaCl) (Arif et al., 2017a). Additionally, the influence of the surface IFT and wettability-associated alteration were analyzed relative to the principle of the trapping mechanism (Iglauder, 2017). With increased pressure and salinity, both receding/advancing contact angles progressed. Further, the rock surface established significant de-wetting (less wet to water) when the pressure increased. In contrast, salinity de-wets the rock system very little. Calcite exhibited slightly CO<sub>2</sub>-wet behavior;

however, mica was intermediate-wet at 308 K and 20 MPa, resulting in a considerable reduction in the geological storage potential of CO<sub>2</sub>. Nevertheless, the extent of the wettability variation increase relative to the pressure is greater when compared to the temperature, resulting in the concept that the rock system becomes nonwetting relative to the depth (Arif et al., 2016b). Additionally, through information on the variation in the wettability of the minerals (rock-forming, such as mica and calcite), high temperature, low salinity, and low pressure are favorable factors for the underground geological storage of CO<sub>2</sub>.

In another study by Arif et al. (2017c) the TOC in shale formation significantly influenced the de-wetting of caprock (Arif et al., 2017c). The low TOC shale was water-wet, and the high TOC shale was less water-wet. Thus, low TOC shale was considered an adequate choice for CO<sub>2</sub> storage based on the wettability information. Nevertheless, the effect of wettability enhancement on these formations has rarely been discussed in actual geo-storage conditions, which are anoxic (contain organic molecules), where reductive conditions exist (Froelich et al., 1979; Townsend et al., 2003).

#### 4.2. Presence of organic acids in geo-storage formations

Since the advent of modern analytical methods in the late 1960s, such as mass spectroscopy and gas chromatography, research scientists have expressed a great geochemical interest in separating organic acids (carboxylic or fatty acids) from the crude oil stream (Kvenvolden, 1967). These fatty acids (recognizable fossils) have been found in numerous geological formations ranging from the Precambrian age (before the development of geological formations) to the recent age (Akob et al., 2015; Kvenvolden, 1967; Lundegard and Kharaka, 1994). The presence of organic acids in geological formations is hypothesized as possible ancestors for the development of hydrocarbons due to the presence of organics in biological substances and similar molecular structures (Caballero et al., 2003; Kvenvolden, 1967). These organic acids may comprise unsaturated straight-chain and branched-chain fatty acids and saturated straight-chain monocarboxylic and dicarboxylic fatty acids (Lundegard and Kharaka, 1994; Waples, 1981). Many researchers have experimentally proved the presence of minute concentrations of organic acids in CO<sub>2</sub> geo-storage formations (i.e., deep saline aquifers) due to diagenesis of organic matter and fossil biodegradation (Akob et al., 2015; Bennett et al., 1993; Jones et al., 2008).

Lundegard and Kharaka (1994) found an abundance of monocarboxylic fatty acids in Cenozoic sedimentary basins, where short-chain fatty acids (i.e., acetate) were commonly present between 80 °C and 140 °C (Lundegard and Kharaka, 1994). They also indicated that organic-acid anion (acetate, C<sub>2</sub>H<sub>3</sub>O<sub>2</sub>) concentrations in these geological formations were less than 3000 mg/L. The authors noted that the alkalinity of geological formation water has a dominance of bicarbonate at temperatures less than 80 °C and more than 140 °C, whereas, in Miocene reservoirs, organic alkalinity dominates bicarbonate alkalinity. Moreover, dicarboxylic acids are rarely found in geological formations, where succinate and methyl-succinate are the most abundant dicarboxylic acids at concentrations of less than 100 mg/L.

Similarly, Akob et al. (2015) conducted a detailed study on microbiology and organic matter composition from Pennsylvania shale gas wells (Akob et al., 2015). They found that these geological formations have an abundance of organic-acid anions (i.e., formate, pyruvate, and acetate) due to microbial activity ranging from 66 to 9400 cells/mL.

Watson et al. (2002) conducted an experimental study on hydrocarbon biodegradation in a laboratory, finding a significant production of organic acids ranging from C<sub>10</sub> to C<sub>20</sub> (Watson et al., 2002). Further biodegradation of hydrocarbons results in heavy molecular weight (>C<sub>20</sub>) cyclic and branched-chain organic acids. Geological formations have traces of hydrocarbons that can produce these organic acids from a more prolonged geological era. Meredith et al. (2000) conducted similar quantitative analyses on 33 crude oil samples from Italy, California, and the UK, which demonstrated that the crucial parameter responsible for

increased acidity in these hydrocarbons is the presence of organic-acid fractions due to biodegradation (Meredith et al., 2000).

Cyr and Strausz (1984) conducted a qualitative analysis of the Alberta (Canada) oil sands, where they found that monocarboxylic concentrations (1% to 14%) are chemisorbed on an inorganic matrix (Cyr and Strausz, 1984). Further detailed studies have revealed the presence of normal, iso-, mono-, and di-unsaturated acids, cyclopropylalkanoic and cyclic terpenoid carboxylic acids, and anteiso alkanoic acids ranging from C<sub>12</sub> to C<sub>32</sub>. The majority of acyclic acids have similarities to those found in Alberta oil sands and petroleum bitumen as a byproduct of biosynthesis (bacterial degradation). Similarly, McGowan et al. (1985) performed an experimental study for kerogen degradation from Green River oil shale to determine the structure of hydrocarbons and found branched-chain fatty acids (McGowan et al., 1985).

The occurrence of these organic acids in fossils may range from C<sub>2</sub> to C<sub>26</sub> (Caballero et al., 2003), where odd-numbered carbon organic acids are rarely found compared to even numbers (Kvenvolden, 1967). These include (but are not limited to) acetic (C<sub>2</sub>), butanoic (C<sub>4</sub>), hexanoic (C<sub>6</sub>), caprylic (C<sub>8</sub>), lauric (C<sub>12</sub>), myristic (C<sub>14</sub>), palmitic (C<sub>16</sub>), stearic (C<sub>18</sub>), behenic (C<sub>22</sub>), lignoceric (C<sub>24</sub>), and cerotic (C<sub>26</sub>) acids (Amaya et al., 2002; Gomari and Hamouda, 2006; Hansen et al., 2000; Jardine et al., 1989; Kharaka et al., 2009; Legens et al., 1999; Madsen and Ida, 1998; Stalker et al., 2013; Yang et al., 2015). Previously, in the presence of organic acids, all wettability studies were related to rock/oil/brine systems for EOR applications (Nazahari et al., 2021). However, there is a severe lack of literature on the influence of these organics in a given rock/CO<sub>2</sub>/brine system. Therefore, we thoroughly reviewed studies that have assessed the effects of organics on CO<sub>2</sub>/brine and oil/brine wettability in various rock minerals and identified gaps for future work.

#### 4.3. Effect of organic acids on CO<sub>2</sub> wettability in real geo-storage conditions

The presence of organic acids in geo-storage formations is well proven in the literature (Akob et al., 2015; Ali, 2018; Lundegard and Kharaka, 1994). In contrast, their influence on wetting characteristics has rarely been tested, which can significantly affect CO<sub>2</sub> trapping capacities (Akhondzadeh et al., 2020; Ali et al., 2019a; Ali et al., 2019b; Ali et al., 2021b; Legens et al., 1999). Previously, wettability studies were conducted on clean mineral surfaces to benchmark the fundamental research for various influencing factors, including the pressure, temperature, salinity, and surface roughness (Al-Yaseri et al., 2016a, 2016b; Arif et al., 2019a; Fauziah et al., 2019). However, actual geological conditions are anoxic (containing organic molecules), where reductive circumstances overcome the fundamental studies on clean mineral substrates (Froelich et al., 1979; Townsend et al., 2003).

The organic effects on wetting characteristics at various physio-thermal conditions and how their minute concentrations may behave in multiple heterogeneous reservoir formations should be considered to fully understand and benchmark natural geological conditions. In the beginning, a series of studies by Anderson (1986, 1987a, 1987b, 1987c) discussed the wettability of geo-storage formations in detail, providing an understanding of oil-wet surfaces (Anderson, 1986; Anderson, 1987a; Anderson, 1987b; Anderson, 1987c). These studies related the adsorption of polar compounds dissolved in crude oil to the oil-wet characteristics of reservoir rock.

Researchers have used silanes to change the wetting characteristics from hydrophilic to hydrophobic conditions to understand the oil-wet nature of reservoir rock (Araujo et al., 1995; Grate et al., 2012; Vanithakumari et al., 2014). However, the presence of silanes in actual geo-storage conditions is not possible due to their highly reactive nature. Therefore, it is pertinent to gauge and simulate actual conditions (the presence of organic acids) at the laboratory scale to determine the thresholds of organics for wettability studies.

The literature seriously lacks information from this perspective, and

very few studies have gauged wettability characteristics in the presence of organic acids. Therefore, we conducted this comprehensive study to fill the gaps in the literature to determine future directions. Recent studies comprising the effects of organic acids on the wettability of rock/oil/brine and rock/CO<sub>2</sub>/brine are summarized in Table 3. However, the published data on the effects of organic acids on contact angles for rock/CO<sub>2</sub>/brine systems is quite sparse due to the precise procedure (explained in Section 3.2.1) and complications related to  $\theta$  measurements in the presence of very minute organic concentrations. This has already been noted in studies conducted by (Ali et al., 2020a; Ali et al., 2019a; Ali et al., 2019b). Fig. 13 summarizes the essence of minute organic contaminations and their associated effects on the wetting characteristics of geo-storage formations in the presence of CO<sub>2</sub>.

The reported data on the effect of organic acids on rock/CO<sub>2</sub>/brine systems demonstrates substantial agreement (Fig. 13 and Table 3), where rock-mineral surfaces became CO<sub>2</sub>-wet in the presence of organic acids (Ali et al., 2020a; Ali et al., 2019a; Ali et al., 2019b; Ali et al., 2021b). To gauge this effect, Ali et al. (2019a, 2019b, 2020a, 2021b) measured the advancing and receding contact angles in the presence of various organic acids (hexanoic, lauric, stearic, lignoceric, and humic acids) for two geo-storage formation proxy minerals (quartz representing sandstone and calcite representing carbonate) and the geo-storage caprock proxy mineral (mica muscovite) in the CO<sub>2</sub> atmosphere. Initially, mineral substrates were cleaned to remove organic contamination (see Section 3.2.2) and placed in monotonically reduced minute concentrations (10<sup>-2</sup> to 10<sup>-9</sup> mol/L) of various organic acids in an n-decane solution for 7 days.

The advancing and receding contact angles were measured on pure and organic-aged mineral substrates in the CO<sub>2</sub> atmosphere in various physio-thermal geo-storage conditions (Fig. 13). The droplet phase used in these studies was 10 wt% NaCl brine (Ali et al., 2020a; Ali et al., 2019a; Ali et al., 2019b) and 0.3 mol% NaCl brine (Ali et al., 2021b). The carbonate geo-storage mineral (calcite) results indicate that pure calcite surfaces were water-wet to intermediate-wet at geo-sequestration conditions (10 MPa, 25 MPa, and 323 K). The advancing and receding contact angles were 48° and 40° at 10 MPa and 68° and 62° at 25 MPa (both measured at 323 K), respectively (Ali et al., 2019a).

However, calcite substrates aged in stearic acid/n-decane solutions drastically shifted the wetting characteristics to CO<sub>2</sub>-wet. The advancing and receding contact angles were 126° and 98.6° at 10 MPa and 141.2° and 131.8° at 25 MPa (both measured at 323 K with 10<sup>-2</sup> mol/L stearic acid concentration). Similarly, the studies conducted on sandstone geo-storage mineral (quartz) and caprock proxy mineral (mica muscovite) demonstrated that pure mineral substrates were weakly water-wet to intermediate-wet in geo-sequestration conditions (25 MPa and 323 K for quartz substrates and 15 MPa, 25 MPa, and 323 K for mica substrates). The advancing and receding contact angles for pure quartz substrates were 56° and 54° at 25 MPa and 323 K (Ali et al., 2019b), and for mica, the substrates were 50.2° and 44.9° at 15 MPa and 65.1° and 60.4° at 25 MPa (both measured at 323 K), respectively (Ali et al., 2020a).

In comparison, hydrophilic mica and quartz substrates substantially reduced their water-wetness after aging in various organic acid/n-decane (hexanoic, lauric, stearic, and lignoceric acids) solutions. The advancing and receding contact angles for quartz mineral substrates were 86.97° and 81.27° for 10<sup>-2</sup> mol/L of hexanoic acid, 89.2° and 83.81° for 10<sup>-2</sup> mol/L of lauric acid, 94.69° and 84.8° for 10<sup>-2</sup> mol/L of stearic acid, and 110.41° and 105.17° for 10<sup>-2</sup> mol/L of lignoceric acid (all measured at 25 MPa and 323 K), respectively. Similarly, advancing and receding contact angles for mica mineral substrates were 98.41° and 93.25° for 10<sup>-2</sup> mol/L of hexanoic acid, 110.12° and 102.26° for 10<sup>-2</sup> mol/L of lauric acid, 121.23° and 113.69° for 10<sup>-2</sup> mol/L of stearic acid, and 132.96° and 124.88° for 10<sup>-2</sup> mol/L of lignoceric acid (all measured at 25 MPa and 323 K), respectively. The change in the degree of the contact angle at a constant organic-acid concentration was different for the respective types of organic acid due to the number of carbon atoms (alkyl chain length; (Ali et al., 2020a; Ali et al., 2019b).

Further, for rock/CO<sub>2</sub>/brine systems, the results of a study conducted by Ali et al. (2021b) revealed that quartz substrates as a representative of sandstone formation were weakly water-wet in geo-storage conditions (20 MPa and 323 K). The advancing contact angle for pure quartz substrate was 40° at 20 MPa and 323 K. However, the aging of quartz mineral surfaces in humic acid/n-decane solutions increases the hydrophobicity of quartz substrates at levels where the residual trapping capacities of CO<sub>2</sub> are significantly affected. For instance, at 10<sup>-3</sup> mol/L of humic acid concentration, the advancing and receding contact angles for the quartz mineral substrates were 100° and 90.12° at 15 MPa and 109.11° and 104.17° at 25 MPa (both measured at 323 K), respectively. Overall, the CO<sub>2</sub>-wettability trend was similar irrespective of the type of organic acid or mineral.

However, the trend in rock/oil/brine systems varies based on the type of organic acids (Table 3) due to the organic contamination in the apparatus, surface roughness, mineral type, salinity, and variable cleaning methodology (Al-Yaseri et al., 2016a, 2016b; Iglauder et al., 2014). However, the wettability data in rock/oil/brine systems are similar, except for a study (Garcia-Olvera et al., 2016) in which the effect of the naphthenic acid on glass chips demonstrated little to no effect on the contact angle measurements and a study (Hamouda and Rezaei Gomari, 2006) in which the aging of heptanoic acid on the calcite surface indicated zero advancing and receding contact angles. In summary, geo-storage formations contain organic molecules. The compiled studies indicate that they substantially affect wetting characteristics of the reservoir rock, reducing the CO<sub>2</sub> trapping capacities (Iglauder et al., 2015b; Iglauder et al., 2011). Therefore, it is crucial to gauge these effects at micro- and nanoporous scales to properly comprehend reservoir schemes for better feasibility of industrial CO<sub>2</sub> storage projects.

#### 4.4. Effect of nanomaterial on CO<sub>2</sub> wettability in real geo-storage conditions

Recently, NPs have been gaining wide acceptance in a diverse range of industries, including biology (De et al., 2008), medicine (Lohse and Murphy, 2012), metal ion removal (Wang et al., 2012), heterogeneous catalysis (Johnson, 2003), food (Wang et al., 2014), tissue penetration, drug delivery (Tong et al., 2012), and oil and gas (Al-Anssari et al., 2021; Alsaba et al., 2020; Mohanty et al., 2021b). In the petroleum industry, NPs are used for various applications of subsurface operations, including optimization of drilling fluids (Aftab et al., 2020a; Aftab et al., 2020b; Ali and Aftab, 2020; Ali et al., 2020b), EOR (Al-Anssari et al., 2019; Al-Anssari et al., 2018a; Al-Anssari et al., 2017d; Yang et al., 2020), IFT reduction (Al-Anssari et al., 2020; Cheraghian and Hendraningrat, 2016), chemical flooding (Akbar et al., 2020; Haghghi et al., 2020), low-salinity water injection (Jha et al., 2018; Jha et al., 2019a; Jha et al., 2020a), wettability alteration (Al-Anssari et al., 2016; Ali et al., 2020c; Naik et al., 2018), adsorption (Awan et al., 2021), and optimizing fracturing fluids (Al-Muntasher et al., 2017; Fakoya and Shah, 2018).

Moreover, NFs are formulated by adding NPs to the base fluid (DI water or brine) at a very low concentration (Al-Anssari et al., 2017c; Al-Anssari et al., 2018b). The practical subsurface applications of NPs in CO<sub>2</sub> geological formations are dependent on various factors, such as stability, dispersion, cost, and injectability, to provide constant migration of NFs in the pore matrix (Al-Anssari et al., 2017a). However, the success ratio of NFs in CO<sub>2</sub> geo-storage formations is adversely affected by various parameters, such as the formation type, salinity, temperature, pressure, pH, zeta-potential, and complex nature of the porous medium (Salama et al., 2015). For instance, the kinetic energy of NPs increases with increased temperature, causing a constant collision between NPs, reducing NF stability (Liu et al., 2013).

Another crucial parameter that affects the stability of NFs is the salinity of CO<sub>2</sub> geological storage formations (i.e., deep saline aquifers), which varies considerably, causing the reduction in NP repulsive forces due to the presence of electrolytes (i.e., brine). This phenomenon constantly increases coagulation and flocculation due to the increased

**Table 3**Summary of wettability studies for rock/CO<sub>2</sub>/brine and rock/oil/brine systems in the presence of organic acids.

Study reference	Experimental procedure	Type of Angle	Type of mineral	Experimental operating conditions					Wettability characteristics	
				Temperature (°K)	Pressure (MPa)	Aqueous and nonaqueous phase	Type of organic acid	Salinity		
(Ali et al., 2019a)	Sessile drop	θ <sub>a</sub> and θ <sub>r</sub>	Calcite	323	0.1, 10, and 25	Drop of brine CO <sub>2</sub> phase	Stearic acid	10 wt% NaCl	20.12 nm	CO <sub>2</sub> -wet
(Ali et al., 2019b)	Sessile drop	θ <sub>a</sub> and θ <sub>r</sub>	Quartz	323	0.1 and 25	Drop of brine CO <sub>2</sub> phase	Hexanoic acid, Lauric acid, Stearic acid, and Lignoceric acid	10 wt% NaCl	1 to 2 nm	CO <sub>2</sub> -wet
(Ali et al., 2020a)	Sessile drop	θ <sub>a</sub> and θ <sub>r</sub>	Mica	323	0.1, 15, and 25	Drop of brine CO <sub>2</sub> phase	Hexanoic acid, Lauric acid, Stearic acid, and Lignoceric acid	10 wt% NaCl	1 to 2 nm	CO <sub>2</sub> -wet
(Ali et al., 2021b)	Sessile drop	θ <sub>a</sub> and θ <sub>r</sub>	Quartz	303, 318, and 333	0.1, 15, and 25	Drop of brine CO <sub>2</sub> phase	Humic acid	DI water, 0.1 M, and 0.3 M NaCl	0.85 nm	CO <sub>2</sub> -wet
(Thomas et al., 1993)	Pendant drop	θ <sub>s</sub>	Calcite <sup>a</sup> , Dolomite <sup>b</sup> , and Magnesite <sup>c</sup>	293, 323, and 353	Atmospheric conditions	Drop of DI water in dodecane phase	<sup>a</sup> Propionic acid <sup>1</sup> , Octanoic acid <sup>2</sup> , Decanoic acid <sup>2</sup> , Palmitic acid <sup>2</sup> , Oleic acid <sup>2</sup> , Stearic acid <sup>2</sup> , Triacanthoic acid <sup>*</sup> , Hexadecanedioic acid <sup>3</sup> , Benzoic acid <sup>3</sup> , 5-phenylvaleric acid <sup>3</sup> , Neopentanoic acid <sup>1</sup> , 2,2-dimethylpentanoic acid <sup>1</sup> , and Neodecanoic acid <sup>1</sup>	DI water	N/A	<sup>a</sup> N/A <sup>1</sup> Water-wet <sup>2</sup> Oil-wet <sup>3</sup> Intermediate-wet
							<sup>b</sup> Octanoic acid <sup>*</sup> , Oleic acid <sup>2</sup>			
							<sup>c</sup> Octanoic acid <sup>*</sup> , Stearic acid <sup>*</sup>			
(Standal et al., 1999)	Sessile drop	θ <sub>a</sub> and θ <sub>r</sub>	Glass	293	Atmospheric conditions	Drop of isoctane in water and drop of water in isoctane	1-naphthoic acid <sup>1</sup> , 5-indanol <sup>1,2,a</sup> , Quinolone <sup>1</sup>	Water, 0.5 M NaCl, and 0.5 M CaCl <sub>2</sub>	N/A	<sup>1</sup> Intermediate-wet <sup>2</sup> Oil-wet <sup>a</sup> Angle increases with salinity
(Legens et al., 1999)	Pendant drop	θ <sub>s</sub>	Calcite	298	Atmospheric conditions	Drop of distilled water in air	Benzoic acid <sup>1</sup> , Lauric acid <sup>2</sup>	Distilled water	N/A	<sup>1</sup> Intermediate-wet <sup>2</sup> Oil-wet
(Lord et al., 2000)	Sessile drop	θ <sub>r</sub>	Quartz	298	Atmospheric conditions	Drop of DI water in air <sup>1,a</sup> and drop of DI-water in o-xylene <sup>1,b</sup>	Dodecylamine	DI-water	N/A	<sup>1</sup> Intermediate-wet <sup>a</sup> Angle increases with pH <sup>b</sup> Angle increase and then decreases with increasing pH
(Hoeiland et al., 2001)	Sessile drop	θ <sub>s</sub>	Glass	293	Atmospheric conditions	Drop of crude oil in distilled water	Naphthenic acid	0.5 M NaCl	N/A	Oil-wet to intermediate-wet due to change in pH
(Gomari and Hamouda, 2006)	Sessile drop	θ <sub>a</sub> and θ <sub>r</sub>	Calcite	296	Atmospheric conditions	Drop of n-decane in air	Quinoline <sup>1,*</sup> , 5-Indanol <sup>1,a</sup> , Heptanoic acid <sup>2,b</sup> , Cyclohexane-pentanoic acid <sup>1,*</sup> , and Decahydronaphthalene-pentanoic acid <sup>2,*</sup>	0.5 M NaCl, 0.5 M MgCl <sub>2</sub> and 0.5 M Na <sub>2</sub> SO <sub>4</sub>	N/A	<sup>1</sup> Oil-wet <sup>2</sup> Intermediate-wet <sup>a</sup> Angle increase with pH <sup>b</sup> Angle decrease with pH <sup>*</sup> Angle does not change
(Hamouda and Rezaei Gomari, 2006)	Sessile drop and imbibition test	θ <sub>a</sub> and θ <sub>r</sub>	Calcite	298, 323, 353, 403	Atmospheric conditions	Drop of n-decane in distilled water	Heptanoic acid <sup>*</sup> , Stearic acid <sup>1,a</sup> , Oleic acid <sup>2,a,b</sup> , 18-Phenoloctadecanoic acid <sup>1,a</sup> , 18-Cyclohexyloctadecanoic acid <sup>1,3</sup>	Distilled water	N/A	<sup>1</sup> Oil-wet <sup>2</sup> Weakly water-wet <sup>3</sup> Intermediate-wet at 353 K <sup>a</sup> Angle decreases with increasing temperature

(continued on next page)

**Table 3 (continued)**

Study reference	Experimental procedure	Type of Angle	Type of mineral	Experimental operating conditions						Wettability characteristics
				Temperature (°K)	Pressure (MPa)	Aqueous and nonaqueous phase	Type of organic acid	Salinity	Surface roughness	
(Tabrizy et al., 2011)	Adsorption isotherm	N/A	Calcite, Quartz, and Kaolinite powders	298	Water vapor pressure conditions	Water vapor adsorption	Stearic acid, N,N-dimethyldodecylamine, and asphaltene	K <sub>2</sub> SO <sub>4</sub>	N/A	Oil-wet
(Fathi et al., 2011)	Spontaneous imbibition and chromatography	N/A	Outcrop chalk cores	383	1	Crude oil and brine	Water-extractable carboxylic acids in crude oil	Formation water and seawater	N/A	Oil-wet
(Garcia-Olvera et al., 2016)	Pendant drop	θs	Glass	323	Atmospheric conditions	Drop of crude oil in brine	Naphthenic acid (NA)	1% Na <sub>2</sub> SO <sub>4</sub> 1% Na <sub>2</sub> SO <sub>4</sub> and 1 vol% NA	N/A	Water-wet
(Mwangi et al., 2018)	Modified Flotation Technique	θs	Austin chalk, Indiana limestone, Silurian dolomite, Berea sandstone	296, 343, and 383	Atmospheric conditions	Flotation in oil and water	Acetic acid, Myristic acid, Naphthenic acid, n-decane	DI-water and three types of mixed brine (1000, 10,000, 100,000 ppm)	N/A	Oil-wet
(Al-Busaidi et al., 2019)	Pendant drop	θs	Calcite	296	Atmospheric conditions	Drop of DI-water in n-decane	Stearic acid <sup>1</sup> , Capric acid <sup>1</sup> , Cyclohexane carboxylic acid <sup>2</sup> , Cyclohexane pentanoic acid <sup>1</sup> , Phenylacetic acid <sup>1</sup> , 1-Naphthaleneacetic acid <sup>2</sup> , Oleic acid <sup>1</sup> , Asphaltene <sup>1</sup>	DI-water	N/A	<sup>1</sup> Oil-wet <sup>2</sup> Intermediate-wet
(Al-Shirawi et al., 2021)	Sessile drop	θs	Calcite, Limestone, Dolomite	298	Atmospheric conditions	Drop of DI-water in n-decane	Stearic acid	DI-water	N/A	Oil-wet

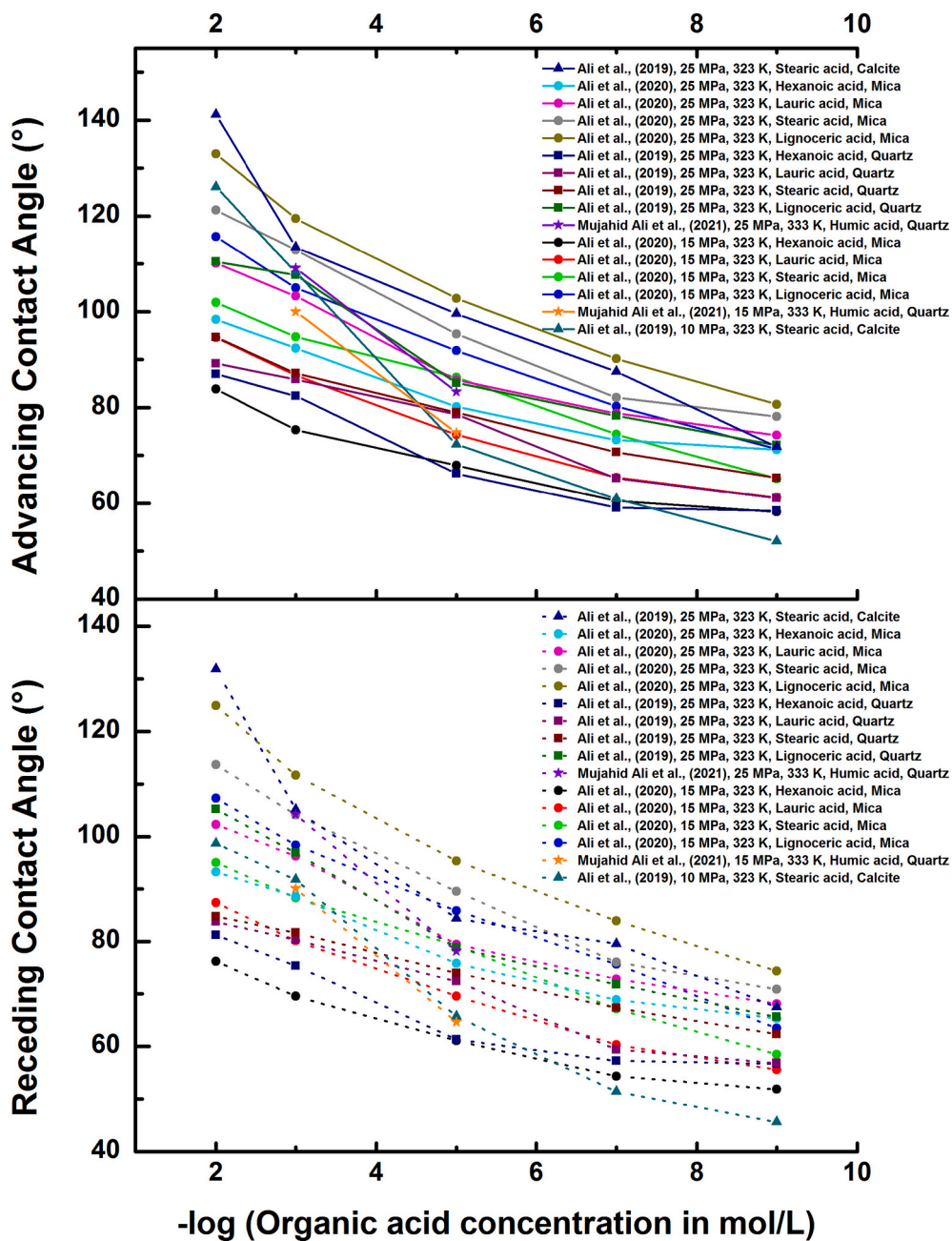


**Fig. 13.** Rock/CO<sub>2</sub>/brine contact angle data in the presence of various organic acids taken from Ali et al. (2020a, 2019a, 2019b, 2021b). Organic-acid concentration on the x-axis is plotted as the negative decadic logarithm, which declines exponentially on the right. The standard deviation in contact angle measurements is  $\pm 3^\circ$  for 10 and 15 MPa and  $\pm 5^\circ$  for 25 MPa.

coalescence and collision in nanosuspensions, causing phase separation (El-sayed et al., 2012). Surface-active agents, such as polymers (ShamsiJazeyi et al., 2014), surfactants (Ahualli et al., 2011; Al-Anssari et al., 2017e) and their combinations (Sharma et al., 2015) are suggested in the base fluid (DI water or brine) to avoid this difficulty and control the properties and stability of NPs for specified subsurface applications. Therefore, the selection of NP types, base fluids, and concentrations should be carefully considered based on the reservoir properties to achieve optimized conditions (Nwiduee et al., 2016). The literature reports that nanosuspensions tend to reduce the IFT (Al-Anssari et al., 2018a; Al-Anssari et al., 2020; Al-Anssari et al., 2018c), altering the hydrophobic wettability to hydrophilic conditions (Jha et al., 2018; Jha et al., 2019a; Jha et al., 2019b).

However, these studies were conducted on clean mineral surfaces in

strong oxidizing conditions, whereas real geo-storage conditions are reductive (containing organic molecules). The literature lacks research from this perspective for comprehending the effect of NPs in the presence of organic acids, and very few studies have gauged the wettability characteristics of nanomaterials in reductive conditions. Therefore, we compiled this comprehensive study to determine the future outlook and fill the gaps in the literature for NP applications in anoxic CO<sub>2</sub> geo-storage conditions. However, the CO<sub>2</sub> saturated brine creates an acidic environment (pH  $\sim 3$ ) in the porous space (Chen et al., 2019; Jha et al., 2019a; Jha et al., 2021). Table 4 lists the recent studies on a given rock/CO<sub>2</sub>/brine and rock/oil/brine systems for NP applications in the presence of organic acids. Fig. 14 summarizes the effects of various NPs on the wetting characteristics of geo-storage formations in the presence of minute organic contamination for rock/CO<sub>2</sub>/brine systems.

**Table 4**Summary of wettability studies for rock/CO<sub>2</sub>/brine and rock/oil/brine systems in the presence of organic acids and nanoparticles.

Study reference	Experimental procedure	Type of angle	Nanoparticles	Type of mineral	Experimental operating conditions					Initial Wettability	Wettability alteration	
					Temperature (°K)	Pressure (MPa)	Aqueous and nonaqueous phase	Organic phase for aging	Salinity	Surface roughness		
(Al-Ansari et al., 2017b)	Sessile drop	θ <sub>a</sub> and θ <sub>r</sub>	Surface modified SiO <sub>2</sub>	Calcite	298–343	0.1–20	Brine, CO <sub>2</sub> phase	Stearic acid/n-decane	0–20 wt% NaCl	79 nm	CO <sub>2</sub> -wet	Weakly water-wet
(Al-Ansari et al., 2018b)	Sessile drop	θ <sub>a</sub> and θ <sub>r</sub>	Surface modified SiO <sub>2</sub>	Calcite	298–343	12	Brine, CO <sub>2</sub> phase	Stearic acid/n-decane	0–30 wt% NaCl	78 nm	CO <sub>2</sub> -wet	Weakly water-wet
(Jha et al., 2019a)	Sessile drop	θ <sub>a</sub> and θ <sub>r</sub>	Surface modified ZrO <sub>2</sub> SiO <sub>2</sub>	Quartz	343	20	Nanofluids, CO <sub>2</sub> phase	n-decane	53 mM brine	1 to 2 nm	Weakly CO <sub>2</sub> -wet	varying
(Ali et al., 2020c)	Sessile drop	θ <sub>a</sub> and θ <sub>r</sub>	Surface modified ZrO <sub>2</sub> SiO <sub>2</sub>	Quartz	323	25	Brine, CO <sub>2</sub> phase	Hexanoic acid, Lauric acid, Stearic acid, and Lignoceric acid/n-decane	10 wt% NaCl	1 to 2 nm	CO <sub>2</sub> -wet	Weakly water-wet
(Jha et al., 2021)	Sessile drop	θ <sub>a</sub> and θ <sub>r</sub>	Surface modified ZrO <sub>2</sub>	Limestone	343	20	Nanofluids, CO <sub>2</sub> phase	n-decane	53 mM brine	80.04 nm	Weakly CO <sub>2</sub> -wet	varying
(Ali et al., 2021a)	Sessile drop	θ <sub>a</sub> and θ <sub>r</sub>	Al <sub>2</sub> O <sub>3</sub>	Mica	323	25	Brine, CO <sub>2</sub> phase	Hexanoic acid, Lauric acid, Stearic acid, and Lignoceric acid/n-decane	10 wt% NaCl	20.12 nm	CO <sub>2</sub> -wet	Weakly water-wet
(Dehghan Monfared et al., 2016)	Captive bubble	θ <sub>w</sub>	SiO <sub>2</sub>	Calcite	Room temperature	Atmospheric conditions	DI water, stearic acid/n-heptane	Stearic acid/n-heptane	0–0.2 M NaCl	N/A	Oil-wet	Weakly water-wet
(Jha et al., 2019b)	USBM	N/A	Surface modified SiO <sub>2</sub>	Sandstone	298	N/A	Nanofluids, low paraffinic oil	Low paraffinic oil	High pH 53 mM brine	N/A	Oil-wet	Weakly water-wet
(Alzobaidi et al., 2021)	Captive bubble	θ <sub>w</sub>	Surface modified SiO <sub>2</sub>	Calcite	298, 353	0.1	Nanofluids, n-decane/crude oil	Stearic acid/n-decane, Crude oil	DI, 3% NaCl, 2% CaCl <sub>2</sub> and 8% NaCl	4.1 ± 2 nm	Oil-wet	Weakly water-wet
(Jha et al., 2020a)	X-ray micro-CT	In-situ contact angle	Surface modified ZrO <sub>2</sub>	Sandstone	Room temperature	Atmospheric conditions	Nanofluids, doped n-decane	Doped n-decane	53 mM brine	N/A	Oil-wet	Weakly water-wet
(Kuang et al., 2020)	X-ray micro-CT	In-situ contact angle	SiO <sub>x</sub> , Al <sub>2</sub> O <sub>3</sub>	Dolomite, and Sandstone	Room temperature	Atmospheric conditions	Nanofluids, doped crude oil	Doped crude oil	1 mM NaCl	N/A	Mixed-wet	Weakly water-wet
(Qin et al., 2020b)	X-ray micro-CT	In-situ contact angle	Surface modified SiO <sub>2</sub>	Sandstone	333 K	Backpressure ~1.38 MPa, Confining pressure ~ 2.76 MPa	Nanofluids, crude oil	Crude oil	Doped 1 M CaCl <sub>2</sub>	N/A	Oil-wet	Weakly water-wet
(Zhang et al., 2020)	X-ray micro-CT	In-situ contact angle	Engineered carbon nano-sheets	Dolomite	323 K	Backpressure ~2.07 MPa, Confining pressure ~ 1.38 MPa	Nanofluids, crude oil	Doped crude oil	30 mM NaCl	N/A	Oil-wet	Weakly water-wet
(Yuan et al., 2021)	Captive bubble	θ <sub>w</sub>	Surface modified SiO <sub>2</sub>	Sandstone	Room temperature	Atmospheric conditions	Nanofluids, crude oil	Crude oil	13,000 ppm brine	N/A	Oil-wet	Weakly water-wet

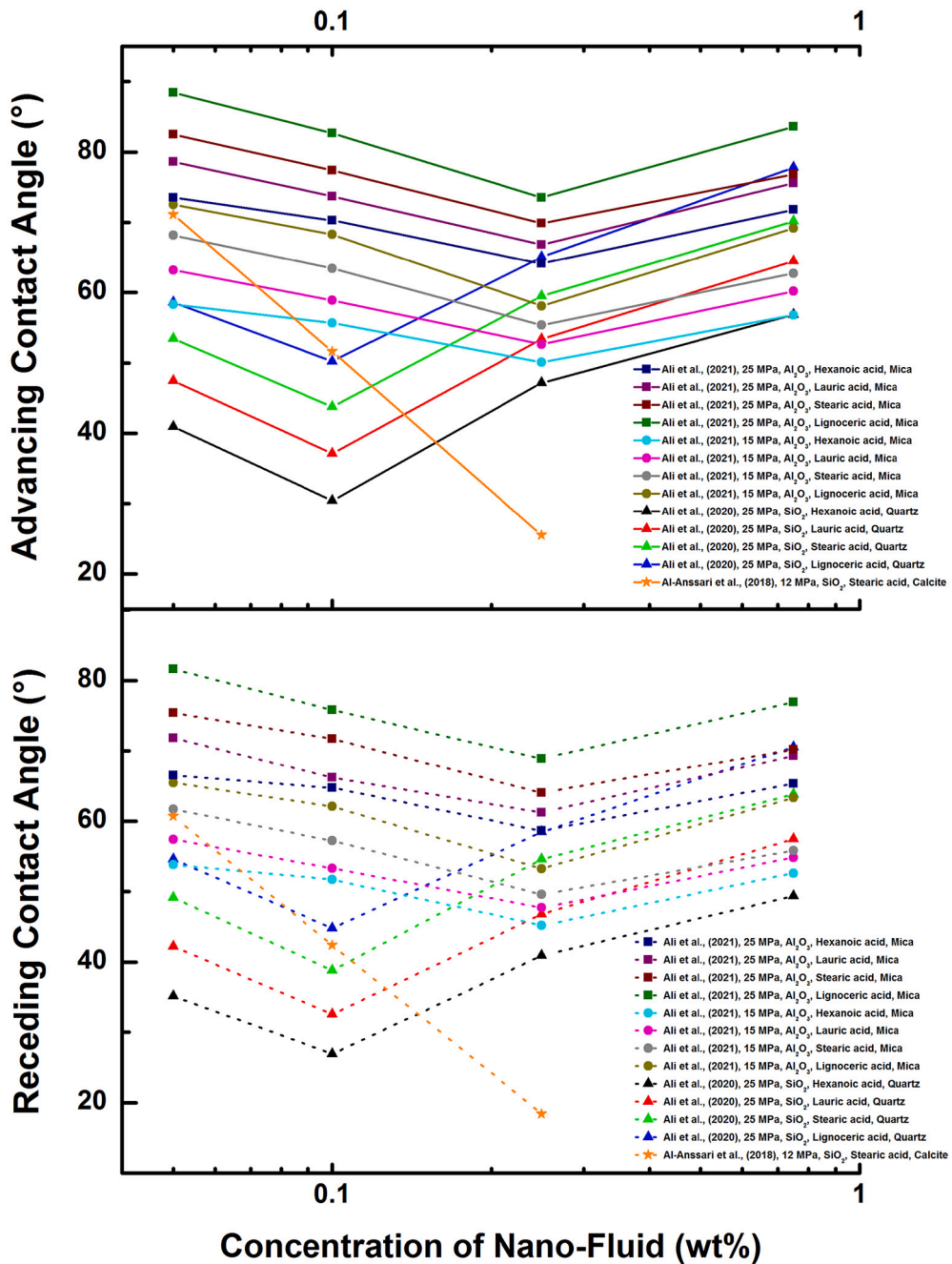


**Fig. 14.** Rock/CO<sub>2</sub>/brine contact angle data in the presence of various nanoparticles and organic acids, from Ali et al. (2021a, 2020c), and Al-Ansari et al. (2018b). Nanofluid concentration on the x-axis is plotted in wt% on the log<sub>10</sub> scale, and all measurements were taken at 323 K. The standard deviation in contact angle measurements was  $\pm 3^\circ$  for 12 and 15 MPa and  $\pm 5^\circ$  for 25 MPa.

The reported data on the effect of NPs in the presence of organic acids on rock/CO<sub>2</sub>/brine systems reveal substantial agreement (Fig. 14 and Table 4). Rock-mineral surfaces became CO<sub>2</sub>-wet in the presence of organic acids (Ali et al., 2020a; Ali et al., 2019a; Ali et al., 2019b; Ali et al., 2021b), and NF concentrations reversed their wetting characteristics to weakly water-wet to intermediate-wet (the degree of wetting reversibility is different for each NF concentration in the same rock/CO<sub>2</sub>/brine system; (Ali et al., 2021a; Ali et al., 2020c). Ali et al. (2020, 2021a) evaluated the effects of SiO<sub>2</sub> and Al<sub>2</sub>O<sub>3</sub>-based NFs on CO<sub>2</sub>-wettability reversal of quartz (sandstone formation representative) and mica (caprock representative), respectively, in the presence of organic acids.

Both hydrophilic NPs were dissolved in DI water to formulate NFs in

the concentration range of 0.05 to 0.75 wt%. Zeta-potential measurements indicated that NPs were reasonably stable in the prepared NF solutions. They followed the cleaning and aging procedure of the substrate as described in Table 2 (Ali et al., 2019b), except that different organic/n-decane substrates aged for one year were further treated with NFs for 5 h. The aging effect for an extended period was observed similarly to the shorter period. The wettability measurements demonstrated that the brine (10 wt% NaCl) contact angles were significantly reduced for NF-treated substrates aged in organic acids, reversing wettability toward a water-wetting (or less CO<sub>2</sub>-wetting) state. For instance, receding contact angles at storage conditions of 25 MPa and 323 K for 0.05 wt% SiO<sub>2</sub> NF-treated ( $10^{-2}$  mol/L of hexanoic acid aged one year) quartz substrates were  $\sim 35^\circ$  compared to  $91.3^\circ$  for without

NF treated substrates. Similar observations were reported for 0.05 wt% SiO<sub>2</sub> NF-treated (10<sup>-2</sup> mol/L of lignoceric acid aged one year) quartz substrate (i.e.,  $\theta_r$  of ~55° vs. 123.44° for without NF treated substrates). The maximum change in wettability (reversal to water-wet) was reported for the optimum concentration of 0.1 wt% SiO<sub>2</sub> NF-treated quartz substrate for all organic-acid aged samples. Similar behavior was observed for mica substrates; however, the optimum concentration of alumina NFs, at which the wettability reversal was the maximum, was for the 0.25 wt% solution. For instance, the receding contact angles at storage conditions of 25 MPa and 323 K for 0.25 wt% alumina NF-treated (10<sup>-2</sup> mol/L of hexanoic acid aged one year) mica substrates were ~ 65° compared to 136.2° for without NF treated substrates (structural leakage of CO<sub>2</sub> is possible at  $\theta_r > 90^\circ$ ).

Al-Anssari et al. (2017b) reported brine contact angle values as a function of pressure, temperature, and salinity for nanotreated natural and oil-wet calcite surfaces (aged in stearic acid) at CO<sub>2</sub> geo-storage conditions (0.1 to 20 MPa, and 296 K to 343 K) (Al-Anssari et al., 2017b). They used a 0.2 wt% SiO<sub>2</sub> NF concentration (prepared in 2 wt% NaCl brine containing 490 mg/L of sodium dodecyl sulfate) to treat the natural and oil-wet calcite surfaces (Al-Anssari et al., 2016; Nwiede et al., 2017). The presence of a small concentration of surfactant (e.g., SDS, SDBS, and CTAB) can actively stabilize NPs in the aqueous phase depending on the NP type (Ahualli et al., 2011; Pal et al., 2019a; Pal et al., 2019b; Pal and Mandal, 2020).

Similarly, Al-Anssari et al. (2018b) investigated brine contact angles as a function of NP concentration, pressure, salinity, and exposure time for NFs (Al-Anssari et al., 2018b). Pure calcite surfaces were rendered oil-wet by aging them in 0.01 mol/L of stearic acid concentration dissolved in n-decane. Calcite-equilibrated DI water contact angles increased with increased pressure and became constant for pressure values in the range of 10 to 20 MPa at 323 K for both nanotreated natural and oil-wet calcite surfaces. The reported constant values for the advancing contact angle were about 40° for the nanotreated oil-wet calcite surface and ~ 30° for the nanotreated natural calcite surface. Nanotreated calcite surfaces became water-wet from the CO<sub>2</sub>-wet state ( $\theta_a \sim 150^\circ$ ) in the storage conditions. They reported that the brine contact angles (at a pressure of ~15 MPa) decreased with temperature (298 K to 343 K) and increased with salinity (0 to 20 wt% NaCl) but remained water-wet for nanotreated calcite surfaces regardless of the initial wetting state. In contrast, the contact angle data as a function of the NF concentration revealed that the contact angle decreased with an increasing NP concentration and became constant for an NF concentration range of 0.2 to 0.5 wt% in typical geo-storage conditions (323 K and 12 MPa).

Jha et al. (2019a, 2021) reported the effect of the divalent cation-sulfate ion ratio (0 to 4.43) and NP concentration (100 to 2000 mg/L) on the CO<sub>2</sub> wettability of n-decane aged (3 weeks) quartz and limestone surfaces, respectively, by directly dispensing ZrO<sub>2</sub>-based NFs on the rock surfaces at 20 MPa and 343 K (Jha et al., 2019a; Jha et al., 2021). They prepared NFs using a low-salinity brine containing SDBS (~1.44 mM) and CTAB (~0.82 mM) surfactants in the respective brines with varying divalent ion and ZrO<sub>2</sub> NP concentrations, keeping the ionic strength and sulfate ion concentration of the aqueous-phase constant. A separate floating piston accumulator was used to directly dispense the NFs on the rock surface in the storage conditions to better control the contamination measurement errors (see Section 3.3.1). For quartz surfaces, the wettability alteration (either water- or CO<sub>2</sub>-wet) is more pronounced when the ZrO<sub>2</sub> concentration was in the range of 100 to 1000 mg/L for divalent cation-sulfate ion ratio values in the range of 2.58 to 4.43. The wettability was altered to a more water-wet state for a low dosage (100 mg/L) of ZrO<sub>2</sub> NPs used in the low-salinity aqueous phase for limestone surfaces.

Further increases in the ZrO<sub>2</sub> NP concentration enhanced the CO<sub>2</sub> wettability state but helped reduce the IFT of the supercritical CO<sub>2</sub>/CO<sub>2</sub> saturated aqueous phase. In addition, Ca<sup>2+</sup> ions in the NFs helped alter the wettability to a more water-wet state for limestone surfaces. Jha

et al. (2019a, 2021) postulated that ZrO<sub>2</sub> NP-CTAB complexes could diffuse into the oil layer, detach the oil layer from the rock surface, turn the surface more water-wet, and some could diffuse back to the water layer and settle on the detached oil and water interface. In addition, the Ca<sup>2+</sup> augments its effect at specific conditions for the ratio of divalent cations to sulfate ion. In summary, synergism and interplay among such factors as coadsorption of surfactant-augmented nanoaggregates on the rock surface, the availability of ions for bridging surfactant molecules and nanosurfaces, and the availability of SO<sub>4</sub><sup>2-</sup> for cations or adsorption on the NP surface (if positively charged) contribute to the wettability trends.

Several other researchers have reported results relevant to EOR in the presence of organic acids or the oil phase or a combination to change the wettability of the rock substrates to oil-wet and later reverse them to water-wet using NPs. However, it is generally observed that oil-wet rocks or rocks with a high TOC are also CO<sub>2</sub>-wet (Arif et al., 2017c; Fauziah et al., 2020; Siddiqui et al., 2018; Yassin et al., 2017).

Alzobaidi et al. (2021) and Dehghan Monfared et al. (2016) used silica NFs to alter the oil-wet calcite surfaces to water-wet in the presence of organic acids (Alzobaidi et al., 2021; Dehghan Monfared et al., 2016). Yuan et al. (2021) used highly surface-modified silicon dioxide NFs to turn oil-wet tight sandstone samples from the lower Montney formation, Alberta, to water-wet (Yuan et al., 2021).

Jha et al. (2019b) used silica NFs at higher pH to evaluate the wettability alteration of sandstone standard cores saturated with low paraffinic oil in USBM experiments using a fully automated centrifuge (Jha et al., 2019b). Jha et al. (2020a) further injected ZrO<sub>2</sub> NFs into oil-saturated sandstone miniature core plugs for EOR by combining the wettability alteration and IFT reduction in the x-ray microcomputed tomography core flood experiments (Jha et al., 2020a). Another set of microcomputed tomography core flood experiments evaluated the effect of aging the sandstones in n-decane (Jha et al., 2020b).

In addition, Kuang et al. (2020) reported a similar observation in a pore-scale experimental study of spontaneous imbibition by SiO<sub>x</sub>- and Al<sub>2</sub>O<sub>3</sub>-based NFs in mixed-wet Fond-du-Lac dolomite and Berea sandstone samples in the x-ray microcomputed tomography core flood experiments (Kuang et al., 2020). Moreover, Qin et al. (2020b) reported results supporting the above observations (Qin et al., 2020b).

Recently, Zhang et al. (2020) also made a similar observation of the wettability alteration and IFT reduction during oil recovery using coal-derived NF as an EOR agent for an oil-wet carbonate via x-ray microcomputed tomography core flood experiments at an elevated temperature and pressure (Zhang et al., 2020). Overall, organic acids have a substantial effect on the wetting characteristics of geo-storage formations that can cause reduced trapping capacities for CO<sub>2</sub>. However, it is proven in the literature that the use of various NPs and their associated nanoformulations can drastically reverse wettability (to more water-wet), increasing the trapping capacities for CO<sub>2</sub>.

## 5. Conclusions

In summary, CO<sub>2</sub> is a major contributor to greenhouse gas emissions. Every year, billions of tons of anthropogenic CO<sub>2</sub> emissions from stationary and nonstationary sources are produced. Half of this is consumed by the natural carbon cycle, whereas the other half is responsible for global warming. A practical solution to this problem is reducing CO<sub>2</sub> emissions using clean energy fuels and capturing CO<sub>2</sub> for permanent immobilization in underground geological formations. Deep saline aquifers and depleted oil and gas reservoirs are pivotal sinks, among others, for underground CO<sub>2</sub> geological storage. To explore their potential, influencing parameters should be investigated for CO<sub>2</sub> geo-storage formations. Wetting and nonwetting properties of geological formations are essential factors directly related to storage capacity and provide an estimation to reduce uncertainties in large-scale EOR and CO<sub>2</sub> geological storage operations.

Previously, many vital parameters related to wettability have been

investigated, such as temperature, pressure, salinity, formation type, and surface roughness. However, these investigations were conducted on clean mineral surfaces, and CO<sub>2</sub> geological storage formations contain organic acids that substantially influence the wetting characteristics of reservoir rock in a given CO<sub>2</sub>/brine and oil/brine systems. Therefore, we compiled this comprehensive study to fill the gaps in the literature to determine the correct measurement procedures, the effects of organic contamination in experimental apparatus and their controls, and the effects of organic acids on the wetting characteristics of geo-storage formations and CO<sub>2</sub> trapping capacities.

Furthermore, recent advances in NPs and their applications in various fields have a promising future. Similarly, we compiled studies in which NF concentrations were used to mitigate the effect of organic acids in various geo-storage formations, increasing the CO<sub>2</sub> trapping capacities. The significant findings of this work are concluded below:

- Carbon capture and storage are the only viable options to capture CO<sub>2</sub> at a rate of 10 billion tons per year to meet the commitment of net zero emissions by 2050 and restrict global warming to less than 2 °C.
- Potential carbon geological sinks include deep saline aquifers, depleted hydrocarbon reservoirs, coal seams, and organic-rich shales. However, other options can also be considered with technological developments, such as tight gas geological formations and basaltic rocks.
- Wettability is a crucial parameter that drives the capability of CO<sub>2</sub> throughout the geological formation and governs the fluid dynamics, injection rate, and containment security. Therefore, it is crucial to critically determine the wetting characteristics to evaluate geological formations and CO<sub>2</sub> trapping capacities.
- Various procedures define the experimental determination of wettability for geological formations; however, organic contamination in experimental apparatus can provide biased measurements. Therefore, proper cleaning procedures should be followed, and controls should be placed to reduce the contact of organic contamination.
- The typical captive bubble method and sessile drop method for rock/CO<sub>2</sub>/brine systems suggest that sandstone, carbonate, and caprock formations are weakly water-wet; however, as the CO<sub>2</sub> pressure and depth increase, they become intermediate-wet. Similar observations also apply to the salinity of the geological formation. In contrast, an increase in temperature suggests contradictions for various geological formations. For instance, sandstone (quartz) formations become weakly water-wet with an increase in temperature, whereas carbonate (calcite) and caprock formations exhibit an increase in water wettability with an increase in temperature (these observations are for chemically clean mineral substrates in strongly oxidizing conditions).
- Real CO<sub>2</sub> geological formations are anoxic (containing organic molecules) with reductive conditions, and clean mineral substrates do not exist. These organic molecules have a substantial effect on CO<sub>2</sub>-wettability. Previous studies have proven that pure mineral surfaces that were initially weakly water-wet become CO<sub>2</sub>-wet due to organic acids.
- Researchers have expressed keen interest in NPs, which are used in various fields. Recent studies have shown that optimum NF concentrations can provide a solution to mitigate the effect caused by organic acids.

Quantifying the wetting characteristics of geological formations in anoxic and reductive geo-storage conditions is crucial. The reservoir schemes and simulation models should also consider effects due to the existence of organic acids and the benefits of nanoconcentrations, as reduced residual and structural trapping capacities may be expected. This review article facilitates determining the correct experimental procedures. The data reviewed in this article offer a proper direction for

the long-term feasibility of CO<sub>2</sub> geo-storage projects.

## 6. Recommendations and future outlook

This research recommends the following regarding the future outlook in determining detailed scenarios for the effects of organics and nanomaterials.

- The current research has been conducted on various subjective organic acids and their associated concentrations to benchmark their development in science. However, the actual composition of organic acids may differ, and a large-scale analysis of natural geological formations may offer a detailed understanding.
- The current research has been conducted on synthetic rock thin sections (calcite, quartz, and mica). However, natural geological storage formations are heterogeneous, and their compositions may differ. Subsequently, the reported investigations and their applications are restricted. Therefore, wettability studies should be conducted to determine the CO<sub>2</sub> geo-storage potential in realistic geological rock thin sections.
- The experimental part of this research comprises a direct quantitative assessment (contact angle measurements) to determine the wettability behavior. However, these measurements are representative of surface chemistry. Therefore, other qualitative methods (e.g., capillary pressure curve, relative permeability, etc.) should also be used to determine the complex wetting characteristics of the pore matrix in the presence of organic acids.
- The types of nanomaterials published in previous research for reversing the wettability of geo-storage formations are minimal. Several other nanomaterials (e.g., TiO<sub>x</sub>, ZrO<sub>x</sub>, ZnO, FeO, etc.) should be formulated to quantify their effects on the wetting characteristics of geo-storage formations in the presence of organic acids.
- In several studies, surface-active agents (e.g., surfactants and polymers) have also exhibited a great potential in reversing wettability. Therefore, these chemicals should be used comparatively with NPs to quantify the wetting characteristics of geo-storage formations in the presence of organic acids.
- These studies indicate that detailed research is required to determine the effect of organic acids and nanomaterials for safe and long-term CO<sub>2</sub> geo-storage projects. It is also recommended that reservoir models and simulation studies that calculate CO<sub>2</sub> storage capacities account for the thresholds of organic acids.
- Optimum nanosuspensions should be injected with formation water at the field scale before supercritical CO<sub>2</sub> injection, which reverses the wetting characteristics of geo-storage formation toward intermediate-wet for increased CO<sub>2</sub> storage potential.

## Declaration of Competing Interest

The authors declare that they have no known competing financial interests or personal relationships that could have appeared to influence the work reported in this paper.

## Acknowledgments

The authors acknowledge Mr. Antonio García, a scientific illustrator from King Abdullah University of Science and Technology, Saudi Arabia for producing the graphical abstract.

## References

- Abbaszadeh, M., Shariatiipour, S., Ifelebuegu, A., 2020. The influence of temperature on wettability alteration during CO<sub>2</sub> storage in saline aquifers. *Int. J. Greenhouse Gas Control* 99, 103101.  
 Abdulkhalik, H., Al-Yaseri, A., Ali, M., Giwelli, A., Negash, B.M., Sarmadivaleh, M., 2021. CO<sub>2</sub>/Basalt's interfacial tension and wettability directly from gas density: Implications for Carbon Geo-sequestration. *J. Pet. Sci. Eng.* 204, 108683.

- Abramov, A., Keshavarz, A., Iglauer, S., 2019. Wettability of fully hydroxylated and alkylated (001)  $\alpha$ -quartz surface in carbon dioxide atmosphere. *J. Phys. Chem. C* 123 (14), 9027–9040.
- Adamson, A.W., Gast, A.P., 1967. *Physical Chemistry of Surfaces*. Interscience Publishers, New York, p. 150.
- Administration, U.E.I., 2011. *Annual Energy Outlook 2011: With Projections to 2035*. Government Printing Office.
- Aftab, A., Ali, M., Arif, M., Panhwar, S., Saady, N.M.C., Al-Khdheewi, E.A., Mahmoud, O., Ismail, A.R., Keshavarz, A., Iglauer, S., 2020a. Influence of tailor-made TiO<sub>2</sub>/API bentonite nanocomposite on drilling mud performance: towards enhanced drilling operations. *Appl. Clay Sci.* 199, 105862.
- Aftab, A., Ali, M., Sahito, M.F., Mohanty, U.S., Jha, N.K., Akhondzadeh, H., Azhar, M.R., Ismail, A.R., Keshavarz, A., Iglauer, S., 2020b. Environmental friendliness and high performance of multifunctional Tween 80/ZnO-nanoparticles-added water-based drilling fluid: an experimental approach. *ACS Sustain. Chem. Eng.* 8 (30), 11224–11243.
- Agartan, E., Trevisan, L., Cihan, A., Birkholzer, J., Zhou, Q., Illangasekare, T.H., 2015. Experimental study on effects of geologic heterogeneity in enhancing dissolution trapping of supercritical CO<sub>2</sub>. *Water Resour. Res.* 51 (3), 1635–1648.
- Aguilar, E., Allende, L., del Toro, F.J., Chung, B.-N., Canto, T., Tenllado, F., 2015. Effects of elevated CO<sub>2</sub> and temperature on pathogenicity determinants and virulence of Potato virus X/Potyvirus-associated synergism. *Mol. Plant-Microbe Interact.* 28 (12), 1364–1373.
- Ahualli, S., Iglesias, G., Wachter, W., Dulle, M., Minami, D., Glatter, O., 2011. Adsorption of anionic and cationic surfactants on anionic colloids: supercharging and destabilization. *Langmuir* 27 (15), 9182–9192.
- Ajaiy, T., Awolayo, A., Gomes, J.S., Parra, H., Hu, J., 2019. Large scale modeling and assessment of the feasibility of CO<sub>2</sub> storage onshore Abu Dhabi. *Energy* 185, 653–670.
- Akbar, I., Zhou, H., Liu, W., Tahir, M.U., Memon, A., Ansari, U., Lv, F., 2020. Experimental investigation of chemical flooding using nanoparticles and polymer on displacement of crude oil for enhanced oil recovery. *Int. J. Chem. Eng.* 2020.
- Akhondzadeh, H., Keshavarz, A., Al-Yaseri, A.Z., Ali, M., Awan, F.U.R., Wang, X., Yang, Y., Iglauer, S., Lebedev, M., 2020. Pore-scale analysis of coal cleat network evolution through liquid nitrogen treatment: a Micro-Computed Tomography investigation. *Int. J. Coal Geol.* 219, 103370.
- Akhondzadeh, H., Keshavarz, A., Awan, F.U.R., Ali, M., Al-Yaseri, A., Liu, C., Yang, Y., Iglauer, S., Gurevich, B., Lebedev, M., 2021. Liquid nitrogen fracturing efficiency as a function of coal rank: a multi-scale tomographic study. *J. Nat. Gas Sci. Eng.* 95, 104177.
- AKhondzadeh, D.M., Cozzarelli, I.M., Dunlap, D.S., Rowan, E.L., Lorah, M.M., 2015. Organic and inorganic composition and microbiology of produced waters from Pennsylvania shale gas wells. *Appl. Geochem.* 60, 116–125.
- Al-Anssari, S., Barifcani, A., Wang, S., Maxim, L., Iglauer, S., 2016. Wettability alteration of oil-wet carbonate by silica nanofluid. *J. Colloid Interface Sci.* 461, 435–442.
- Al-Anssari, S., Arif, M., Wang, S., Barifcani, A., Iglauer, S., 2017a. Stabilizing nanofluids in saline environments. *J. Colloid Interface Sci.* 508, 222–229.
- Al-Anssari, S., Arif, M., Wang, S., Barifcani, A., Lebedev, M., Iglauer, S., 2017b. CO<sub>2</sub> geo-storage capacity enhancement via nanofluid priming. *Int. J. Greenhouse Gas Control* 63, 20–25.
- Al-Anssari, S., Arif, M., Wang, S., Barifcani, A., Lebedev, M., Iglauer, S., 2017c. Wettability of nano-treated calcite/CO<sub>2</sub>/brine systems: implication for enhanced CO<sub>2</sub> storage potential. *Int. J. Greenhouse Gas Control* 66, 97–105.
- Al-Anssari, S., Nwiduee, L., Ali, M., Sangwai, J.S., Wang, S., Barifcani, A., Iglauer, S., 2017d. Retention of silica nanoparticles in limestone porous media. In: SPE/IATMI Asia Pacific Oil & Gas Conference and Exhibition. Society of Petroleum Engineers.
- Al-Anssari, S., Wang, S., Barifcani, A., Iglauer, S., 2017e. Oil-water interfacial tensions of silica nanoparticle-surfactant formulations. *Tenside Surfactants Detergents* 54 (4), 334–341.
- Al-Anssari, S., Arain, Z.-U.-A., Barifcani, A., Keshavarz, A., Ali, M., Iglauer, S., 2018a. Influence of Pressure and Temperature on CO<sub>2</sub>-Nanofluid Interfacial Tension: Implication for Enhanced Oil Recovery and Carbon Geosequestration. Abu Dhabi International Petroleum Exhibition & Conference. Society of Petroleum Engineers.
- Al-Anssari, S., Arif, M., Wang, S., Barifcani, A., Lebedev, M., Iglauer, S., 2018b. Wettability of nanofluid-modified oil-wet calcite at reservoir conditions. *Fuel* 211, 405–414.
- Al-Anssari, S., Barifcani, A., Keshavarz, A., Iglauer, S., 2018c. Impact of nanoparticles on the CO<sub>2</sub>-brine interfacial tension at high pressure and temperature. *J. Colloid Interface Sci.* 532, 136–142.
- Al-Anssari, S., Ali, M., Memon, S., Bhatti, M.A., Lagat, C., Sarmadivaleh, M., 2019. Reversible and irreversible adsorption of bare and hybrid silica nanoparticles onto carbonate surface at reservoir condition. *Petroleum* 6 (3), 277–285.
- Al-Anssari, S., Arain, Z.-U.-A., Shanshool, H.A., Ali, M., Keshavarz, A., Iglauer, S., Sarmadivaleh, M., 2020. Effect of Nanoparticles on the Interfacial Tension of CO-oil System at High Pressure and Temperature: An Experimental Approach. SPE Asia Pacific Oil & Gas Conference and Exhibition. Society of Petroleum Engineers.
- Al-Anssari, S., Ali, M., Alajmi, M., Akhondzadeh, H., Khaksar Manshad, A., Kalantariasl, A., Iglauer, S., Keshavarz, A., 2021. Synergistic effect of nanoparticles and polymers on the rheological properties of injection fluids: implications for enhanced oil recovery. *Energy Fuel* 35 (7), 6125–6135.
- Al-Bayati, D., Saeedi, A., Myers, M., White, C., Xie, Q., 2019. Insights into immiscible supercritical CO<sub>2</sub> EOR: An XCT scanner assisted flow behaviour in layered sandstone porous media. *J. CO<sub>2</sub> Util.* 32, 187–195.
- Al-Busaidi, I.K., Al-Maamari, R.S., Karimi, M., Naser, J., 2019. Effect of different polar organic compounds on wettability of calcite surfaces. *J. Pet. Sci. Eng.* 180, 569–583.
- Ali, M., 2018. Effect of Organic Surface Concentration on CO<sub>2</sub>-wettability of Reservoir Rock. Curtin University.
- Ali, M., 2021. Effect of Organics and Nanoparticles on CO<sub>2</sub>-Wettability of Reservoir Rock; Implications for CO<sub>2</sub> Geo-Storage. Curtin University.
- Ali, M., Aftab, A., 2020. Topic Review Unconventional Reservoirs Subjects: Energy & Fuel Technology.
- Ali, M., Dahraj, N.U., Haider, S.A., 2015. Study of Asphaltene Precipitation During CO<sub>2</sub> Injection in Light Oil Reservoirs. SPE/PAPG Pakistan Section Annual Technical Conference. Society of Petroleum Engineers.
- Ali, M., Al-Anssari, S., Shakeel, M., Arif, M., Dahraj, N.U., Iglauer, S., 2017. Influence of Miscible CO<sub>2</sub> Flooding on Wettability and Asphaltene Precipitation in Indiana Lime Stone. SPE/IATMI Asia Pacific Oil & Gas Conference and Exhibition. Society of Petroleum Engineers.
- Ali, M., Al-Anssari, S., Arif, M., Barifcani, A., Sarmadivaleh, M., Stalker, L., Lebedev, M., Iglauer, S., 2019a. Organic acid concentration thresholds for ageing of carbonate minerals: implications for CO<sub>2</sub> trapping/storage. *J. Colloid Interface Sci.* 534, 88–94.
- Ali, M., Arif, M., Sahito, M.F., Al-Anssari, S., Keshavarz, A., Barifcani, A., Stalker, L., Sarmadivaleh, M., Iglauer, S., 2019b. CO<sub>2</sub>-wettability of sandstones exposed to traces of organic acids: implications for CO<sub>2</sub> geo-storage. *Int. J. Greenhouse Gas Control* 83, 61–68.
- Ali, M., Aftab, A., Arain, Z.U., Al-Yaseri, A., Roshan, H., Saeedi, A., Iglauer, S., Sarmadivaleh, M., 2020a. Influence of organic acid concentration on wettability alteration of cap-rock: implications for CO<sub>2</sub> trapping/storage. *ACS Appl. Mater. Interfaces* 12 (35), 39850–39858.
- Ali, M., Jarni, H.H., Aftab, A., Ismail, A.R., Saady, N.M.C., Sahito, M.F., Keshavarz, A., Iglauer, S., Sarmadivaleh, M., 2020b. Nanomaterial-based drilling fluids for exploitation of unconventional reservoirs: a review. *Energies* 13 (13), 3417.
- Ali, M., Sahito, M.F., Jha, N.K., Arain, Z.U., Memon, S., Keshavarz, A., Iglauer, S., Saeedi, A., Sarmadivaleh, M., 2020c. Effect of nanofluid on CO<sub>2</sub>-wettability reversal of sandstone formation: implications for CO<sub>2</sub> geo-storage. *J. Colloid Interface Sci.* 559, 304–312.
- Ali, M., Aftab, A., Awan, F.U.R., Akhondzadeh, H., Keshavarz, A., Saeedi, A., Iglauer, S., Sarmadivaleh, M., 2021a. CO<sub>2</sub>-wettability reversal of cap-rock by alumina nanofluid: Implications for CO<sub>2</sub> geo-storage. *Fuel Process. Technol.* 214, 106722.
- Ali, M., Awan, F.U.R., Ali, M., Al-Yaseri, A., Arif, M., Sanchez-Roman, M., Keshavarz, A., Iglauer, S., 2021b. Effect of humic acid on CO<sub>2</sub>-wettability in sandstone formation. *J. Colloid Interface Sci.* 588, 315–325.
- Ali, M., Jha, N.K., Al-Yaseri, A., Zhang, Y., Iglauer, S., Sarmadivaleh, M., 2021c. Hydrogen wettability of quartz substrates exposed to organic acids: implications for hydrogen trapping/storage in sandstone reservoirs. *J. Pet. Sci. Eng.*, 109081.
- Ali, M., Yeeken, N., Pal, N., Keshavarz, A., Iglauer, S., Hoteit, H., 2021d. Influence of pressure, temperature and organic surface concentration on hydrogen wettability of caprock; implications for hydrogen geo-storage. *Energy Rep.* 7, 5988–5996.
- Ali, M., Shar, A.M., Mahesar, A.A., Al-Yaseri, A., Yeeken, N., Memon, K.R., Keshavarz, A., Hoteit, H., 2022a. Experimental evaluation of liquid nitrogen fracturing on the development of tight gas carbonate rocks in the Lower Indus Basin, Pakistan. *Fuel* 309, 122192.
- Ali, M., Yeeken, N., Pal, N., Keshavarz, A., Iglauer, S., Hoteit, H., 2022b. Influence of organic molecules on wetting characteristics of mica/H<sub>2</sub>/brine systems: implications for hydrogen structural trapping capacities. *J. Colloid Interface Sci.* 608 (2), 1739–1749.
- Al-Khdheewi, E.A., Vialle, S., Barifcani, A., Sarmadivaleh, M., Iglauer, S., 2017. Influence of CO<sub>2</sub>-wettability on CO<sub>2</sub> migration and trapping capacity in deep saline aquifers. *Greenhouse Gas* 7 (2), 328–338.
- Al-Khdheewi, E.A., Vialle, S., Barifcani, A., Sarmadivaleh, M., Iglauer, S., 2017a. Impact of reservoir wettability and heterogeneity on CO<sub>2</sub>-plume migration and trapping capacity. *Int. J. Greenhouse Gas Control* 58, 142–158.
- Al-Khdheewi, E.A., Vialle, S., Barifcani, A., Sarmadivaleh, M., Iglauer, S., 2017b. Influence of injection well configuration and rock wettability on CO<sub>2</sub> plume behaviour and CO<sub>2</sub> trapping capacity in heterogeneous reservoirs. *J. Nat. Gas Sci. Eng.* 43, 190–206.
- Al-Khdheewi, E.A., Mahdi, D.S., Ali, M., Fauziah, C.A., Barifcani, A., 2020. Impact of Caprock Type on Geochemical Reactivity and Mineral Trapping Efficiency of CO<sub>2</sub>. Offshore Technology Conference Asia. Offshore Technology Conference.
- Al-Khdheewi, E.A., Mahdi, D.S., Ali, M., Iglauer, S., Barifcani, A., 2021. Reservoir Scale Porosity-Permeability Evolution in Sandstone Due to CO<sub>2</sub> Geological Storage (Available at SSRN 3818887).
- Al-Menhal, A.S., Krevor, S., 2016. Capillary trapping of CO<sub>2</sub> in oil reservoirs: observations in a mixed-wet carbonate rock. *Environ. Sci. Technol.* 50 (5), 2727–2734.
- Al-Muntasher, G.A., Liang, F., Hull, K.L., 2017. Nanoparticle-enhanced hydraulic-fracturing fluids: a review. *SPE Product. Operat.* 32 (02), 186–195.
- Al-Rubaye, A., Al-Yaseri, A., Ali, M., Mahmud, H.B., 2021. Characterization and analysis of naturally fractured gas reservoirs based on stimulated reservoir volume and petrophysical parameters. *J. Petrol. Explor. Product.* 11 (2), 639–649.
- Alsaba, M.T., Al-Dushaishi, M.F., Abbas, A.K., 2020. A comprehensive review of nanoparticles applications in the oil and gas industry. *J. Petrol. Explor. Product. Technol.* 10 (4), 1389–1399.
- Al-Shirawi, M., Karimi, M., Al-Maamari, R.S., 2021. Impact of carbonate surface mineralogy on wettability alteration using stearic acid. *J. Pet. Sci. Eng.* 203, 108674.
- Al-Yaseri, A., Jha, N.K., 2021. On hydrogen wettability of basaltic rock. *J. Pet. Sci. Eng.*, 108387.
- Al-Yaseri, A., Sarmadivaleh, M., Saeedi, A., Lebedev, M., Barifcani, A., Iglauer, S., 2015. N<sub>2</sub>+ CO<sub>2</sub>+ NaCl brine interfacial tensions and contact angles on quartz at CO<sub>2</sub> storage site conditions in the Gippsland basin, Victoria/Australia. *J. Pet. Sci. Eng.* 129, 58–62.

- Al-Yaseri, A.Z., Lebedev, M., Barifcani, A., Iglauer, S., 2016a. Receding and advancing ( $\text{CO}_2$ + brine+ quartz) contact angles as a function of pressure, temperature, surface roughness, salt type and salinity. *J. Chem. Thermodyn.* 93, 416–423.
- Al-Yaseri, A.Z., Roshan, H., Lebedev, M., Barifcani, A., Iglauer, S., 2016b. Dependence of quartz wettability on fluid density. *Geophys. Res. Lett.* 43 (8), 3771–3776.
- Al-Yaseri, A., Roshan, H., Zhang, Y., Rahman, T., Lebedev, M., Barifcani, A., Iglauer, S., 2017. Effect of the temperature on  $\text{CO}_2$ /brine/dolomite wettability: hydrophilic versus hydrophobic surfaces. *Energy Fuel* 31 (6), 6329–6333.
- Al-Yaseri, A., Abdulelah, H., Yeeken, N., Ali, M., Negash, B.M., Zhang, Y., 2021a. Assessment of  $\text{CO}_2$ /shale interfacial tension. *Colloids Surf. A Physicochem. Eng. Asp.* 627, 127118.
- Al-Yaseri, A., Ali, M., Ali, M., Taheri, R., Wolff-Boenisch, D., 2021b. Western Australia basalt- $\text{CO}_2$ -Brine wettability at geo-storage conditions. *J. Colloid Interface Sci.* 603, 165–171.
- Alzobaidi, S., Wu, P., Da, C., Zhang, X., Hackbarth, J., Angeles, T., Rabat-Torki, N.J., MacAuliffe, S., Panja, S., Johnston, K.P., 2021. Effect of surface chemistry of silica nanoparticles on contact angle of oil on calcite surfaces in concentrated brine with divalent ions. *J. Colloid Interface Sci.* 581, 656–668.
- Amaya, J., Rana, D., Hornof, V., 2002. Dynamic interfacial tension behavior of water/oil systems containing in situ-formed surfactants. *J. Solut. Chem.* 31 (2), 139–148.
- Ampomah, W., Balch, R., Cather, M., Rose-Coss, D., Dai, Z., Heath, J., Dowers, T., Mozley, P., 2016. Evaluation of  $\text{CO}_2$  storage mechanisms in  $\text{CO}_2$  enhanced oil recovery sites: application to Morrow sandstone reservoir. *Energy Fuel* 30 (10), 8545–8555.
- Anderson, W., 1986. Wettability literature survey-part 2: wettability measurement. *J. Pet. Technol.* 38 (11), 1246–1262.
- Anderson, W.G., 1987a. Wettability literature survey-part 4: effects of wettability on capillary pressure. *J. Pet. Technol.* 39 (10), 1283–1300.
- Anderson, W.G., 1987b. Wettability literature survey-part 6: the effects of wettability on waterflooding. *J. Pet. Technol.* 39 (12), 1605–1622.
- Anderson, W.G., 1987c. Wettability literature survey part 5: the effects of wettability on relative permeability. *J. Pet. Technol.* 39 (11), 1453–1468.
- Araujo, Y.C., Toledo, P.G., Leon, V., Gonzalez, H.Y., 1995. Wettability of silane-treated glass slides as determined from X-ray photoelectron spectroscopy. *J. Colloid Interface Sci.* 176 (2), 485–490.
- Arif, M., Al-Yaseri, A.Z., Barifcani, A., Lebedev, M., Iglauer, S., 2016a. Impact of pressure and temperature on  $\text{CO}_2$ -brine-mica contact angles and  $\text{CO}_2$ -brine interfacial tension: implications for carbon geo-sequestration. *J. Colloid Interface Sci.* 462, 208–215.
- Arif, M., Barifcani, A., Iglauer, S., 2016b. Solid/ $\text{CO}_2$  and solid/water interfacial tensions as a function of pressure, temperature, salinity and mineral type: implications for  $\text{CO}_2$ -wettability and  $\text{CO}_2$  geo-storage. *Int. J. Greenhouse Gas Control* 53, 263–273.
- Arif, M., Barifcani, A., Lebedev, M., Iglauer, S., 2016c. Structural trapping capacity of oil-wet caprock as a function of pressure, temperature and salinity. *Int. J. Greenhouse Gas Control* 50, 112–120.
- Arif, M., Jones, F., Barifcani, A., Iglauer, S., 2017a. Electrochemical investigation of the effect of temperature, salinity and salt type on brine/mineral interfacial properties. *Int. J. Greenhouse Gas Control* 59, 136–147.
- Arif, M., Lebedev, M., Barifcani, A., Iglauer, S., 2017b.  $\text{CO}_2$  storage in carbonates: wettability of calcite. *Int. J. Greenhouse Gas Control* 62, 113–121.
- Arif, M., Lebedev, M., Barifcani, A., Iglauer, S., 2017c. Influence of shale-total organic content on  $\text{CO}_2$  geo-storage potential. *Geophys. Res. Lett.* 44 (17), 8769–8775.
- Arif, M., Abu-Khamsin, S., Iglauer, S., 2019a. Wettability of rock/ $\text{CO}_2$ /brine and rock/oil/ $\text{CO}_2$ -enriched-brine systems: critical parametric analysis and future outlook. In: *Advances in Colloid and Interface Science*.
- Arif, M., Abu-Khamsin, S.A., Iglauer, S., 2019b. Wettability of rock/ $\text{CO}_2$ /brine and rock/oil/ $\text{CO}_2$ -enriched-brine systems: critical parametric analysis and future outlook. *Adv. Colloid Interf. Sci.* 268, 91–113.
- Arif, M., Abu-Khamsin, S.A., Zhang, Y., Iglauer, S., 2020. Experimental investigation of carbonate wettability as a function of mineralogical and thermo-physical conditions. *Fuel* 264, 116846.
- Arif, M., Zhang, Y., Iglauer, S., 2021. Shale wettability: data sets, challenges, and outlook. *Energy Fuel* 35 (4), 2965–2980.
- Awan, F.U.R., Keshavarz, A., Akhondzadeh, H., Al-Ansari, S.F., Al-Yaseri, A.Z., Nosrati, A., Ali, M., Iglauer, S., 2020. Stable dispersion of coal fines during hydraulic fracturing flowback in coal seam gas reservoirs—an experimental study. *Energy Fuel* 34 (5), 5566–5577.
- Awan, F.U.R., Keshavarz, A., Azhar, M.R., Akhondzadeh, H., Ali, M., Al-Yaseri, A., Abid, H.R., Iglauer, S., 2021. Adsorption of nanoparticles on glass bead surface for enhancing proppant performance: a systematic experimental study. *J. Mol. Liq.* 328, 115398.
- Bachu, S., Adams, J., 2003. Sequestration of  $\text{CO}_2$  in geological media in response to climate change: capacity of deep saline aquifers to sequester  $\text{CO}_2$  in solution. *Energy Convers. Manag.* 44 (20), 3151–3175.
- Bachu, S., Gunter, W., Perkins, E., 1994. Aquifer disposal of  $\text{CO}_2$ : hydrodynamic and mineral trapping. *Energy Convers. Manag.* 35 (4), 269–279.
- Beaumont, V., Robert, F., 1999. Nitrogen isotope ratios of kerogens in Precambrian cherts: a record of the evolution of atmosphere chemistry? *Precambrian Res.* 96 (1–2), 63–82.
- Bennett, P.C., Siegel, D., Baedecker, M.J., Hult, M., 1993. Crude oil in a shallow sand and gravel aquifer—I. Hydrogeology and inorganic geochemistry. *Appl. Geochem.* 8 (6), 529–549.
- Berger, P.M., Yoksoulian, L., Freiburg, J.T., Butler, S.K., Roy, W.R., 2019. Carbon sequestration at the Illinois Basin-Decatur Project: experimental results and geochemical simulations of storage. *Environ. Earth Sci.* 78 (22), 646.
- Bikkina, P.K., 2011. Contact angle measurements of  $\text{CO}_2$ -water-quartz/calcite systems in the perspective of carbon sequestration. *Int. J. Greenhouse Gas Control* 5 (5), 1259–1271.
- Bikkina, P.K., 2012. Reply to the comments on “Contact angle measurements of  $\text{CO}_2$ -water-quartz/calcite systems in the perspective of carbon sequestration”. *Int. J. Greenhouse Gas Control* 7, 263–264.
- Blunt, M., Fayers, F.J., Orr Jr., F.M., 1993. Carbon dioxide in enhanced oil recovery. *Energy Convers. Manag.* 34 (9–11), 1197–1204.
- Boden, T.A., Marland, G., Andres, R., 1995. Estimates of Global, Regional, and National Annual  $\text{CO}_2$  Emissions From Fossil-fuel Burning, Hydraulic Cement Production, and Gas Flaring, pp. 1950–1992.
- Britannica, T.E.O.E., 2017. Petroleum Trap. *Encyclopedia Britannica*.
- Brocks, J.J., 2011. Millimeter-scale concentration gradients of hydrocarbons in Archean shales: live-oil escape or fingerprint of contamination? *Geochim. Cosmochim. Acta* 75 (11), 3196–3213.
- Brocks, J.J., Buick, R., Logan, G.A., Summons, R.E., 2003a. Composition and syngeneity of molecular fossils from the 2.78 to 2.45 billion-year-old Mount Bruce Supergroup, Pilbara Craton, Western Australia. *Geochim. Cosmochim. Acta* 67 (22), 4289–4319.
- Brocks, J.J., Buick, R., Summons, R.E., Logan, G.A., 2003b. A reconstruction of Archean biological diversity based on molecular fossils from the 2.78 to 2.45 billion-year-old Mount Bruce Supergroup, Hamersley Basin, Western Australia. *Geochim. Cosmochim. Acta* 67 (22), 4321–4335.
- Brocks, J.J., Grosjean, E., Logan, G.A., 2008. Assessing biomarker syngeneity using branched alkanes with quaternary carbon (BAQCs) and other plastic contaminants. *Geochim. Cosmochim. Acta* 72 (3), 871–888.
- Broseta, D., Tonnet, N., Shah, V., 2012. Are rocks still water-wet in the presence of dense  $\text{CO}_2$  or  $\text{H}_2\text{S}$ ? *Geofluids* 12 (4), 280–294.
- Budisa, N., Schulze-Makuch, D., 2014. Supercritical carbon dioxide and its potential as a life-sustaining solvent in a planetary environment. *Life* 4 (3), 331–340.
- Bui, M., Adjiman, C.S., Bardow, A., Anthony, E.J., Boston, A., Brown, S., Fennell, P.S., Fuss, S., Galindo, A., Hackett, L.A., 2018. Carbon capture and storage (CCS): the way forward. *Energy Environ. Sci.* 11 (5), 1062–1176.
- Busch, A., Alles, S., Gensterblum, Y., Prinz, D., Dewhurst, D.N., Raven, M.D., Stanjek, H., Kroos, B.M., 2008. Carbon dioxide storage potential of shales. *Int. J. Greenhouse Gas Control* 2 (3), 297–308.
- Butt, H., Graf, K., Kappl, M., 2006. *Physics and Chemistry of Interfaces*. Wiley, Weinheim.
- Caballero, B., Trugo, L.C., Finglas, P.M., 2003. *Encyclopedia of Food Sciences and Nutrition*. Academic.
- Carré, A., Gastel, J.-C., Shanahan, M.E., 1996. Viscoelastic effects in the spreading of liquids. *Nature* 379 (6564), 432–434.
- Chahal, P., 2020. Global Warming and Greenhouse Effect. Conservation, Sustainability, and Environmental Justice in India, p. 95.
- Chalbaud, C., Robin, M., Lombard, J., Martin, F., Egermann, P., Bertin, H., 2009. Interfacial tension measurements and wettability evaluation for geological  $\text{CO}_2$  storage. *Adv. Water Resour.* 32 (1), 98–109.
- Chang, Y.-B., Coats, B.K., Nolen, J.S., 1996. A Compositional Model for  $\text{CO}_2$  Floods Including  $\text{CO}_2$  Solubility in Water, Permian Basin Oil and Gas Recovery Conference. Society of Petroleum Engineers.
- Chaturvedi, K.R., Sharma, T., 2020. Single-step silica nanofluid for improved carbon dioxide flow and reduced formation damage in porous media for carbon utilization. *Energy* 197, 117276.
- Chaudhary, K., Bayani Cardenas, M., Wolfe, W.W., Maisano, J.A., Ketcham, R.A., Bennett, P.C., 2013. Pore-scale trapping of supercritical  $\text{CO}_2$  and the role of grain wettability and shape. *Geophys. Res. Lett.* 40 (15), 3878–3882.
- Chen, Y., Sari, A., Xie, Q., Saeedi, A., 2019. Excess  $\text{H}^+$  increases hydrophilicity during  $\text{CO}_2$ -assisted enhanced oil recovery in sandstone reservoirs. *Energy Fuel* 33 (2), 814–821.
- Cheraghian, G., Hendraningrat, L., 2016. A review on applications of nanotechnology in the enhanced oil recovery part A: effects of nanoparticles on interfacial tension. *Int. Nano Lett.* 6 (2), 129–138.
- Chiquet, P., Broseta, D., Thibeau, S., 2007. Wettability alteration of caprock minerals by carbon dioxide. *Geofluids* 7 (2), 112–122.
- Chu, S., Majumdar, A., 2012. Opportunities and challenges for a sustainable energy future. *nature* 488 (7411), 294–303.
- Cyr, T., Strausz, O., 1984. Bound carboxylic acids in the Alberta oil sands. *Org. Geochem.* 7 (2), 127–140.
- Dahraj, N.U., Ali, M., Khan, M.N., 2016. End of Linear Flow Time Picking in Long Transient Hydraulically Fractured Wells to Correctly Estimate the Permeability, Fracture Half-length and Original Gas in Place in Liquid Rich Shales, PAPG/SPE Pakistan Section Annual Technical Conference and Exhibition. Society of Petroleum Engineers.
- Davis, S.J., Caldeira, K., Matthews, H.D., 2010. Future  $\text{CO}_2$  emissions and climate change from existing energy infrastructure. *Science* 329 (5997), 1330–1333.
- Davis, S., Williams, S., Boundy, R., 2016. Transportation Energy Data Book: Edition 35 (No. ORNL/TM-2016/470). Oak Ridge National Laboratory (ORNL), Oak Ridge.
- De, G.P., 1985. Wetting: statics and dynamics. *Rev. Mod. Phys.* 57 (3), 827.
- De, M., Ghosh, P.S., Rotello, V.M., 2008. Applications of nanoparticles in biology. *Adv. Mater.* 20 (22), 4225–4241.
- Dehghan Monfared, A., Ghazanfari, M.H., Jamialahmadi, M., Helalizadeh, A., 2016. Potential application of silica nanoparticles for wettability alteration of oil-wet calcite: a mechanistic study. *Energy Fuel* 30 (5), 3947–3961.
- dell'energia, A.I., 2010. *Energy Technology Perspectives 2010: Scenarios & Strategies to 2050* (ill).

- Derenne, S., Robert, F., Skrzypczak-Bonduelle, A., Gourier, D., Binet, L., Rouzaud, J.-N., 2008. Molecular evidence for life in the 3.5 billion year old Warrawoona chert. *Earth Planet. Sci. Lett.* 272 (1–2), 476–480.
- Ding, S., Xi, Y., Jiang, H., Liu, G., 2018. CO<sub>2</sub> storage capacity estimation in oil reservoirs by solubility and mineral trapping. *Appl. Geochem.* 89, 121–128.
- Donaldson, E.C., Alam, W., 2013. Wettability. Elsevier.
- Donaldson, E.C., Thomas, R.D., Lorenz, P.B., 1969. Wettability determination and its effect on recovery efficiency. *Soc. Pet. Eng. J.* 9 (01), 13–20.
- Druckenmiller, M.L., Maroto-Valer, M.M., Hill, M., 2006. Investigation of carbon sequestration via induced calcite formation in natural gas well brine. *Energy Fuel* 20 (1), 172–179.
- Durand, B., 2005. Carbon Dioxide Capture and Storage.
- El-Maghriby, R., Pentland, C., Iglauder, S., Blunt, M., 2012. A fast method to equilibrate carbon dioxide with brine at high pressure and elevated temperature including solubility measurements. *J. Supercrit. Fluids* 62, 55–59.
- El-sayed, G.M., Kamel, M., Morsy, N., Taher, F., 2012. Encapsulation of nano Disperse Red 60 via modified miniemulsion polymerization. I. Preparation and characterization. *J. Appl. Polym. Sci.* 125 (2), 1318–1329.
- Eral, H., Oh, J., 2013. Contact angle hysteresis: a review of fundamentals and applications. *Colloid Polym. Sci.* 291 (2), 247–260.
- Espinosa, D.N., Santamarina, J.C., 2010. Water-CO<sub>2</sub>-mineral systems: interfacial tension, contact angle, and diffusion—implications to CO<sub>2</sub> geological storage. *Water Resour. Res.* 46 (7).
- Fakoya, M.F., Shah, S.N., 2018. Effect of silica nanoparticles on the rheological properties and filtration performance of surfactant-based and polymeric fracturing fluids and their blends. *SPE Drill. Compleat.* 33 (02), 100–114.
- Farokhpour, R., Bjørkvik, B.J., Lindeberg, E., Torsæter, O., 2013. Wettability behaviour of CO<sub>2</sub> at storage conditions. *Int. J. Greenhouse Gas Control* 12, 18–25.
- Fathi, S.J., Aoustad, T., Strand, S., 2011. Effect of water-extractable carboxylic acids in crude oil on wettability in carbonates. *Energy Fuel* 25 (6), 2587–2592.
- Fauziah, C.A., Al-Khdheewi, E.A., Barifcani, A., Iglauder, S., 2019. Wettability measurements of mixed clay minerals at elevated temperature and pressure: implications for CO<sub>2</sub> geo-storage. In: SPE Gas & Oil Technology Showcase and Conference. Society of Petroleum Engineers.
- Fauziah, C.A., Al-Yaseri, A.Z., Jha, N.K., Lagat, C., Roshan, H., Barifcani, A., Iglauder, S., 2020. Carbon dioxide wettability of South West Hub sandstone, Western Australia: implications for carbon geo-storage. *Int. J. Greenhouse Gas Control* 98, 103064.
- Froehlich, P.N., Klinkhammer, G., Bender, M.L., Luedtke, N., Heath, G.R., Cullen, D., Dauphin, P., Hammond, D., Hartman, B., Maynard, V., 1979. Early oxidation of organic matter in pelagic sediments of the eastern equatorial Atlantic: suboxic diagenesis. *Geochim. Cosmochim. Acta* 43 (7), 1075–1090.
- Gaines, G.L., 1966. Insoluble Monolayers at Liquid-gas Interfaces.
- Garcia, S., Kaminska, S., Mercedes Maroto-Valer, M., 2010. Underground carbon dioxide storage in saline formations. In: Proceedings of the Institution of Civil Engineers-Waste and Resource Management. Thomas Telford Ltd, pp. 77–88.
- Garcia-Olvera, G., Reilly, T.M., Lehmann, T.E., Alvarado, V., 2016. Effects of asphaltenes and organic acids on crude oil-brine interfacial visco-elasticity and oil recovery in low-salinity waterflooding. *Fuel* 185, 151–163.
- Gauteplass, J., Almenningen, S., Ersland, G., Barth, T., Yang, J., Chapoy, A., 2020. Multiscale investigation of CO<sub>2</sub> hydrate self-sealing potential for carbon geo-sequestration. *Chem. Eng. J.* 381, 122646.
- Gerard, E., Moreira, D., Philippot, P., Van Kranendonk, M.J., Lopez-Garcia, P., 2009. Modern subsurface bacteria in pristine 2.7 Ga-old fossil stromatolite drillcore samples from the Fortescue Group, Western Australia. *PLoS One* 4 (4), e5298.
- Gerber, P.J., Henderson, B., Makkar, H.P., 2013. Mitigation of Greenhouse Gas Emissions in Livestock Production: A Review of Technical Options for Non-CO<sub>2</sub> Emissions. Food and Agriculture Organization of the United Nations (FAO).
- Gislason, S.R., Oelkers, E.H., 2014. Carbon storage in basalt. *Science* 344 (6182), 373–374.
- Gislason, S.R., Wolff-Boenisch, D., Stefansson, A., Oelkers, E.H., Gunnlaugsson, E., Sigurdardottir, H., Sigfusson, B., Broecker, W.S., Matter, J.M., Stute, M., 2010. Mineral sequestration of carbon dioxide in basalt: a pre-injection overview of the CarbFix project. *Int. J. Greenhouse Gas Control* 4 (3), 537–545.
- Gislason, S.R., Sigurdardottir, H., Aradottir, E.S., Oelkers, E.H., 2018. A brief history of CarbFix: challenges and victories of the project's pilot phase. *Energy Proc.* 146, 103–114.
- Godec, M.L., Kuuskraa, V.A., Dipietro, P., 2013. Opportunities for using anthropogenic CO<sub>2</sub> for enhanced oil recovery and CO<sub>2</sub> storage. *Energy Fuel* 27 (8), 4183–4189.
- Golding, S., Uysal, I., Boreham, C., Kirste, D., Baublys, K., Esterle, J., 2011. Adsorption and mineral trapping dominate CO<sub>2</sub> storage in coal systems. *Energy Proc.* 4, 3131–3138.
- Gomari, K.R., Hamouda, A., 2006. Effect of fatty acids, water composition and pH on the wettability alteration of calcite surface. *J. Pet. Sci. Eng.* 50 (2), 140–150.
- Good, R.J., Girifalco, L., 1960. A theory for estimation of surface and interfacial energies. III. Estimation of surface energies of solids from contact angle data. *J. Phys. Chem.* 64 (5), 561–565.
- Goodman, A., Sanguinito, S., Kutchko, B., Natesakhawat, S., Cvetic, P., Allen, A.J., 2020. Shale pore alteration: Potential implications for hydrocarbon extraction and CO<sub>2</sub> storage. *Fuel* 265, 116930.
- Grate, J.W., Dehoff, K.J., Warner, M.G., Pittman, J.W., Wietsma, T.W., Zhang, C., Oostrom, M., 2012. Correlation of oil–water and air–water contact angles of diverse silanized surfaces and relationship to fluid interfacial tensions. *Langmuir* 28 (18), 7182–7188.
- Grim, C., 2017. Cape Grim Greenhouse Gas Web Data.
- Gunning, J., Ennis-King, J., LaForce, T., Jenkins, C., Paterson, L., 2020. Bayesian well-test 2D tomography inversion for CO<sub>2</sub> plume detection. *Int. J. Greenhouse Gas Control* 94, 102804.
- Gunter, W.D., Bachu, S., Benson, S., 2004. The role of hydrogeological and geochemical trapping in sedimentary basins for secure geological storage of carbon dioxide. *Geol. Soc. Lond. Spec. Publ.* 233 (1), 129–145.
- Gutiérrez, F., Lizaga, I., 2016. Sinkholes, collapse structures and large landslides in an active salt dome submerged by a reservoir: the unique case of the Ambal ridge in the Karun River, Zagros Mountains, Iran. *Geomorphology* 254, 88–103.
- Haghghi, O.M., Zargar, G., Khaksar Manshad, A., Ali, M., Takassi, M.A., Ali, J.A., Keshavarz, A., 2020. Effect of environment-friendly non-ionic surfactant on interfacial tension reduction and wettability alteration; implications for enhanced oil recovery. *Energies* 13 (15), 3988.
- Hamouda, A.A., Rezaei Gomari, K.A., 2006. Influence of temperature on wettability alteration of carbonareous reservoirs. In: SPE/DOE Symposium on Improved Oil Recovery. Society of Petroleum Engineers.
- Hansen, G., Hamouda, A., Denoyel, R., 2000. The effect of pressure on contact angles and wettability in the mica/water/n-decane system and the calcite+ stearic acid/water/n-decane system. *Colloids Surf. A Physicochem. Eng. Asp.* 172 (1–3), 7–16.
- Herrero, M., Henderson, B., Havlik, P., Thornton, P.K., Conant, R.T., Smith, P., Wirsenius, S., Hristov, A.N., Gerber, P., Gill, M., 2016. Greenhouse gas mitigation potentials in the livestock sector. *Nat. Clim. Chang.* 6 (5), 452–461.
- Hinkle, H., Hargett, T., Bailon, W., 2017. BamCore and Global Warming. BamCore, Windsor.
- Hoeland, S., Barth, T., Blokhuis, A., Skauge, A., 2001. The effect of crude oil acid fractions on wettability as studied by interfacial tension and contact angles. *J. Pet. Sci. Eng.* 30 (2), 91–103.
- Holloway, S., 2007. Carbon dioxide capture and geological storage. *Philos. Trans. R. Soc. A Math. Phys. Eng. Sci.* 365 (1853), 1095–1107.
- Huang, W., Chen, W., Anandarajah, G., 2017. The role of technology diffusion in a decarbonizing world to limit global warming to well below 2 C: an assessment with application of Global TIMES model. *Appl. Energy* 208, 291–301.
- Hussain, M., Butt, A.R., Uzma, F., Ahmed, R., Islam, T., Yousaf, B., 2019. A comprehensive review of sectorial contribution towards greenhouse gas emissions and progress in carbon capture and storage in Pakistan. *Greenhouse Gas*. 9 (4), 617–636.
- Idouw, N., Long, H., Øren, P.-E., Carnerup, A.M., Fogden, A., Bondino, I., Sundal, L., AS, D.N., 2015. Wettability analysis using micro-CT, FESEM and QEMSCAN, and its applications to digital rock physics. In: International Symposium of the Society of Core Analysts, pp. 16–21.
- IEA, 2020. Global Energy Review 2020. IEA, Paris.
- Iglauder, S., 2011. Dissolution Trapping of Carbon Dioxide in Reservoir Formation Brine—A Carbon Storage Mechanism, Mass Transfer—advanced Aspects. InTechOpen 48 (3), e2020GL090814.
- Iglauder, S., 2017. CO<sub>2</sub>–water–rock wettability: variability, influencing factors, and implications for CO<sub>2</sub> geostorage. *Acc. Chem. Res.* 50 (5), 1134–1142.
- Iglauder, S., 2018. Optimum storage depths for structural CO<sub>2</sub> trapping. *Int. J. Greenhouse Gas Control* 77, 82–87.
- Iglauder, S., Wülling, W., Pentland, C.H., Al-Mansoori, S.K., Blunt, M.J., 2011. Capillary-trapping capacity of sandstones and sandpacks. *SPE J.* 16 (04), 778–783.
- Iglauder, S., Ferno, M., Shearing, P., Blunt, M., 2012a. Comparison of residual oil cluster size distribution, morphology and saturation in oil-wet and water-wet sandstone. *J. Colloid Interface Sci.* 375 (1), 187–192.
- Iglauder, S., Mathew, M., Bresme, F., 2012b. Molecular dynamics computations of brine–CO<sub>2</sub> interfacial tensions and brine–CO<sub>2</sub>–quartz contact angles and their effects on structural and residual trapping mechanisms in carbon geo-sequestration. *J. Colloid Interface Sci.* 386 (1), 405–414.
- Iglauder, S., Salamat, A., Sarmadivaleh, M., Liu, K., Phan, C., 2014. Contamination of silica surfaces: impact on water–CO<sub>2</sub>–quartz and glass contact angle measurements. *Int. J. Greenhouse Gas Control* 22, 325–328.
- Iglauder, S., Al-Yaseri, A.Z., Rezaee, R., Lebedev, M., 2015a. CO<sub>2</sub> wettability of caprocks: implications for structural storage capacity and containment security. *Geophys. Res. Lett.* 42 (21), 9279–9284.
- Iglauder, S., Pentland, C., Busch, A., 2015b. CO<sub>2</sub> wettability of seal and reservoir rocks and the implications for carbon geo-sequestration. *Water Resour. Res.* 51 (1), 729–774.
- Iglauder, S., Paluszny, A., Rahman, T., Zhang, Y., Wülling, W., Lebedev, M., 2019. Residual trapping of CO<sub>2</sub> in an oil-filled, oil-wet sandstone core: results of three-phase pore-scale imaging. *Geophys. Res. Lett.* 46 (20), 11146–11154.
- Iglauder, S., Ali, M., Keshavarz, A., 2020. Hydrogen wettability of sandstone reservoirs: implications for hydrogen geo-storage. *Geophys. Res. Lett.* 48 (3), e2020GL090814.
- III, I.P.O.C.C.W.G., 2013. IPCC Special Report on Carbon Dioxide Capture and Storage. Published for the Intergovernmental Panel on Climate Change, Cambridge.
- Illing, C.J., Hallmann, C., Miller, K.E., Summons, R.E., Strauss, H., 2014. Airborne hydrocarbon contamination from laboratory atmospheres. *Org. Geochem.* 76, 26–38.
- Ingrossi, F., Ruiz-López, M.F., 2017. Modeling solvation in supercritical CO<sub>2</sub>. *ChemPhysChem* 18 (19), 2560–2572.
- Jackson, M.D., Valvatne, P.H., Blunt, M.J., 2005. Prediction of wettability variation within an oil/water transition zone and its impact on production. *SPE J.* 10 (02), 185–195.
- Jadhunandan, P., Morrow, N.R., 1995. Effect of wettability on waterflood recovery for crude-oil/brine/rock systems. *SPE Reserv. Eng.* 10 (01), 40–46.
- Jardine, P., McCarthy, J., Weber, N., 1989. Mechanisms of dissolved organic carbon adsorption on soil. *Soil Sci. Soc. Am. J.* 53 (5), 1378–1385.

- Jha, N.K., Iglauer, S., Sangwai, J.S., 2017. Effect of monovalent and divalent salts on the interfacial tension of n-heptane against aqueous anionic surfactant solutions. *J. Chem. Eng. Data* 63 (7), 2341–2350.
- Jha, N., Ali, M., Sarmadivaleh, M., Iglauer, S., Barifcani, A., Lebedev, M., Sangwai, J., 2018. Low salinity surfactant nanofluids for enhanced CO<sub>2</sub> storage application at high pressure and temperature. In: Fifth CO<sub>2</sub> Geological Storage Workshop. European Association of Geoscientists & Engineers, pp. 1–4.
- Jha, N.K., Ali, M., Iglauer, S., Lebedev, M., Roshan, H., Barifcani, A., Sangwai, J.S., Sarmadivaleh, M., 2019a. Wettability alteration of quartz surface by low-salinity surfactant nanofluids at high-pressure and high-temperature conditions. *Energy Fuel* 33 (8), 7062–7068.
- Jha, N.K., Iglauer, S., Barifcani, A., Sarmadivaleh, M., Sangwai, J.S., 2019b. Low-salinity surfactant nanofluid formulations for wettability alteration of sandstone: role of the SiO<sub>2</sub> nanoparticle concentration and divalent cation/SO<sub>4</sub><sup>2-</sup>-ratio. *Energy Fuel* 33 (2), 739–746.
- Jha, N.K., Lebedev, M., Iglauer, S., Ali, M., Roshan, H., Barifcani, A., Sangwai, J.S., Sarmadivaleh, M., 2020a. Pore scale investigation of low salinity surfactant nanofluid injection into oil saturated sandstone via X-ray micro-tomography. *J. Colloid Interface Sci.* 562, 370–380.
- Jha, N.K., Lebedev, M., Iglauer, S., Sangwai, J.S., Sarmadivaleh, M., 2020b. In situ wettability investigation of aging of sandstone surface in alkane via X-ray microtomography. *Energies* 13 (21), 5594.
- Jha, N.K., Ivanova, A., Lebedev, M., Barifcani, A., Cheremisin, A., Iglauer, S., Sangwai, J.S., Sarmadivaleh, M., 2021. Interaction of low salinity surfactant nanofluids with carbonate surfaces and molecular level dynamics at fluid-fluid interface at ScCO<sub>2</sub> loading. *J. Colloid Interface Sci.* 586, 315–325.
- Ji, X., Zhu, C., 2015. CO<sub>2</sub> storage in deep saline aquifers. In: NOVEL Materials for Carbon Dioxide Mitigation Technology. Elsevier, pp. 299–332.
- Jing, J., Yang, Y., Tang, Z., 2021. Assessing the influence of injection temperature on CO<sub>2</sub> storage efficiency and capacity in the sloping formation with fault. *Energy* 215, 119097.
- Johnson, B.F., 2003. Nanoparticles in catalysis. *Top. Catal.* 24 (1), 147–159.
- Jones, D., Head, I., Gray, N., Adams, J., Rowan, A., Aitken, C., Bennett, B., Huang, H., Brown, A., Bowler, B., 2008. Crude-oil biodegradation via methanogenesis in subsurface petroleum reservoirs. *Nature* 451 (7175), 176–180.
- Juanes, R., Spiteri, E., Orr Jr., F., Blunt, M., 2006. Impact of relative permeability hysteresis on geological CO<sub>2</sub> storage. *Water Resour. Res.* 42 (12).
- Jung, J.-W., Wan, J., 2012. Supercritical CO<sub>2</sub> and ionic strength effects on wettability of silica surfaces: Equilibrium contact angle measurements. *Energy Fuel* 26 (9), 6053–6059.
- Kalam, S., Olaiyiwola, T., Al-Rubaii, M.M., Amaechi, B.I., Jamal, M.S., Awotunde, A.A., 2020. Carbon dioxide sequestration in underground formations: review of experimental, modeling, and field studies. *J. Petrol. Explor. Product. Technol.* 1–23.
- Kang, S.M., Fathi, E., Ambrose, R.J., Akkutlu, I.Y., Sigal, R.F., 2011. Carbon dioxide storage capacity of organic-rich shales. *SPE J.* 16 (4), 842–855.
- Karl, T.R., Melillo, J.M., Peterson, T.C., Hassel, S.J., 2009. Global Climate Change Impacts in the United States. Cambridge University Press.
- Kaveh, N.S., Wolf, K., Ashrafizadeh, S., Rudolph, E., 2012. Effect of coal petrology and pressure on wetting properties of wet coal for CO<sub>2</sub> and flue gas storage. *Int. J. Greenhouse Gas Control* 11, S91–S101.
- Kazemifar, F., Blois, G., Kyritsis, D.C., Christensen, K.T., 2016. Quantifying the flow dynamics of supercritical CO<sub>2</sub>-water displacement in a 2D porous micromodel using fluorescent microscopy and microscopic PIV. *Adv. Water Resour.* 95, 352–368.
- Keshavarz, A., Abid, H., Ali, M., Iglauer, S., 2022. Hydrogen diffusion in coal: implications for hydrogen geo-storage. *J. Colloid Interface Sci.* 608, 1457–1462.
- Kharaka, Y.K., Thorsen, J.J., Hovorka, S.D., Nance, H.S., Cole, D.R., Phelps, T.J., Knauss, K.G., 2009. Potential environmental issues of CO<sub>2</sub> storage in deep saline aquifers: Geochemical results from the Frio-I Brine Pilot test, Texas, USA. *Appl. Geochem.* 24 (6), 1106–1112.
- King, M., Bott, T.R., 2012. Extraction of Natural Products Using Near-critical Solvents. Springer Science & Business Media.
- Klutse, N.A.B., Ajayi, V.O., Gboganiyi, E.O., Egbebiyi, T.S., Kouadio, K., Nkrumah, F., Quagrainie, K.A., Olusegun, C., Diasso, U., Abiodun, B.J., 2018. Potential impact of 1.5 C and 2 C global warming on consecutive dry and wet days over West Africa. *Environ. Res. Lett.* 13 (5), 055013.
- Krevor, S.C., Pini, R., Zuo, L., Benson, S.M., 2012. Relative permeability and trapping of CO<sub>2</sub> and water in sandstone rocks at reservoir conditions. *Water Resour. Res.* 48 (2).
- Krever, S., Blunt, M.J., Benson, S.M., Pentland, C.H., Reynolds, C., Al-Mehdhi, A., Niu, B., 2015. Capillary trapping for geologic carbon dioxide storage—from pore scale physics to field scale implications. *Int. J. Greenhouse Gas Control* 40, 221–237.
- Kuang, W., Saraji, S., Piri, M., 2020. Nanofluid-induced wettability gradient and imbibition enhancement in natural porous media: a pore-scale experimental investigation. *Transp. Porous Media* 134 (3), 593–619.
- Kuhn, H., Möbius, D., 1971. Systems of monomolecular layers—assembling and physico-chemical behavior. *Angew. Chem. Int. Ed. Engl.* 10 (9), 620–637.
- Kumar, A., Noh, M., Pope, G., Sepehrnoori, K., Bryant, S., Lake, L., 2004. Reservoir simulation of CO<sub>2</sub> storage in deep saline aquifers. In: SPE/DOE Symposium on Improved Oil Recovery. Society of Petroleum Engineers.
- Kumar, A., Malik, G., Goyal, K., Sardana, N., Chandra, R., Mulik, R.S., 2020. Controllable synthesis of tunable aspect ratios novel h-BN nanorods with an enhanced wetting performance for water repellent applications. *Vacuum* 184, 109927.
- Kvenvolden, K.A., 1967. Normal fatty acids in sediments. *J. Am. Oil Chem. Soc.* 44 (11), 628–636.
- Lackner, K.S., 2003. A guide to CO<sub>2</sub> sequestration. *Science* 300 (5626), 1677–1678.
- Lander, L.M., Siewierski, L.M., Brittain, W.J., Vogler, E.A., 1993. A systematic comparison of contact angle methods. *Langmuir* 9 (8), 2237–2239.
- Legens, C., Toulhoat, H., Cuiec, L., Villieras, F., Palermo, T., 1999. Wettability change related to adsorption of organic acids on calcite: experimental and ab initio computational studies. *SPE J.* 4 (04), 328–333.
- Lemonnier, P., Ainsworth, E.A., 2018. Crop responses to rising atmospheric [CO<sub>2</sub>] and global climate change. In: Food Security and Climate Change. John Wiley & Sons Ltd., Chichester, pp. 51–69.
- Li, W., Nan, Y., Zhang, Z., You, Q., Jin, Z., 2020a. Hydrophilicity/hydrophobicity driven CO<sub>2</sub> solubility in kaolinite nanopores in relation to carbon sequestration. *Chem. Eng. J.* 398, 125449.
- Li, W., Zhang, M., Nan, Y., Pang, W., Jin, Z., 2020b. Molecular Dynamics Study on CO<sub>2</sub> Storage in Water-filled Kerogen Nanopores in Shale Reservoirs: Effects of Kerogen Maturity and Pore Size. *Langmuir*.
- Lindeberg, E., Wessel-Berg, D., 1997. Vertical convection in an aquifer column under a gas cap of CO<sub>2</sub>. *Energy Convers. Manag.* 38, S229–S234.
- Liu, Q., Maroto-Valer, M.M., 2011. Parameters affecting mineral trapping of CO<sub>2</sub> sequestration in brines. *Greenhouse Gas* 1 (3), 211–222.
- Liu, Y., Sun, C., Bolin, T., Wu, T., Liu, Y., Sternberg, M., Sun, S., Lin, X.-M., 2013. Kinetic pathway of palladium nanoparticle sulfidation process at high temperatures. *Nano Lett.* 13 (10), 4893–4901.
- Lohse, S.E., Murphy, C.J., 2012. Applications of colloidal inorganic nanoparticles: from medicine to energy. *J. Am. Chem. Soc.* 134 (38), 15607–15620.
- Looyestijn, W.J., 2008. Wettability index determination from NMR logs. *Petrophysics* 49 (02).
- Lord, D., Demond, A., Hayes, K., 2000. Effects of organic base chemistry on interfacial tension, wettability, and capillary pressure in multiphase subsurface waste systems. *Transp. Porous Media* 38 (1), 79–92.
- Louk, K., Ripepi, N., Luxbacher, K., Gilliland, E., Tang, X., Keles, C., Schlosser, C., Diminick, E., Keim, S., Amante, J., 2017. Monitoring CO<sub>2</sub> storage and enhanced gas recovery in unconventional shale reservoirs: results from the Morgan County, Tennessee injection test. *J. Nat. Gas Sci. Eng.* 45, 11–25.
- Love, J.C., Estroff, L.A., Kriebel, J.K., Nuzzo, R.G., Whitesides, G.M., 2005. Self-assembled monolayers of thiols on metals as a form of nanotechnology. *Chem. Rev.* 105 (4), 1103–1170.
- Lu, Y., Najafabadi, N.F., Firoozabadi, A., 2017. Effect of temperature on wettability of oil/brine/rock systems. *Energy Fuel* 31 (5), 4989–4995.
- Lundegård, P.D., Kharaka, Y.K., 1994. Distribution and occurrence of organic acids in subsurface waters. In: Organic Acids in Geological Processes. Springer, pp. 40–69.
- Maboudian, R., Howe, R.T., 1997. Critical review: adhesion in surface micromechanical structures. *J. Vacuum Sci. Technol. B* 15 (1), 1–20.
- MacAllister, D.J., Miller, K.C., Graham, S.K., Yang, C.-T., 1993. Application of X-ray CT scanning to determine gas/water relative permeabilities. *SPE Form. Eval.* 8 (03), 184–188.
- Mackay, E.J., 2013. Modelling the injectivity, migration and trapping of CO<sub>2</sub> in carbon capture and storage (CCS). In: Geological Storage of Carbon Dioxide (CO<sub>2</sub>). Elsevier, pp. 45–70.
- Madsen, L., Ida, I., 1998. Adsorption of carboxylic acids on reservoir minerals from organic and aqueous phase. *SPE Reserv. Eval. Eng.* 1 (01), 47–51.
- Mahadevan, J., 2012. Comments on the paper titled “Contact angle measurements of CO<sub>2</sub>-water-quartz/calcite systems in the perspective of carbon sequestration”: a case of contamination? *Int. J. Greenhouse Gas Control* 7, 261–262.
- Mahesar, A.A., Ali, M., Shar, A.M., Memon, K.R., Mohanty, U.S., Akhondzadeh, H., Tunio, A.H., Iglauer, S., Keshavarz, A., 2020a. Effect of cryogenic liquid nitrogen on the morphological and petrophysical characteristics of tight gas sandstone rocks from kirthar fold belt, Indus Basin, Pakistan. *Energy Fuels* 34 (11), 14548–14559.
- Mahesar, A.A., Shar, A.M., Ali, M., Tunio, A.H., Uqailli, M.A., Mohanty, U.S., Akhondzadeh, H., Iglauer, S., Keshavarz, A., 2020b. Morphological and petro physical estimation of eocene tight carbonate formation cracking by cryogenic liquid nitrogen; a case study of Lower Indus basin, Pakistan. *J. Pet. Sci. Eng.*, 107318.
- Marmur, A., 2006. Soft contact: measurement and interpretation of contact angles. *Soft Matter* 2 (1), 12–17.
- Marshall, C.P., Love, G.D., Snape, C.E., Hill, A.C., Allwood, A.C., Walter, M.R., Van Kranendonk, M.J., Bowden, S.A., Sylva, S.P., Summons, R.E., 2007. Structural characterization of kerogen in 3.4 Ga Archaean cherts from the Pilbara Craton, Western Australia. *Precambrian Res.* 155 (1–2), 1–23.
- Matter, J.M., Kelemen, P.B., 2009. Permanent storage of carbon dioxide in geological reservoirs by mineral carbonation. *Nat. Geosci.* 2 (12), 837–841.
- Matter, J.M., Takahashi, T., Goldberg, D., 2007. Experimental evaluation of in situ CO<sub>2</sub>-water-rock reactions during CO<sub>2</sub> injection in basaltic rocks: implications for geological CO<sub>2</sub> sequestration. *Geochim. Geophys. Geosyst.* 8 (2).
- Matter, J.M., Stute, M., Snæbjörnsdóttir, S.Ó., Oelkers, E.H., Gislason, S.R., Aradottir, E. S., Sigfusson, B., Gunnarsson, I., Sigurdardottir, H., Gunnlaugsson, E., 2016. Rapid carbon mineralization for permanent disposal of anthropogenic carbon dioxide emissions. *Science* 352 (6291), 1312–1314.
- Matthews, H.D., Gillett, N.P., Stott, P.A., Zickfeld, K., 2009. The proportionality of global warming to cumulative carbon emissions. *Nature* 459 (7248), 829–832.
- McCaffery, F., Bennion, D., 1974. The effect of wettability on two-phase relative penneabilities. *J. Can. Pet. Technol.* 13 (04).
- McGowan, C.W., Pearce, R.C., Diehl, H., 1985. A comparison of the dissolution of model compounds and the kerogen of Green River oil shale by oxidation with perchloric acid—a model for the kerogen of Green River oil shale. *Fuel Process. Technol.* 10 (2), 195–204.
- Meinshausen, M., Meinshausen, N., Hare, W., Raper, S.C., Frieler, K., Knutti, R., Frame, D.J., Allen, M.R., 2009. Greenhouse-gas emission targets for limiting global warming to 2 °C. *Nature* 458 (7242), 1158–1162.
- Memon, K.R., Mahesar, A.A., Ali, M., Tunio, A.H., Mohanty, U.S., Akhondzadeh, H., Awan, F.U.R., Iglauer, S., Keshavarz, A., 2020. Influence of cryogenic liquid nitrogen

- on petro-physical characteristics of mancos shale: an experimental investigation. *Energy Fuel* 34 (2), 2160–2168.
- Memon, K.R., Ali, M., Awan, F.U.R., Mahesar, A.A., Abbasi, G.R., Mohanty, U.S., Akhondzadeh, H., Tunio, A.H., Iglauer, S., Keshavarz, A., 2021a. Influence of cryogenic liquid nitrogen cooling and thermal shocks on petro-physical and morphological characteristics of Eagle Ford shale. *J. Nat. Gas Sci. Eng.*, 104313.
- Memon, S., Feng, R., Ali, M., Bhatti, M.A., Giweli, A., Keshavarz, A., Xie, Q., Sarmadivaleh, M., 2021b. Supercritical CO<sub>2</sub>-Shale interaction induced natural fracture closure: implications for scCO<sub>2</sub> hydraulic fracturing in shales. *Fuel*, 122682.
- Meredith, W., Kelland, S.-J., Jones, D., 2000. Influence of biodegradation on crude oil acidity and carboxylic acid composition. *Org. Geochem.* 31 (11), 1059–1073.
- Metz, B., Davidson, O., De Coninck, H., 2005. Carbon Dioxide Capture and Storage: Special Report of the Intergovernmental Panel on Climate Change. Cambridge University Press.
- Mills, J., Riazi, M., Sohrabi, M., 2011. Wettability of common rock-forming minerals in a CO<sub>2</sub>-brine system at reservoir conditions. In: International Symposium of the Society of Core Analysts. Society of Core Analysts Fredericton, Canada, pp. 19–21.
- Mohanty, U.S., Ali, M., Azhar, M.R., Al-Yaseri, A., Keshavarz, A., Iglauer, S., 2021a. Current advances in syngas (CO + H<sub>2</sub>) production through bi-reforming of methane using various catalysts: a review. *Int. J. Hydrogen Energy* 46 (65), 32809–32845.
- Mohanty, U.S., Awan, F.U.R., Ali, M., Aftab, A., Keshavarz, A., Iglauer, S., 2021b. Physicochemical characterization of zirconia nanoparticle-based sodium alginate polymer suspension for enhanced oil recovery. *Energy Fuel*.
- Morrow, N.R., 1990. Wettability and its effect on oil recovery. *J. Pet. Technol.* 42 (12), 1476–1484.
- Muller, É., Thomazo, C., Stüeken, E.E., Hallmann, C., Leider, A., Chaduteau, C., Buick, R., Baton, F., Philippot, P., Ader, M., 2018. Bias in carbon concentration and δ<sup>13</sup>C measurements of organic matter due to cleaning treatments with organic solvents. *Chem. Geol.* 493, 405–412.
- Mwangi, P., Brady, P.V., Radonjic, M., Thyne, G., 2018. The effect of organic acids on wettability of sandstone and carbonate rocks. *J. Pet. Sci. Eng.* 165, 428–435.
- Naik, S., Malgaresi, G., You, Z., Bedrikovetsky, P., 2018. Well productivity enhancement by applying nanofluids for wettability alteration. *APPEA J.* 58 (1), 121–129.
- NASA, NOAA, 2016. Warmest Year on Record Globally.
- Nazarahari, M.J., Manshad, A.K., Ali, M., Ali, J.A., Shafiei, A., Sajadi, S.M., Moradi, S., Iglauer, S., Keshavarz, A., 2021. Impact of a novel biosynthesized nanocomposite (SiO<sub>2</sub>@ Montmorillonite@ Xanthan) on wettability shift and interfacial tension: applications for enhanced oil recovery. *Fuel* 298, 120773.
- Neumann, A., Good, R., 1972. Thermodynamics of contact angles. I. Heterogeneous solid surfaces. *J. Colloid Interface Sci.* 38 (2), 341–358.
- Newell, R., Raimi, D., Aldana, G., 2019. Global energy outlook 2019: the next generation of energy. *Resour. Future* 8–19.
- Nordhaus, W., 2014. A Question of Balance: Weighing the Options on Global Warming Policies. Yale University Press.
- Nunes, L.J., Meireles, C.I., Pinto Gomes, C.J., Almeida Ribeiro, N., 2020. Forest contribution to climate change mitigation: management oriented to carbon capture and storage. *Climate* 8 (2), 21.
- Nwidue, L., Al-Anssari, S., Barifcane, A., Sarmadivaleh, M., Iglauer, S., 2016. Nanofluids for enhanced oil recovery processes: wettability alteration using zirconium oxide. In: Offshore Technology Conference Asia. Offshore Technology Conference.
- Nwidue, L.N., Al-Anssari, S., Barifcane, A., Sarmadivaleh, M., Lebedev, M., Iglauer, S., 2017. Nanoparticles influence on wetting behaviour of fractured limestone formation. *J. Pet. Sci. Eng.* 149, 782–788.
- Orr, F.M., 2009. Onshore geologic storage of CO<sub>2</sub>. *Science* 325 (5948), 1656–1658.
- Page, B., Turan, G., Zapantis, A., Burrows, J., Consoli, C., Erikson, J., Havercroft, I., Kearns, D., Liu, H., Rassool, D., 2020. The Global Status of CCS 2020: Vital to Achieve Net Zero.
- Pai, N., Zhang, X., Ali, M., Mandal, A., Hoteit, H., 2022. Carbon dioxide Thickening: A Review of Technological aspects. *Advances and Challenges for Oilfield application. Fuel*.
- Pai, N., Mandal, A., 2020. Oil recovery mechanisms of Pickering nanoemulsions stabilized by surfactant-polymer-nanoparticle assemblies: a versatile surface energies' approach. *Fuel* 276, 118138.
- Pai, N., Kumar, N., Mandal, A., 2019a. Stabilization of dispersed oil droplets in nanoemulsions by synergistic effects of the gemini surfactant, PHPA polymer, and silica nanoparticle. *Langmuir* 35 (7), 2655–2667.
- Pai, N., Kumar, N., Saw, R.K., Mandal, A., 2019b. Gemini surfactant/polymer/silica stabilized oil-in-water nanoemulsions: Design and physicochemical characterization for enhanced oil recovery. *J. Pet. Sci. Eng.* 183, 106464.
- Pan, B., Li, Y., Zhang, M., Wang, X., Iglauer, S., 2020. Effect of total organic carbon (TOC) content on shale wettability at high pressure and high temperature conditions. *J. Pet. Sci. Eng.* 193, 107374.
- Pearce, J., Underschultz, J., La Croix, A., 2019. Mineralogy, Geochemical CO<sub>2</sub>-water-rock Reactions and Associated Characterisation.
- Pentland, C., El-Maghriby, R., Georgiadis, A., Iglauer, S., Blunt, M., 2011a. Immiscible displacements and capillary trapping in CO<sub>2</sub> storage. *Energy Proc.* 4, 4969–4976.
- Pentland, C.H., El-Maghriby, R., Iglauer, S., Blunt, M.J., 2011b. Measurements of the capillary trapping of super-critical carbon dioxide in Berea sandstone. *Geophys. Res. Lett.* 38 (6).
- Pentland, C.H., Iglauer, S., Gharbi, O., Okada, K., Suekane, T., 2012. The influence of pore space geometry on the entrapment of carbon dioxide by capillary forces. In: SPE Asia Pacific Oil and Gas Conference and Exhibition. Society of Petroleum Engineers.
- Plaisant, A., Maiu, A., Maggio, E., Pettinai, A., 2017. Pilot-scale CO<sub>2</sub> sequestration test site in the Sulcis Basin (SW Sardinia): preliminary site characterization and research program. *Energy Procedia* 114, 4508–4517.
- Porrostami, R., Zahedi Amiri, G., Etemad, V., 2020. Spatial variability of carbon storage and sequestration in leaf litter and layers of soil in the forest area of Jahannama Park. *Iran. J. Forest* 12 (3), 317–330.
- Qin, C., Jiang, Y., Luo, Y., Zhou, J., Liu, H., Song, X., Li, D., Zhou, F., Xie, Y., 2020a. Effect of supercritical CO<sub>2</sub> saturation pressures and temperatures on the methane adsorption behaviours of Longmaxi shale. *Energy* 206, 118150.
- Qin, T., Goual, L., Piri, M., Hu, Z., Wen, D., 2020b. Nanoparticle-stabilized microemulsions for enhanced oil recovery from heterogeneous rocks. *Fuel* 274, 117830.
- Rackley, S.A., 2017. Carbon Capture and Storage. Butterworth-Heinemann.
- Rahman, T., Lebedev, M., Barifcane, A., Iglauer, S., 2016. Residual trapping of supercritical CO<sub>2</sub> in oil-wet sandstone. *J. Colloid Interface Sci.* 469, 63–68.
- Rao, Z., Bao, S., Liu, X., Taylor, R.A., Liao, S., 2020. Estimating allowable energy flux density for the supercritical carbon dioxide solar receiver: a service life approach. *Appl. Therm. Eng.* 182, 116024.
- Reddy, K.R., Gopakumar, A., Chetri, J.K., 2019. Critical review of applications of iron and steel slags for carbon sequestration and environmental remediation. *Rev. Environ. Sci. Biotechnol.* 18 (1), 127–152.
- Rezk, M.G., Foroozesh, J., Zivar, D., Mumtaz, M., 2019. CO<sub>2</sub> storage potential during CO<sub>2</sub> enhanced oil recovery in sandstone reservoirs. *J. Nat. Gas Sci. Eng.* 66, 233–243.
- Riaz, A., Cinar, Y., 2014. Carbon dioxide sequestration in saline formations: part I—review of the modeling of solubility trapping. *J. Pet. Sci. Eng.* 124, 367–380.
- Rochelle, C.A., Czernichowski-Lauriol, I., Milodowski, A., 2004. The impact of chemical reactions on CO<sub>2</sub> storage in geological formations: a brief review. *Geol. Soc. Lond., Spec. Publ.* 233 (1), 87–106.
- Rosenberg, N.J., 1981. The increasing CO<sub>2</sub> concentration in the atmosphere and its implication on agricultural productivity. *Clim. Chang.* 3 (3), 265–279.
- Ruprecht, C., Pini, R., Falta, R., Benson, S., Murdoch, L., 2014. Hysteretic trapping and relative permeability of CO<sub>2</sub> in sandstone at reservoir conditions. *Int. J. Greenhouse Gas Control* 27, 15–27.
- Rushton, J.C., Wagner, D., Pearce, J.M., Rochelle, C.A., Purser, G., 2020. Red-bed bleaching in a CO<sub>2</sub> storage analogue: insights from Entrada Sandstone fracture-hosted mineralization. *J. Sediment. Res.* 90 (1), 48–66.
- Sahle, M., Saito, O., Fürst, C., Yeshitela, K., 2018. Quantification and mapping of the supply of and demand for carbon storage and sequestration service in woody biomass and soil to mitigate climate change in the socio-ecological environment. *Sci. Total Environ.* 624, 342–354.
- Salama, A., Negara, A., El Amin, M., Sun, S., 2015. Numerical investigation of nanoparticles transport in anisotropic porous media. *J. Contam. Hydrol.* 181, 114–130.
- Saraji, S., Goual, L., Piri, M., Plancher, H., 2013. Wettability of supercritical carbon dioxide/water/quartz systems: simultaneous measurement of contact angle and interfacial tension at reservoir conditions. *Langmuir* 29 (23), 6856–6866.
- Saraji, S., Piri, M., Goual, L., 2014. The effects of SO<sub>2</sub> contamination, brine salinity, pressure, and temperature on dynamic contact angles and interfacial tension of supercritical CO<sub>2</sub>/brine/quartz systems. *Int. J. Greenhouse Gas Control* 28, 147–155.
- Sarmadivaleh, M., Al-Yaseri, A.Z., Iglauer, S., 2015. Influence of temperature and pressure on quartz–water–CO<sub>2</sub> contact angle and CO<sub>2</sub>–water interfacial tension. *J. Colloid Interface Sci.* 441, 59–64.
- Schiermeier, Q., Tollefson, J., Scully, T., Witze, A., Morton, O., 2008. Energy alternatives: electricity without carbon. *Nat. News* 454 (7206), 816–823.
- Shafrin, E., Zisman, W., 1962. Effect of progressive fluorination of a fatty acid on the wettability of its adsorbed monolayer. *J. Phys. Chem.* 66 (4), 740–748.
- ShamsiJazeyi, H., Miller, C.A., Wong, M.S., Tour, J.M., Verduzco, R., 2014. Polymer-coated nanoparticles for enhanced oil recovery. *J. Appl. Polym. Sci.* 131 (15).
- Sharma, T., Kumar, G.S., Sangwai, J.S., 2015. Comparative effectiveness of production performance of Pickering emulsion stabilized by nanoparticle-surfactant-polymerover surfactant-polymer (SP) flooding for enhanced oil recoveryfor Brownfield reservoir. *J. Pet. Sci. Eng.* 129, 221–232.
- Siddiqui, M.A.Q., Ali, S., Fei, H., Roshan, H., 2018. Current understanding of shale wettability: a review on contact angle measurements. *Earth Sci. Rev.* 181, 1–11.
- Snippe, J., Berg, S., Ganga, K., Brussee, N., Gdanski, R., 2020. Experimental and numerical investigation of wormholing during CO<sub>2</sub> storage and water alternating gas injection. *Int. J. Greenhouse Gas Control* 94, 102901.
- Solomon, S., Plattner, G.-K., Knutti, R., Friedlingstein, P., 2009. Irreversible climate change due to carbon dioxide emissions. *Proc. Natl. Acad. Sci.* 106 (6), 1704–1709.
- Song, J., Zhang, D., 2013. Comprehensive review of caprock-sealing mechanisms for geologic carbon sequestration. *Environ. Sci. Technol.* 47 (1), 9–22.
- Soong, Y., Goodman, A., McCarthy-Jones, J., Baltrus, J., 2004. Experimental and simulation studies on mineral trapping of CO<sub>2</sub> with brine. *Energy Convers. Manag.* 45 (11–12), 1845–1859.
- Soong, Y., Fauth, D., Howard, B., Jones, J., Harrison, D., Goodman, A., Gray, M., Frommell, E., 2006. CO<sub>2</sub> sequestration with brine solution and fly ashes. *Energy Convers. Manag.* 47 (13–14), 1676–1685.
- Stalker, L., Varma, S., Van Gent, D., Haworth, J., Sharma, S., 2013. South West Hub: a carbon capture and storage project. *Aust. J. Earth Sci.* 60 (1), 45–58.
- Standal, S., Haavik, J., Blokhus, A., Skauge, A., 1999. Effect of polar organic components on wettability as studied by adsorption and contact angles. *J. Pet. Sci. Eng.* 24 (2–4), 131–144.
- Stumm, W., Morgan, J., 1996. Aquatic Chemistry: Chemical Equilibria and Rates in Natural Waters. John Wiley & Sons, Inc, New York, p. 1022.
- Su, E., Liang, Y., Zou, Q., Niu, F., Li, L., 2019. Analysis of effects of CO<sub>2</sub> injection on coalbed permeability: implications for coal seam CO<sub>2</sub> sequestration. *Energy Fuel* 33 (7), 6606–6615.

- Sun, Q., Ampomah, W., Kutsienyo, E.J., Appold, M., Adu-Gyamfi, B., Dai, Z., Soltanian, M.R., 2020. Assessment of CO<sub>2</sub> trapping mechanisms in partially depleted oil-bearing sands. *Fuel* 278, 118356.
- Tabrizy, V.A., Denoyel, R., Hamouda, A., 2011. Characterization of wettability alteration of calcite, quartz and kaolinite: surface energy analysis. *Colloids Surf. A Physicochem. Eng. Asp.* 384 (1–3), 98–108.
- Tang, Y., Hu, S., He, Y., Wang, Y., Wan, X., Cui, S., Long, K., 2020. Experiment on CO<sub>2</sub>-brine-rock interaction during CO<sub>2</sub> injection and storage in gas reservoirs with aquifer. *Chem. Eng. J.* 413, 127567.
- Thomas, M.M., Clouse, J.A., Longo, J.M., 1993. Adsorption of organic compounds on carbonate minerals: 1. Model compounds and their influence on mineral wettability. *Chem. Geol.* 109 (1–4), 201–213.
- Tokunaga, T.K., Wan, J., 2013. Capillary pressure and mineral wettability influences on reservoir CO<sub>2</sub> capacity. *Rev. Mineral. Geochem.* 77 (1), 481–503.
- Tong, R., Hemmati, H.D., Langer, R., Kohane, D.S., 2012. Photoswitchable nanoparticles for triggered tissue penetration and drug delivery. *J. Am. Chem. Soc.* 134 (21), 8848–8855.
- Toquero, C.M., 2020. Challenges and opportunities for higher education amid the COVID-19 pandemic: the Philippine context. *Pedagog. Res.* 5 (4).
- Tosun, Y.İ., 2020. Microwave Caustic Slurry Carbonation of Flue Gas of Coal Power Plants in Double Hot Tube Bed for CO<sub>2</sub> Sequestration, Carbon Capture. IntechOpen.
- Townsend, G.T., Prince, R.C., Suflita, J.M., 2003. Anaerobic oxidation of crude oil hydrocarbons by the resident microorganisms of a contaminated anoxic aquifer. *Environ. Sci. Technol.* 37 (22), 5213–5218.
- Tudek, J., Crandall, D., Fuchs, S., Werth, C.J., Valocchi, A.J., Chen, Y., Goodman, A., 2017. In situ contact angle measurements of liquid CO<sub>2</sub>, brine, and Mount Simon sandstone core using micro X-ray CT imaging, sessile drop, and Lattice Boltzmann modeling. *J. Pet. Sci. Eng.* 155, 3–10.
- Vanithakumari, S., George, R., Mudali, U.K., 2014. Influence of silanes on the wettability of anodized titanium. *Appl. Surf. Sci.* 292, 650–657.
- Viete, D.R., Ranjith, P.G., 2006. The effect of CO<sub>2</sub> on the geomechanical and permeability behaviour of brown coal: implications for coal seam CO<sub>2</sub> sequestration. *Int. J. Coal Geol.* 66 (3), 204–216.
- Walspurger, S., Cobden, P.D., Safonova, O.V., Wu, Y., Anthony, E.J., 2010. High CO<sub>2</sub> storage capacity in alkali-promoted hydrotalcite-based material: in situ detection of reversible formation of magnesium carbonate. *Chemistry* 16 (42), 12694–12700.
- Wang, H., Yan, N., Li, Y., Zhou, X., Chen, J., Yu, B., Gong, M., Chen, Q., 2012. Fe nanoparticle-functionalized multi-walled carbon nanotubes: one-pot synthesis and their applications in magnetic removal of heavy metal ions. *J. Mater. Chem.* 22 (18), 9230–9236.
- Wang, S., Edwards, I.M., Clarens, A.F., 2013a. Wettability phenomena at the CO<sub>2</sub>-brine-mineral interface: implications for geologic carbon sequestration. *Environ. Sci. Technol.* 47 (1), 234–241.
- Wang, S., Tao, Z., Persily, S.M., Clarens, A.F., 2013b. CO<sub>2</sub> adhesion on hydrated mineral surfaces. *Environ. Sci. Technol.* 47 (20), 11858–11865.
- Wang, Y., Yuan, L., Yao, C., Ding, L., Li, C., Fang, J., Sui, K., Liu, Y., Wu, M., 2014. A combined toxicity study of zinc oxide nanoparticles and vitamin C in food additives. *Nanoscale* 6 (24), 15333–15342.
- Waples, D.W., 1981. Organic Geochemistry for Exploration Geologists. Burgess Pub. Co.
- Watson, J., Jones, D., Swannell, R., Van Duin, A., 2002. Formation of carboxylic acids during aerobic biodegradation of crude oil and evidence of microbial oxidation of hopanes. *Org. Geochem.* 33 (10), 1153–1169.
- Wesch, A., Dahmen, N., Ebert, K., Schön, J., 1997. Grenzflächenspannungen, Tropfengrößen und Kontaktwinkel im Zweiphasensystem H<sub>2</sub>O/CO<sub>2</sub> bei Temperaturen von 298 bis 333 K und Drücken bis 30 MPa. *Chemie Ingenieur Technik* 69 (7), 942–946.
- Wright, I.P., Yates, P., Hutchison, R., Pillinger, C., 1997. The content and stable isotopic composition of carbon in individual micrometeorites from Greenland and Antarctica. *Meteorit. Planet. Sci.* 32 (1), 79–89.
- Xu, L., Yu, G., He, N., Wang, Q., Gao, Y., Wen, D., Li, S., Niu, S., Ge, J., 2018. Carbon storage in China's terrestrial ecosystems: a synthesis. *Sci. Rep.* 8 (1), 1–13.
- Yang, D., Gu, Y., Tontiwachwuthikul, P., 2008. Wettability determination of the reservoir brine–reservoir rock system with dissolution of CO<sub>2</sub> at high pressures and elevated temperatures. *Energy Fuel* 22 (1), 504–509.
- Yang, L., Xu, T., Wei, M., Feng, G., Wang, F., Wang, K., 2015. Dissolution of arkose in dilute acetic acid solution under conditions relevant to burial diagenesis. *Appl. Geochem.* 54, 65–73.
- Yang, Y., Cheng, T., Wu, H., You, Z., Shang, D., Hou, J., 2020. Enhanced oil recovery using oleic acid-modified titania nanofluids: underlying mechanisms and oil-displacement performance. *Energy Fuel* 34 (5), 5813–5822.
- Yassin, M.R., Begum, M., Dehghanpour, H., 2017. Organic shale wettability and its relationship to other petrophysical properties: a Duvernay case study. *Int. J. Coal Geol.* 169, 74–91.
- Yuan, L., Zhang, Y., Dehghanpour, H., 2021. A theoretical explanation for wettability alteration by adding nanoparticles in oil-water-tight rock systems. *Energy Fuel* 35 (9), 7787–7798.
- Zasadzinski, J., Viswanathan, R., Madsen, L., Garnaes, J., Schwartz, D., 1994. Langmuir-blodgett films. *Science* 263 (5154), 1726–1733.
- Zhang, D., Song, J., 2014. Mechanisms for geological carbon sequestration. *Proc. IUTAM* 10, 319–327.
- Zhang, W., Li, Y., Xu, T., Cheng, H., Zheng, Y., Xiong, P., 2009. Long-term variations of CO<sub>2</sub> trapped in different mechanisms in deep saline formations: a case study of the Songliao Basin, China. *Int. J. Greenhouse Gas Control* 3 (2), 161–180.
- Zhang, X., Xiao, S., Zhou, J., Tang, J., 2014. Experimental analysis of the feasibility of CF<sub>3</sub> /CO<sub>2</sub> substituting SF<sub>6</sub> as insulation medium using needle-plate electrodes. *IEEE Trans. Dielectr. Electr. Insul.* 21 (4), 1895–1900.
- Zhang, Y., Kogure, T., Nishizawa, O., Xue, Z., 2017. Different flow behavior between 1-to-1 displacement and co-injection of CO<sub>2</sub> and brine in Berea sandstone: Insights from laboratory experiments with X-ray CT imaging. *Int. J. Greenhouse Gas Control* 66, 76–84.
- Zhang, B., Mohamed, A.I., Goual, L., Piri, M., 2020. Pore-scale experimental investigation of oil recovery enhancement in oil-wet carbonates using carbonaceous nanofluids. *Sci. Rep.* 10 (1), 1–16.
- Zheng, H., Zhong, Y., Mao, Z., Zheng, L., 2018. CO<sub>2</sub> utilization for the waterless dyeing: characterization and properties of Disperse Red 167 in supercritical fluid. *J. CO<sub>2</sub> Util.* 24, 266–273.
- Zheng, J., Chong, Z.R., Qureshi, M.F., Linga, P., 2020. Carbon dioxide sequestration via gas hydrates: a potential pathway toward decarbonization. *Energy Fuel* 34 (9), 10529–10546.